THE UNIVERSITY OF OKLAHOMA

GRADUATE COLLEGE

STUDIES OF LINE WIDTH OF MICROWAVE SPECTRA OF SYMMETRIC TOP MOLECULES

A DISSERTATION

SUBMITTED TO THE GRADUATE FACULTY

in partial fulfillment of the requirements for the

degree of

DOCTOR OF PHILOSOPHY

BY

JAMES ANDREW ROBERTS

Norman, Oklahoma

1967

STUDIES OF LINE WIDTH OF MICROWAVE SPECTRA

OF SYMMETRIC TOP MOLECULES

APPROVED BY

Chun C. Lin

Charles W. Bert

[illegible]

Robert F. St. John

William N. Hughes

ACKNOWLEDGMENTS

The author wishes to thank Professor Chun C. Lin for assigning this problem and directing it to completion.

Grateful thanks are expressed to Professor Ralph W. Parsons of the University of Queensland, Brisbane, Australia, for suggesting the problems of doppler broadening and overlapping spectral lines in the inversion spectrum of NH_3 for K = 1, for his invaluable aid in theoretical discussion of phases of these problems and in numerical analysis of much of the data.

The author wishes to express appreciation to the Ford Foundation for financial assistance during the 1965-66 school year.

Most of all the author wishes to express appreciation to his wife, Pat, and daughters, Judi and Kim, for their patience and understanding while the work encompassed by this dissertation was being performed.

TABLE OF CONTENTS

LIST OF TABLES

LIST OF ILLUSTRATIONS

STUDIES OF LINE WIDTH OF MICROWAVE SPECTRA OF SYMMETRIC TOP MOLECULES

CHAPTER I

INTRODUCTION

Microwave line width spectroscopy has become important in the last twenty years as a means of determining interaction processes between molecules. From a systematic and careful determination of the line widths of spectral lines it is possible to infer interaction parameters and interaction processes which take place between the molecules being observed. Two groups of interactions are studied. These are broadly classified under the two headings "self-broadening" and "foreign gas broadening."

When investigations of self broadening are being made all of the molecules within the absorption cell are of one kind. On the other hand, in the foreign gas broadening scheme interactions between different types of molecules are observed.

In the self broadening scheme the gas being observed is admitted into the absorption cell in small samples from a dosing system. After each sample of gas has been allowed to stabilize within the cell, the line width of the transition being observed is measured carefully and recorded along with the cell pressure. This procedure is continued

with increasing pressure until sufficient data for line width, $\Delta\nu$, and pressure, P, are obtained to obtain a reliable graph of $\Delta\nu$ versus P. From this graph the slope of the curve, called the line width parameter $\Delta\nu_p$, is obtained for the transition being made. This line width parameter is used in conjunction with other molecular parameters to infer an effective collision cross section for self collision of the molecules.

In the foreign gas broadening scheme a small sample of gas to be examined is admitted into the collision cell and allowed to stabilize. The spectrograph is then tuned to the desired transition to be observed and the half-width of this line measured. Fixed samples of a "foreign" gas molecule are then admitted into the absorption cell in a systematic manner with the line width of the observed line and pressure in the cell being measured after admission of each sample. These results are tabulated and plotted to determine the line width parameter. From line width parameters and a knowledge of other parameters of the molecules it is possible to determine an effective collision cross section for interaction between the type molecules being studied. If the origin of the interaction is known, it is possible to infer magnitudes of the type interactions and gain insight into the collision processes which take place between molecules.

Recent developments in instrumentation and line width measuring techniques have made it possible to determine line width of spectral lines to an accuracy of better than 2%. [1]

In order to appreciate some of the problems encountered in developing electronic devices and measuring line widths, it is well to

look briefly at some of these.

A basic apparatus for observing absorption spectra is shown in Figure 1.

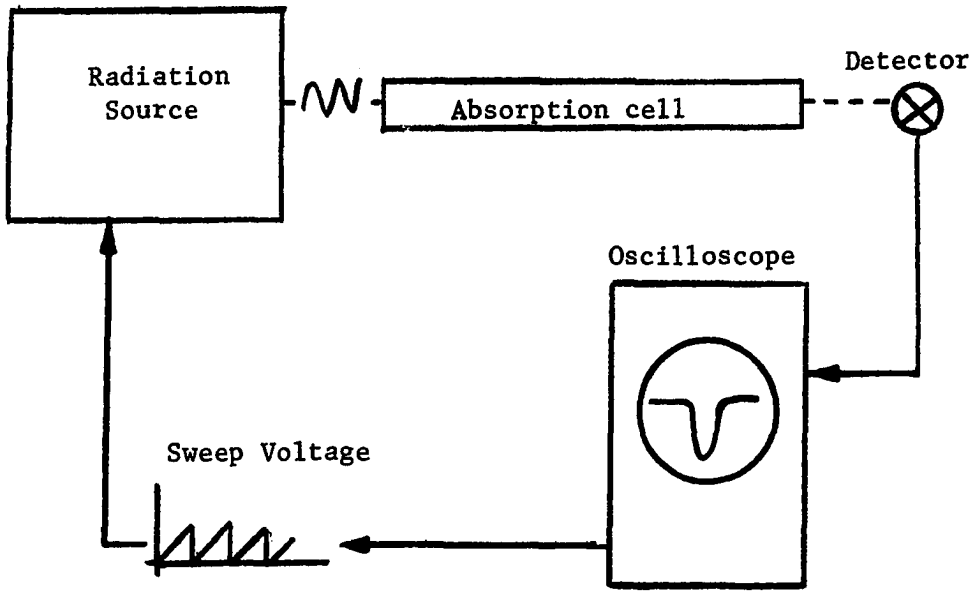

Figure 1. Basic apparatus for observing absorption spectra.

The source of radiation is varied in frequency by a saw-tooth voltage pulse in such a way that the frequency output produces time varying signals from the molecular transitions being induced. As the frequency of the source is swept through a frequency corresponding to an allowed transition within the molecule, some of the radiation will be absorbed from the source. This absorption will appear as a power "dip" at the detector. Application of the time varying sawtooth to the radiation source will produce a display on the read-out device, here an oscilloscope. The display will have a shape characteristic dependent upon several parameters which attend the measuring process.

The apparatus of Figure 1 is very basic and supplies only

the minimum requirements for doing microwave spectroscopy. In the more complex spectrograph generally used, the line shape appearing on the read-out apparatus for most spectral lines is not a true reproduction of the absorption line appearing at the input of the detector unless the detector loading and response are taken into account. The signal also undergoes distortion from amplification when it is necessary to amplify the signals. A more detailed discussion of the problem of detector loading and amplification is found in Chapter III.

The addition of any components to the spectrograph shown in Figure 1 makes it necessary to study in detail any effect arising which may produce error in line width determination when this basic spectrograph is made more complex. As pointed out earlier, the distortion of line shape by amplification must be considered and proper corrections made. One way of compensating for the non-linear distortion in the amplifier is to keep the amplitude within a range over which the amplifier responds in a linear way. The most effective way of compensating for non-linear response in the amplifier system is to make observations on the derivative of the line shape. The critical points of the line shape are not as sensitive to non-linearity of the amplifier system as is the non-differentiated signal. In Figure 2 is shown the line shape and the derivative of the line shape. The derivative of the line shape is obtained easily and information obtained from the points of steepest slope via the derivative signal are more reliable than half-power points for the spectral line observed directly.

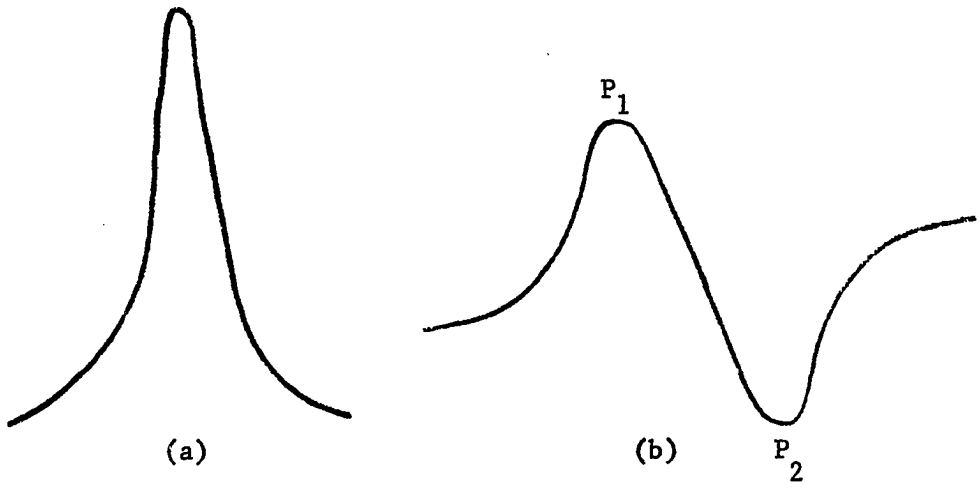

Figure 2. (a) Line shape at the detector

(b) Line shape after chopping with a square wave and amplifying

The derivative of the line shape, Figure 2(b), is obtained by applying a square wave of 5 kc/sec to the repeller electrode of the klystron which serves as a microwave source. This square wave has a two-fold function. Chopping of the spectral signal produces an ac signal which is more easily amplified. The square wave also serves to differentiate the line shape, hence, produces the well defined points of steepest slope, P_1 and P_2. These points are more easily located and more reliable than are the half-power points of Figure 2(a). The half-power points of Figure 2(a) can be found merely by measuring the one-half amplitude of the signal above the background noise. Two problems arise here which must be considered. First, it is sometimes difficult to establish a well-defined base line for the noise. Secondly, the amplifier may be saturating and "chopping" some of the peak from the signal. Obviously errors in finding half-power points arise if either the

base line is not properly located or the peak of the signal is shifted by saturation or non-linear response within the amplifier.

Both of these problems can be overcome by looking at the derivative of the line shape and relating the points of steepest slope to the half-power points for the non-differentiated line. This relationship is given by [2]

$$\delta\nu = \frac{\Delta\nu}{\sqrt{3}}\left[1+1/4\left(\frac{\omega}{\Delta\nu}\right)^2 + \left(\frac{\nu}{\Delta\nu}\right)^2\right] \qquad \text{(I-1)}$$

Where: $\Delta\nu$ = one half true line width.
$\delta\nu$ = one half apparent line width.
ω = angular frequency excursion of the klystron due to the applied square-wave modulation signal.
ν = angular frequency of the modulation.

By measuring the spacing between points of steepest slope it is no longer necessary to find the base line for background noise or loacte the point of maximum power for the spectral line. It is necessary to continue to exercise care to reproduce the true line shape but the method of measuring the line derivative allows some relaxation of the strict requirement of reproducing the line shape near its peak value.

A problem related to the base line or background noise level is the lack of a flat mode response over a broad frequency range. Most microwave sources have flat mode response only over a narrow range of frequencies. When spectral lines are being observed superimposed upon this mode there may occur some line width distortion due to this non-flat response. This amounts to taking the line shape derivative over a curved time axis, shifting the points of steepest slope accordingly. The location of the spectral line along the klystron mode will deter-

mine the nature of the distortion in line width measurements. From the following sketch can be seen the nature of distortion for the line when observed relative to a curved background. Extreme care must be exercised to obtain a flat background upon which to observe the spectral lines.

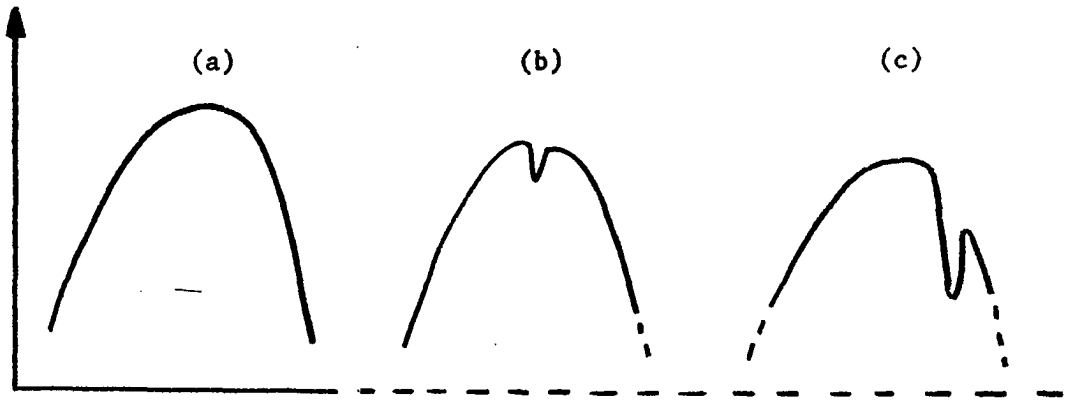

Figure 3. (a) Power mode sketch for a klystron output

(b) Power mode plus spectral line with the spectral line centered on the mode

(c) Power mode with spectral line shifted to one edge of the mode

Figure 3(a) shows the approximate shape of the power mode output for a klystron. Most klystrons have two or three modes like this for the same coarse frequency setting.

The line shape of Figure 3(b) will be a near faithful reproduction of the line shape characteristic of the molecular transition if $\Delta\nu$ is very small or the mode is flat over most of the range. It is difficult to obtain klystrons which have flat mode response over a very large frequency spread. A device referred to as a "mode leveler" has been developed by Rinehart and Legan to produce a flat mode. [3] This

device flattens the mode by means of a feedback loop and enables broad, flat frequency response for the system. The chief drawback of this device is that enough power is required such that the feedback loop will not attenuate the power below usable amounts at the absorption cell. The spread of flatness for the mode can be controlled by the feed-back loop.

Figure 3(c) is an extreme case of spectral line distortion due to non-flatness of the klystron mode. The setting of the spectral line at the edge of the mode of the klystron, where its curvature is greatest, will radically distort the line shape and produce gross errors in line width determinations. This is remedied by keeping the absorption line near the center of the mode where it is flattest.

Some other contributing factors to line width distortion are the following.

Since an absorption cell is utilized in microwave spectroscopy some problems arise due to the cell wall shape and finite extent. This arises as follows. As the mean free path of the molecules in the molecular aggregate becomes comparable to the cross-sectional dimensions of the wave guide there will be broadening of the line which is referred to as wall broadening. Generally a rectangular wave-guide is used to contain the gas. The mean free path of the molecules becomes comparable to a and b, the dimensions of the wave guide, respectively as the gas pressure is lowered. Each of these dimensions will offer a constant line width factor to the overall line width. This contribution to line width should be considered in determining the line width when the cell pressure is extrapolated to zero. If absolute line widths

are not desired but only $\Delta\nu_p$, it is not imperative to consider the wall broadening contribution to spectral line widths, as this width distortion is a constant which only translates the graph of $\Delta\nu_p$.

A spectral line shape may be distorted when it is very close to other spectral lines. Because of the importance of this line width distortion, a detailed treatment of this problem is given in Chapter V.

The spectral lines are also distorted in shape by doppler broadening when the cell pressure is very low. In Chapter VI a discussion of the origin and solution of this problem is given.

Once the problems of instrumentation and measuring techniques were solved and understood, a systematic study was made to determine the validity of previous data and the Anderson collision theory. [4] Detailed discussions of instrumentation requirements of this investigation are found in Chapters II, III, and IV.

CHAPTER II

GENERAL INSTRUMENTATION

One of the most important phases of microwave line width spectroscopy is the instrumentation needed to produce a dependable spectrograph that can be used to obtain reliable data. A great amount of effort has been expended to understand or eliminate the problems arising when the basic spectrograph of Figure 1 is enlarged to become a reliable research tool.

The problem of amplification of spectral signals is discussed in Chapter III. This is perhaps the most important facet of instrumentation for several reasons. First of all, microwave line width spectroscopy would be severely limited without some means of amplifying the spectral signals, since many microwave transitions are very weak. Secondly, many problems attend amplification and must be coped with when the necessity to amplify a signal arises.

A block diagram of the overall spectrograph is shown in Figure 5. Each block within the system serves a unique function to make the spectrograph a useful tool of research. Circuit diagrams for the units which are not commercially available are given for reference. These units were designed and constructed to satisfy the requirements of the line width spectrograph used to obtain all of the data recorded in this

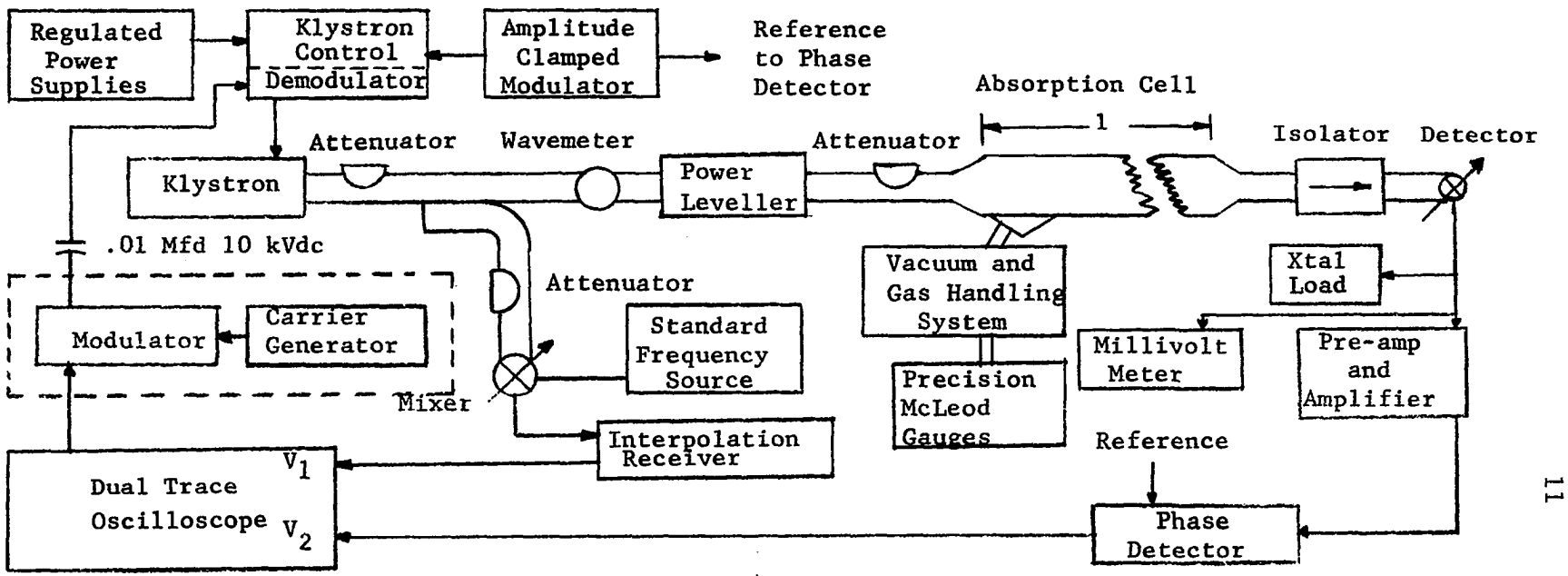

Figure 5. Block Diagram of the Complete Microwave Spectrograph used for Obtaining Line Widths of Microwave Spectral Lines

work. Some of the general instrumentation which has not been described by earlier investigators is discussed and recorded here.

The requirement that the klystron mode be broad and flat led to the development of the linear sweep circuit used to supply a saw tooth wave form to the repeller electrode of the reflex klystron. A choice of sweeping the repeller electrode or the focus electrode of the klystron is dependent upon the output properties sought for the klystron and the type klystron being used. Both focus and repeller electrode sweeping have been used and the merits of one over the other are debatable.

Focus sweeping of the klystron can give a long, flat mode response from some klystrons, with reduced power output for some klystrons and critical voltage settings at the focus electrode for others. It has been observed that sweeping of the focus electrode for OKI type klystrons produces gross power variations at the output for some voltage settings. The reason for this can be seen in the following way.

The effective circuit of the klystron is basically a triode amplifier with the plate load resistance being the resonant cavity and cavity grid structure. In Figure 4 is shown both the tube structure and the equivalent circuit when focus sweep is applied.

The klystron acts as an amplifier, but a very interesting one, in the following way. Any voltage change at the focus electrode will produce a voltage change at the "plate" of the triode due to the amplifying property of the tube; at the same time there is a frequency change at the cavity due to a change in the bunching of the electrons streaming from the cathode toward the repeller electrode. The resonant

cavity, therefore, feels the resultant of two signals; one an amplification signal and the other a frequency changing impulse. These two blend to give an output mode.

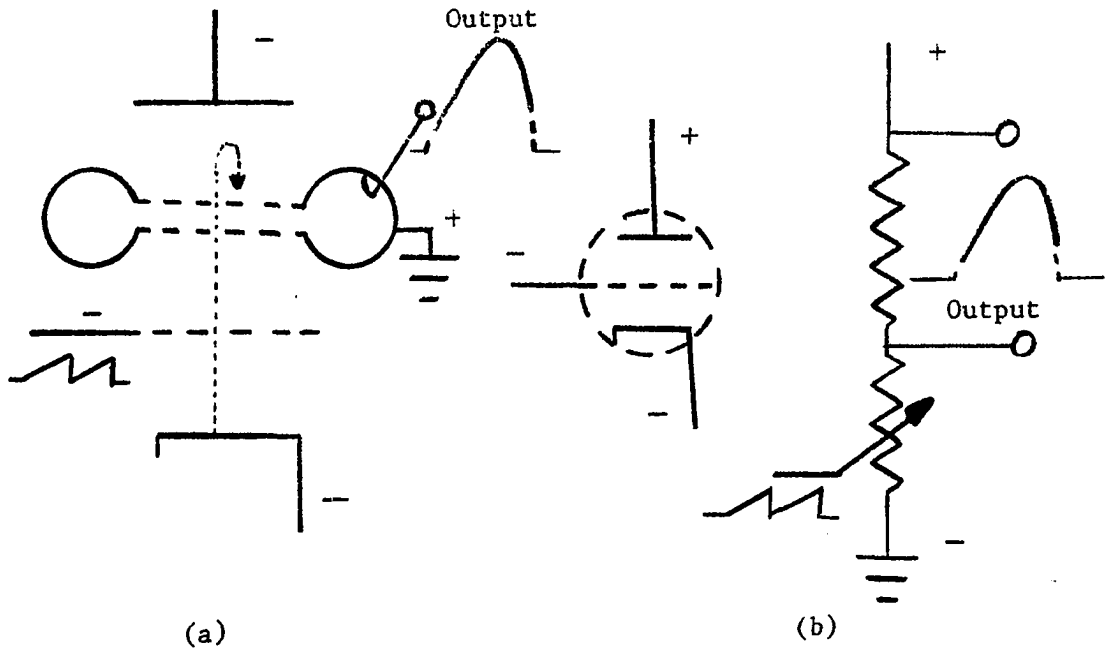

Figure 4. Reflex klystron and equivalent circuit

Tests have been made to check the amplifying property of the klystron and signals of strong magnitude have been transferred from the focus electrode to the mode by applying a square wave to the focus electrode. The amplitudes of these signals are strongly dependent upon the voltage setting of the focus electrode. The reason for this is that the reflex klystron has a characteristic "amplification" curve that has the same trend as for any triode type tube. The klystron can be operated along this dynamic curve and produce a variety of output modes, not all of which are suitable to line width determination requirements.

Because of the sensitivity of the OKI klystrons to focus voltage

settings, extreme care must be exercised when it is desired to sweep the focus electrode. Sweeping the repeller electrode does not produce the same difficulties but mode curvature becomes more of a problem when using repeller sweep. Both types of klystron sweeps have their merits and the choice of type sweep is determined by the requirements for the klystron output spectrum.

A modified klystron control circuit has been designed and constructed to enable repeller sweeping of the OKI type klystrons. This control circuit has some advantages over the former circuits used. The control circuit is simpler and it is possible to bypass any disturbing a.c. voltage which appears on the focus electrode. The noise appearing in the frequency markers has been reduced considerably by restoring the focus to d.c. voltage levels and sweeping the repeller electrode of the OKI klystrons.

A circuit diagram of the filament power supply and control circuit for sweeping the OKI klystrons is shown in Figure 6. Since a common power supply is used for the focus potential and repeller potential it was found necessary to sweep the repeller by impressing the sweep voltage across a high valued resistor in series with the lead to the repeller electrode. By filtering the sweep variations at R in Figure 6 it was possible to eliminate coupling of the sweep into the focus electrode. The biasing potentiometers were chosen to have high values in order to reduce the importance of the internal resistance of the power supply and thus produce minimum coupling of the sweep voltage into the power supply resistance where it would reflect onto the focus electrode.

The sawtooth sweep voltage applied to the focus or repeller

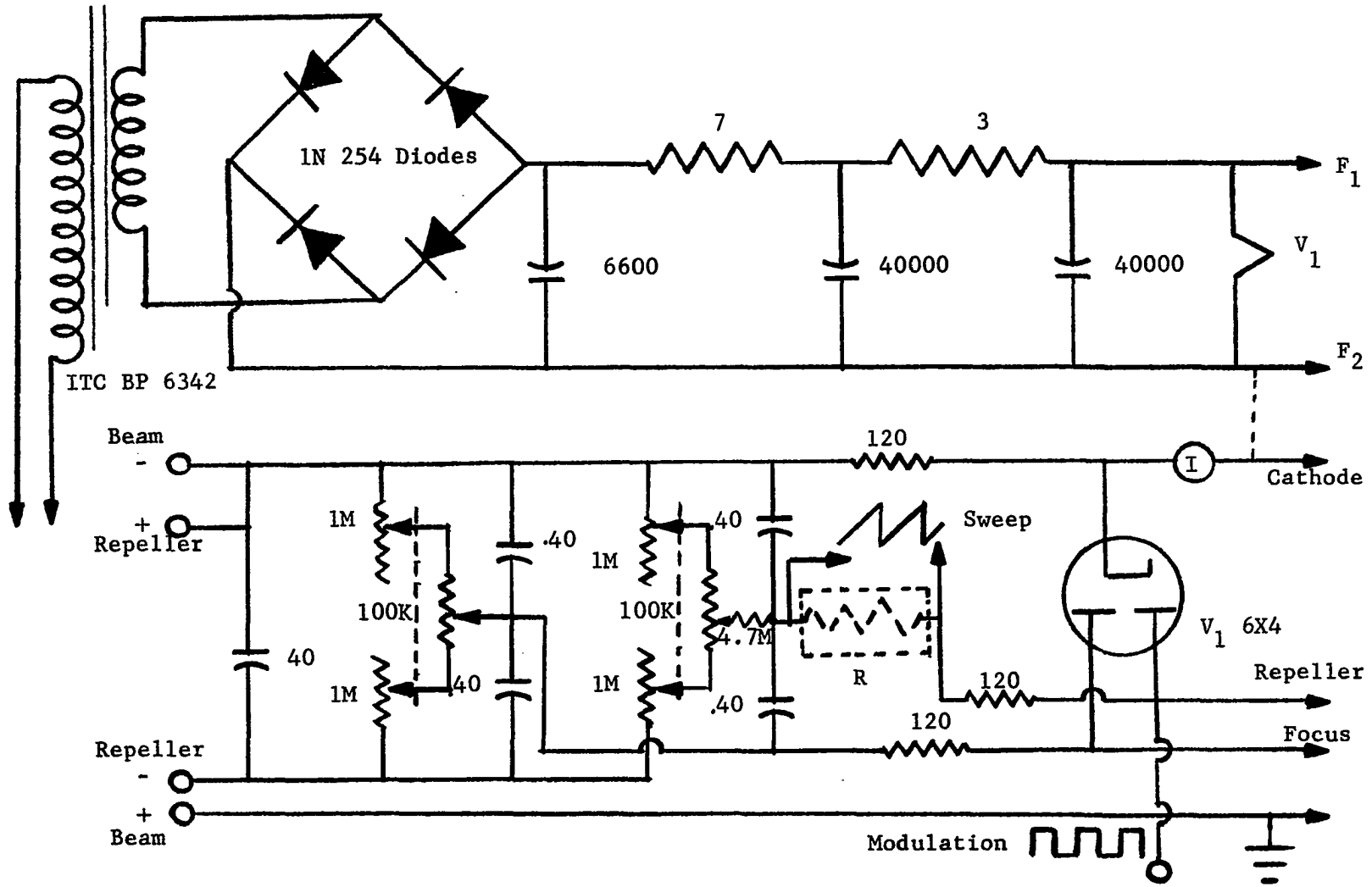

Figure 6. Filament Supply and Control Circuit for Repeller Sweeping OKI Klystrons

electrode of the reflex klystron must be very linear in order to obtain a uniform power mode output from the klystron. Several methods of sweeping the klystron have been tried to achieve a linear sawtooth sweep.

The earliest method employed was an electro-mechanical sweep circuit which consisted of a linear potentiometer driven by a synchronous motor. The wiper arm of the potentiometer served as a source of varying voltage. The amplitude of the sweep was controlled by varying the voltage applied across the potentiometer terminals. This sweep circuit was very simple but not as versatile as needed for general line width spectroscopy.

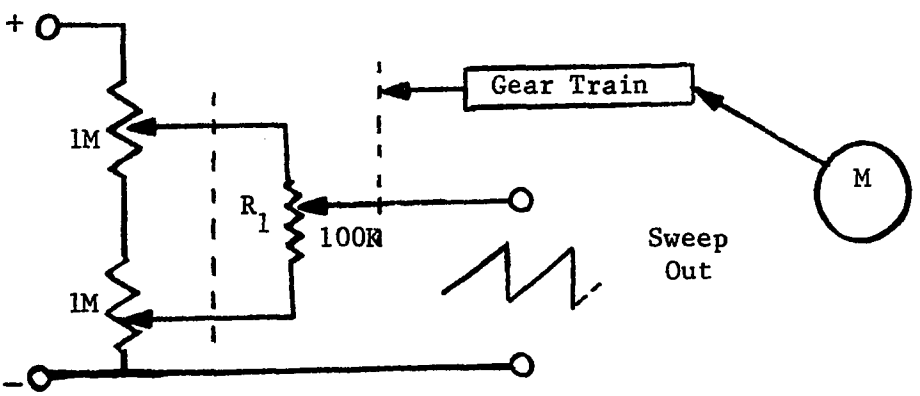

Figure 7. Sketch of earliest sweep circuit tried.

The sweep speed was controlled by using a series of geared synchronous motors, M. Each time the sweep speed was to be changed from a speed suitable for search to a slower speed suitable for making line width measurements, the motor had to be changed. This was a very awkward and time consuming procedure. The amplitude of the sweep was changed by adjusting R_1 to vary the voltage drop across the sweep potentiometer.

Two types of potentiometers, wire wound and carbon deposited, were tried in an attempt to get a very uniform voltage change at the wiper arm as it was moved by the synchronous motor. Neither the carbon nor wire wound type potentiometers satisfied the requirements. The carbon deposited type resistors were not as linear as required over their entire range and were abandoned for wire wound type. The wire wound type produced jitter in the voltage as the wiper arm moved over the wire turns. This could not be tolerated as it broadened the frequency markers and reduced the resolution of the apparatus.

Several electronic sweep circuits were constructed to eliminate mechanical noises generated in the sweep. Some of these were discarded as marginal for the resolution requirements sought as the linearity of the sawtooth voltages produced was not very good. Electronic sawtooth generators were constructed that would satisfy the requirement for a linear sweep voltage for the reflex klystron. A difficulty arose in applying this sweep voltage to the repeller or focus electrode of the klystron. This voltage could not be applied directly to either of these electrodes as both electrodes resided at a voltage in excess of 1500 volts relative to ground. In order to overcome this difficulty a modulator and demodulator circuit was employed.

Figure 8 shows the circuit diagram of the carrier generator and modulator circuit used to transfer the sawtooth voltage from the oscilloscope output to the desired electrode of the klystron. The two signals, sawtooth and carrier signal, are mixed in the modulator section. This a.c. signal can readily be transferred through a capacitor to be referenced to any d.c. voltage desired. Once the carrier plus sawtooth

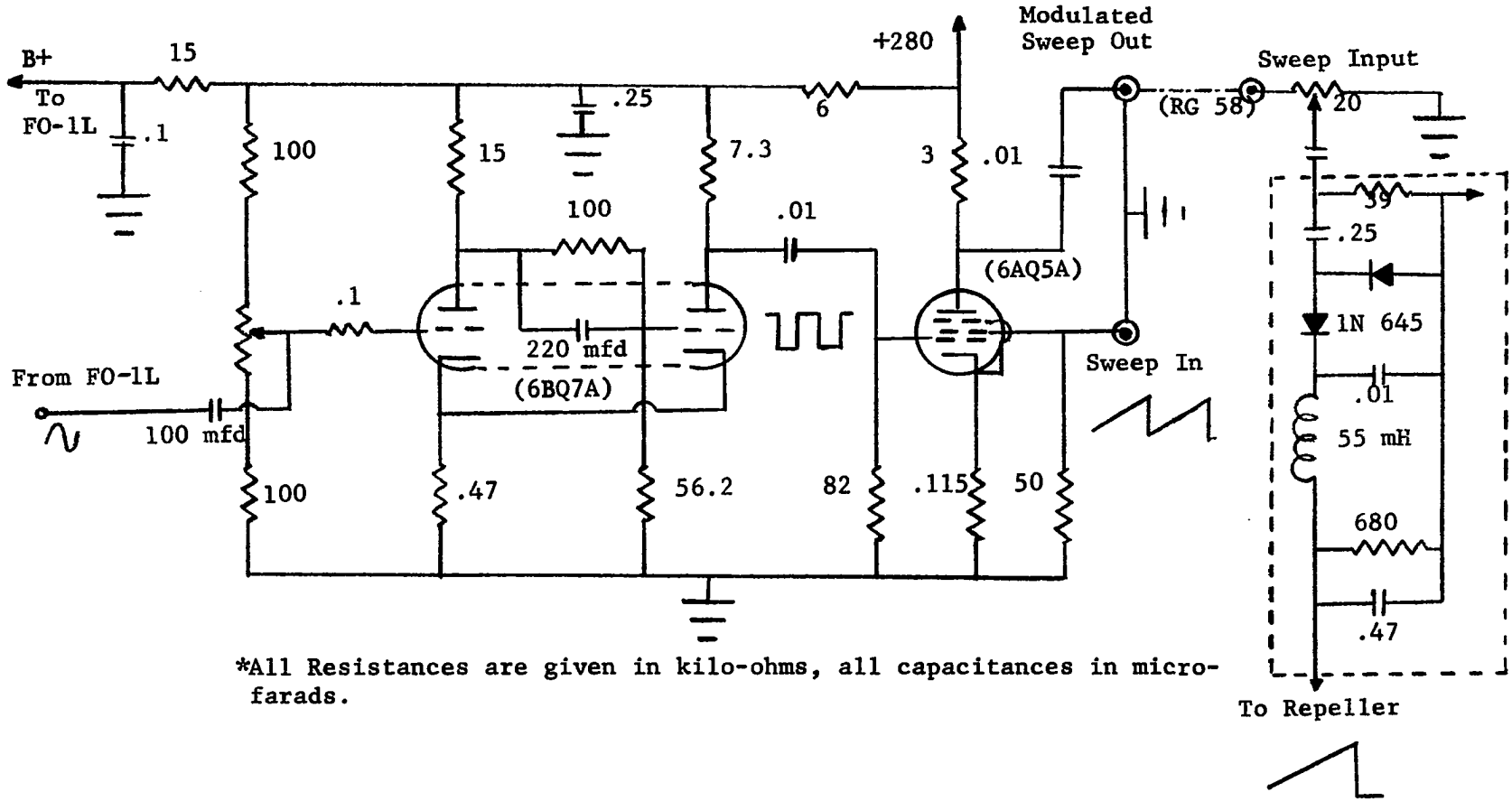

*All Resistances are given in kilo-ohms, all capacitances in micro-farads.

Figure 8. Modulator and Demodulator Circuits

signal has been transferred through the isolation capacitor in Figure 5, the composite signals are separated by demodulation, the carrier filtered by the proper RLC circuit, and a sawtooth voltage of very linear property obtained to be applied to the klystron electrode as a sweep voltage.

An attempt to simplify the sweep circuitry was made with fruitful results. Tests upon sawtooth sweep output used in Tektronix oscilloscopes have shown this output voltage to be very linear over the allowed sweep intervals of the oscilloscope. This sweep was "made to order" for the sawtooth voltage requirements of the klystron. Not only was the sawtooth voltage satisfactory in shape and linearity but the problem of sychronization of the oscilloscope sweep and klystron sweep was solved in that the same voltage sweep drove both of these units in synchronization. The klystron sweep frequency could be displayed directly along the time axis of the oscilloscope. By choosing proper demodulation of the signal in the demodulator circuit a positive or negative going sawtooth pulse could be obtained. The choice of direction of this sweep was arbitrary, but it is advantageous to choose the direction of sweep that sweeps the klystron from lower frequency to higher frequency as the oscilloscope traces from left to right.

Use of the sawtooth output of the oscilloscope and the modulator circuit of Figure 8 has led to great simplification of the klystron sweep circuit. The electronic sawtooth generator and its power supply are no longer needed to produce a sawtooth voltage but this voltage sweep is readily available from the oscilloscope.

The modulator and carrier generator circuits are of general design. The carrier source consists of a Schmitt trigger circuit

driven by a crystal controlled oscillator. The oscillator used for driving the Schmitt trigger is commercially available and is shown schematically in Appendix I. [5] Mixing of the carrier signal and the sawtooth sweep voltage is achieved by the output tube V_2. The output signal is coupled through RG 58 coaxial cable to an isolation capacitor which serves to isolate this signal from the high voltages found in the klystron control circuit. After rectification and filtering the sawtooth voltage is reclaimed and found to be as linear as it was before being transferred through the isolation capacitor.

The demodulator circuit is specially designed such that the signal from the modulator is both doubled and demodulated at the same time. The two 1N645 diodes in Figure 8 are used to double and rectify the incoming signal to reclaim the sawtooth sweep voltage. This produces a voltage of sufficient amplitude to sweep most of the klystrons used through 50 to 60 megacycles per second sweep range for search purposes.

Some other phases of development of instrumentation for the spectrograph shown in Figure 5 are given in the following chapters.

CHAPTER III

SIGNAL AMPLIFICATION

A central problem in line width microwave spectroscopy is to obtain sufficiently strong signals to make accurate measurements of the half-power points of the spectral lines. It is adequate in frequency determinations to measure the frequency when only a small signal appears at any suitable pressure. In the case of line width determinations not only must the signal be strong at a given pressure, but the signal must be strong and readable over the entire pressure range at which the investigation of line width behavior is being made. This requirement of strong signals limited the early line width investigation problems to only those molecules which offered strong spectral lines. By development of suitable amplifiers it is now possible to observe directly the line widths of spectral lines of $10^{-7}cm^{-1}$ intensity. An amplifier to enable investigations of these spectral lines has been developed and is described in the following paragraphs.

The requirements for an amplifier capable of producing readable display signals from signals of $10^{-7}cm^{-1}$ intensity were investigated and the following conclusions drawn.

1. The amplifier must have very high gain, greater than 10^6.
2. Little signal distortion by the amplifier can be tolerated.

3. The amplifier must have linear response over a very wide range of signal inputs.

4. The noise generated within the amplifier components must be sufficiently low such that effective input noise is less than 0.2 microvolt.

5. The signal-to-noise ratio of the amplifier and especially of the input stage must be very high.

6. The amplifier must be sufficiently narrow band to exclude noise not near the modulation frequency but not too narrow band to distort the resonance signal.

With these requirements in mind the design and construction of the amplifier system was begun. In order to reduce input noise a series tuned resonant circuit was used. This circuit was tuned to the modulation frequency of the klystron square-wave modulation signal. The amplifier tubes were high gain, low noise pentodes of 6AK5 type selected from a large number available, thus reducing the possibility of noise arising from random selection of tubes. The circuits were constructed in such a way that mechanical coupling to the tube bases was minimal. The first stage of amplification was mounted on rubber cushions with very flexible connecting leads in order to minimize the coupling of vibration of the chassis to this stage. A rigid steel chassis was used in order to reduce mechanical coupling to succeeding stages. Adequate tuning of the stages was made to exclude random noises which were not near the modulation frequency. The final stage of amplification was tuned with a high Q parallel network in such a way that any signals not near the modulation frequency would be shunted to ground. A schematic

diagram of the amplifier is shown in Figure 9.

A thorough study of the response of each stage of amplification was made individually for various voltage inputs. The gains of each stage were investigated for different voltages and any distortion noted. Finally the overall response of the amplifier was tested for linearity, saturation and distortion.

The characteristic curves for some of the possible gain settings of the amplifier are plotted in Figure 10. Operational settings of the amplifier were determined by the magnitude of the input signal. A detailed investigation of the characteristics of the amplifier yielded the following conclusions. The signal inputs must be kept below 100 microvolts by proper attenuation of the signal at the detector in order to assure linear response from the amplifier at gains of 10^6. Most of the signals to be observed were sufficiently weak that this requirement did not pose a problem. The effective noise input at a gain of 10^6 was found to be less than 0.2 microvolt.

A detailed study of the detector response and loading parameter of the detector produced calibration curves to be used with a given detector. These curves furnished power and loading requirements that would enable the detector to be operated in the square-law response region. All investigations of this work which were made between 15 and 35 kmc/sec were made using detector #17 of the calibrated set. The detector load and input power to the detector were kept within the range allowed by the calibration curve to retain square-law response of the detector. The characteristic curves for detector #17 are shown in Figure 11. The pre-amplifier was provided with an attenuator net-

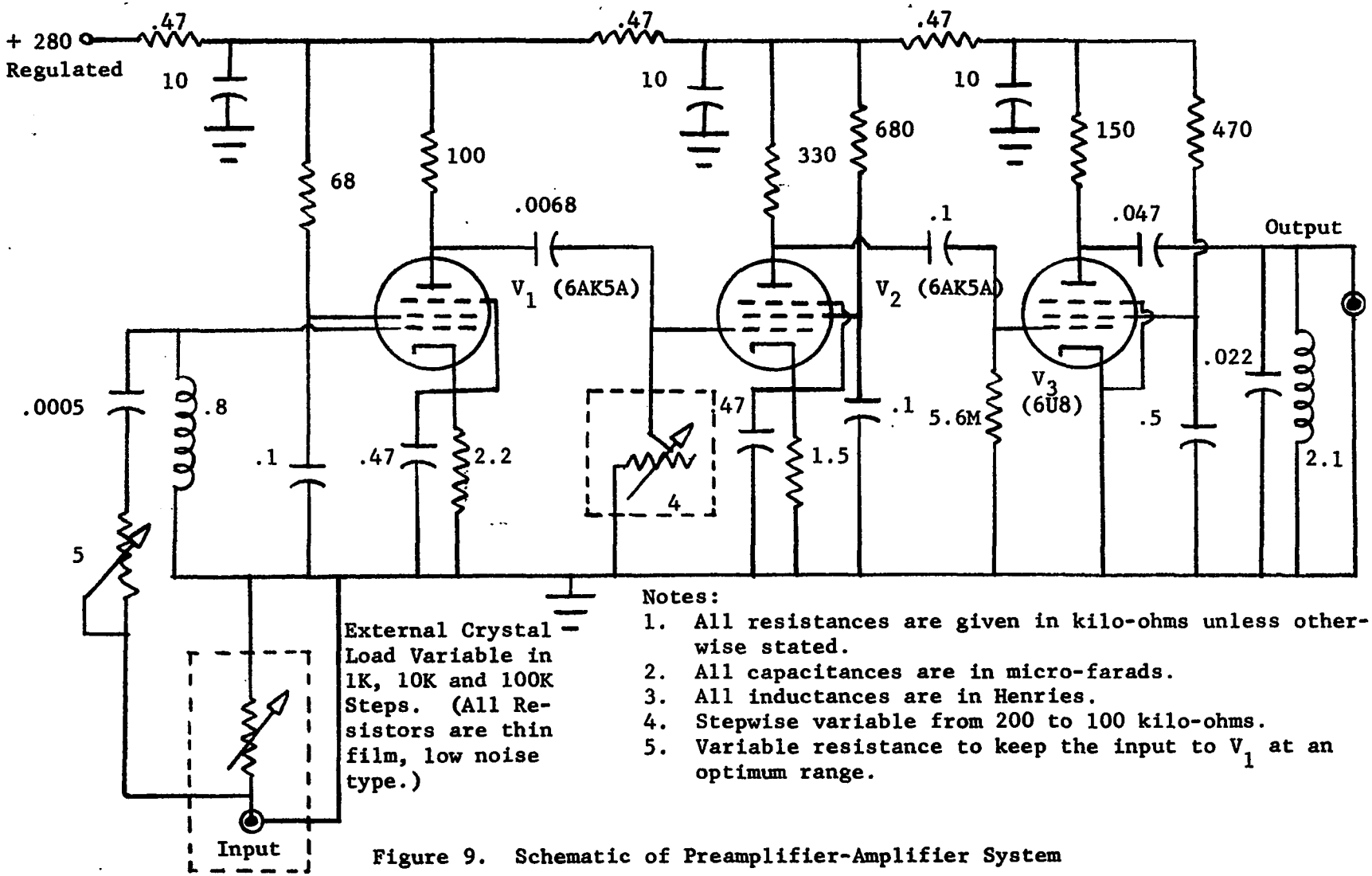

Notes:

1. All resistances are given in kilo-ohms unless otherwise stated.
2. All capacitances are in micro-farads.
3. All inductances are in Henries.
4. Stepwise variable from 200 to 100 kilo-ohms.
5. Variable resistance to keep the input to V_1 at an optimum range.

Figure 9. Schematic of Preamplifier-Amplifier System

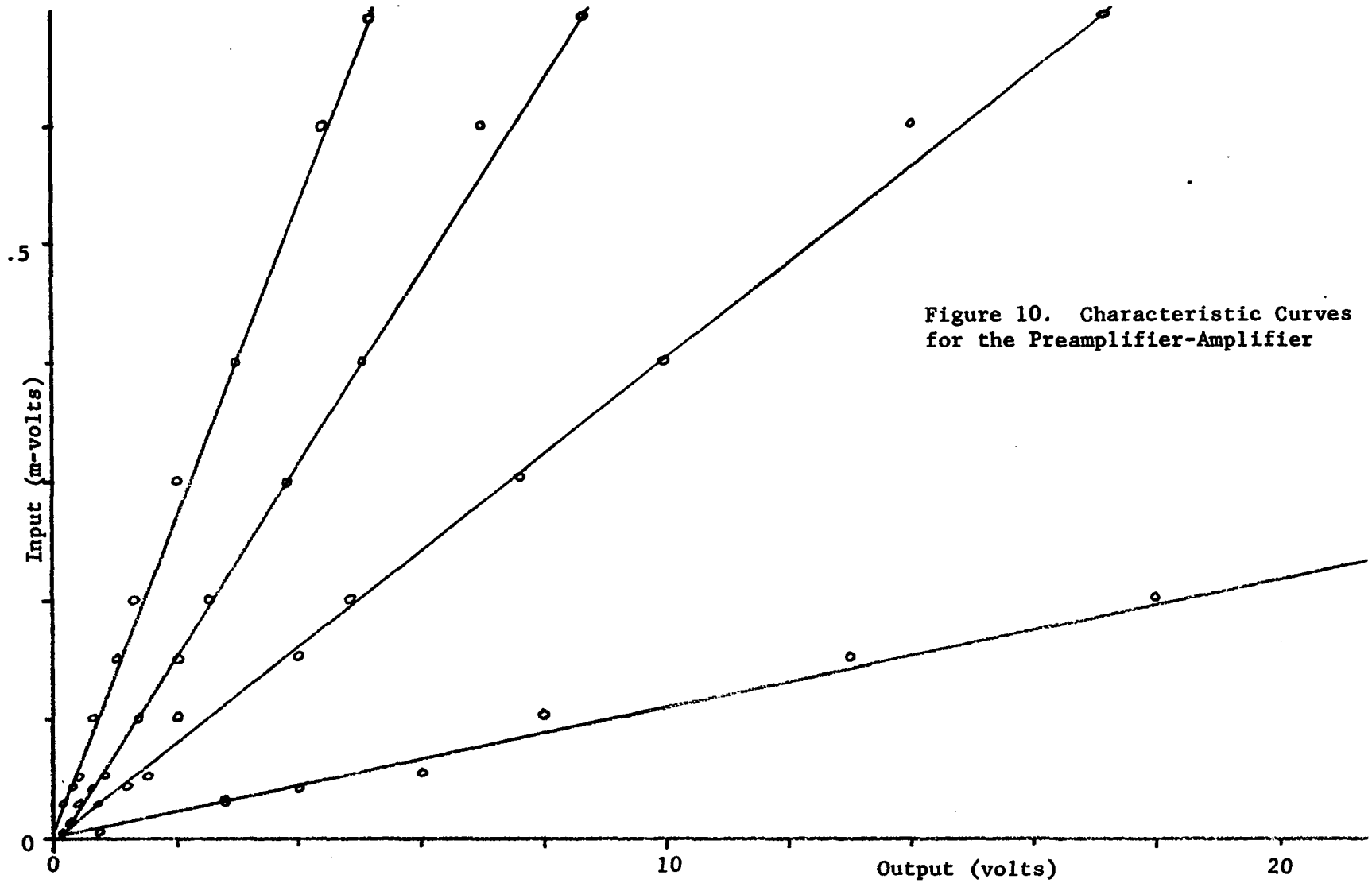

Figure 10. Characteristic Curves for the Preamplifier-Amplifier

TABLE 1.--Data used to plot characteristic curves of the pre-amplifier-amplifier system. (This tabulated data is used to obtain proper gain setting for searching and proper gain setting for line width measurements.)

Input (m volts)	Output in volts for each gain setting							
	1	2	3	4	5	6	7	8
0.001	.05	.09	.2	.75	1.2	2	3	5
.025	.15	.4	.7	2.2	5	7	11	18
.03	.175	.5	.75	2.8	5	8	12.5	20
.04	.28	.6	1.2	4	7	10	17	
.05	.35	.8	1.5	6	10	15	20	
.1	.6	1.4	2.5	8	15	25		
.15	1.0	2	4	13	20			
.2	1.3	2.5	4.8	18	30			
.3	2	3.8	7.6	22	35			
.4	3	5	10	30	42			
.6	4.4	7	14	40	75			
.72	5.3	9	17.7					
.8	6	10	20	50	100			
1	7.3	11.5	20	60				

Figure 11. Output potential versus microwave power input for 1N26 type detector #17

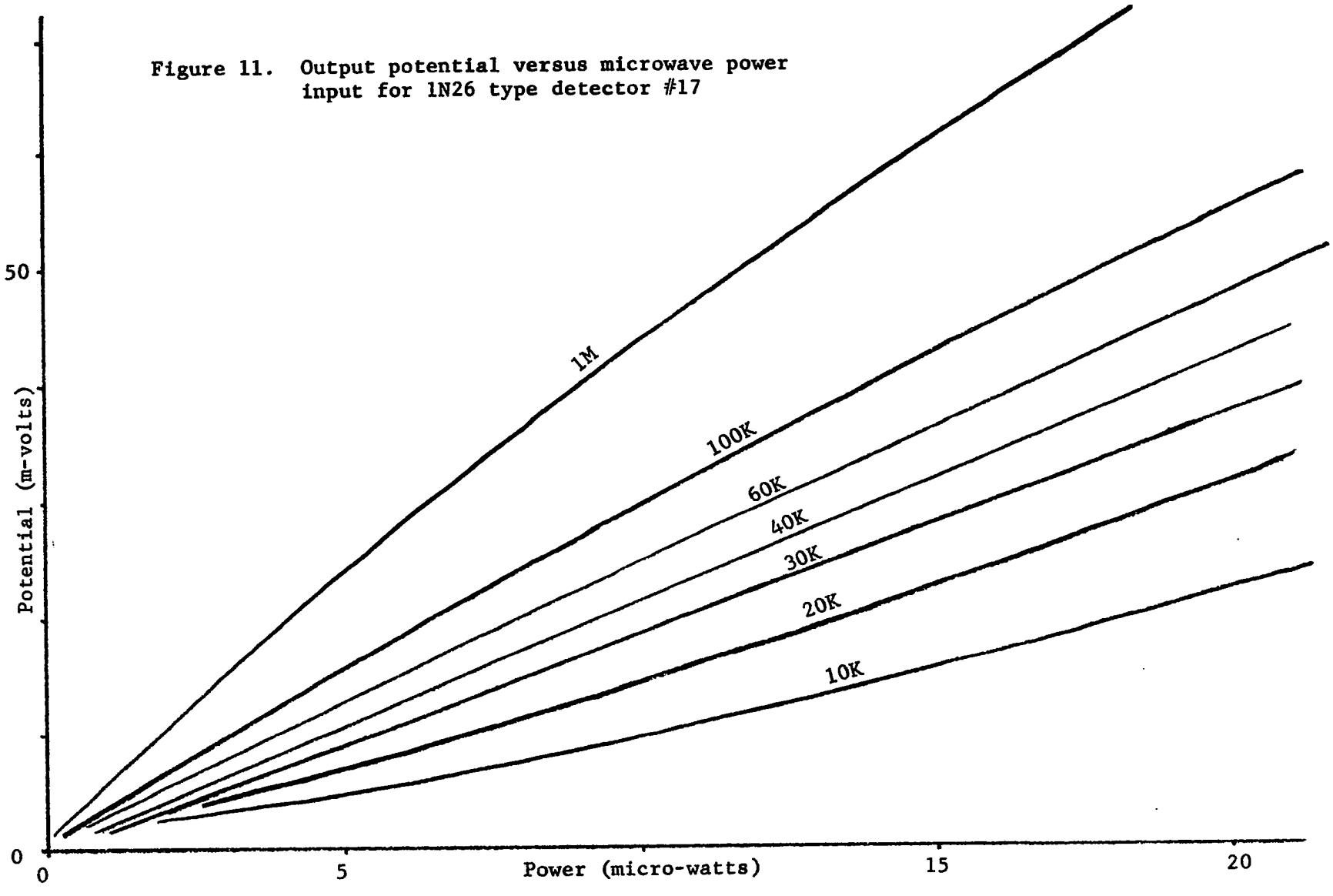

work such than when power requirements at the detector and signal input requirement to the amplifier could not be matched by adjustment of power to the detector, there remained a means of adjusting the signal input to the first stage of the amplifier. This attenuation network was needed for only a few of the very strong lines. Most of the lines investigated were sufficiently weak that the main problem was amplification and not attenuation.

It is believed that the amplifier developed surpasses any available on the commercial market for this specific application. The high gain and overall performance of the amplifier has made it possible to make line width investigations of many spectral lines heretofore not observable. By proper gain setting and adjustment of the input signal level the amplifier system produces no observable broadening of the spectral line display, thus producing a true reproduction of the line shape as seen by the detector diode.

CHAPTER IV

FREQUENCY MULTIPLIERS

In the course of this investigation it became necessary to use microwave radiation with frequencies which were higher than those ordinarily available directly from klystron sources. This frequency requirement led to the construction of a frequency multiplier which is capable of producing harmonics of a fundamental input frequency produced by the standard klystrons. The frequency multiplier was constructed in the general way, using a crossed waveguide arrangement. [6] The overall functioning of the frequency multiplier has been found to be quite good and spectral lines have been observed in excess of 78 kmc/sec using the output of a 35V10 OKI klystron as the fundamental source while detecting the second harmonic output of the frequency multiplier. The fourth harmonic output at a frequency of 85 kmc/sec has been observed while driving the frequency multiplier with a 20V10 OKI klystron.

The power requirements for operation of the frequency multiplier were adequately satisfied by these klystrons. Other klystrons, among these the EMI type R-9518 and Raytheon type 2K33, were used as drivers for the harmonic generator and these were found to work quite well at the second harmonic of the fundamental. Adequate power requirements to produce higher order harmonics of sufficient intensity were not satis-

fied, however, by the EMI and Raytheon klystrons available in the laboratory. A minimum power requirement of 25 milliwatts was needed to produce second harmonics of sufficient intensity to be usable in line width determinations. The power requirements for third and fourth harmonic generation were adequately satisfied by an input power of 165 milliwatts.

A detailed drawing of the frequency multiplier designed and constructed to produce the high frequencies required is shown in Figure 12. The harmonic output of the multiplier was filtered to eliminate any low order undesirable harmonics. Harmonics which were higher than those desired were eliminated by keeping low power input to the multiplier. When possible the second harmonic was utilized, since it had adequate intensity to stimulate transitions within the molecules even when the fourth harmonic was sufficiently weak to fail to appear in the spectrum.

When producing 70 kmc/sec radiation from a fundamental frequency of 35 kmc/sec the fourth harmonic occurs at 140 kmc/sec and may produce rotational transitions in the molecule being observed. For the detector used, IN53C, there should be poor detector response at 140 kmc/sec, unless the detector is an extremely good one. The IN53C type detectors are designed to rectify over a range extending from 60 to 90 kmc/sec. It is conceivable that these detectors can rectify at 105 kmc/sec, or at the third harmonic. The frequency multiplier is not designed to produce odd harmonics even though odd harmonics of the fundamental do occur in measurable intensity. By proper tuning the multiplier has produced sufficiently high power at the third harmonic of 19 kmc/sec

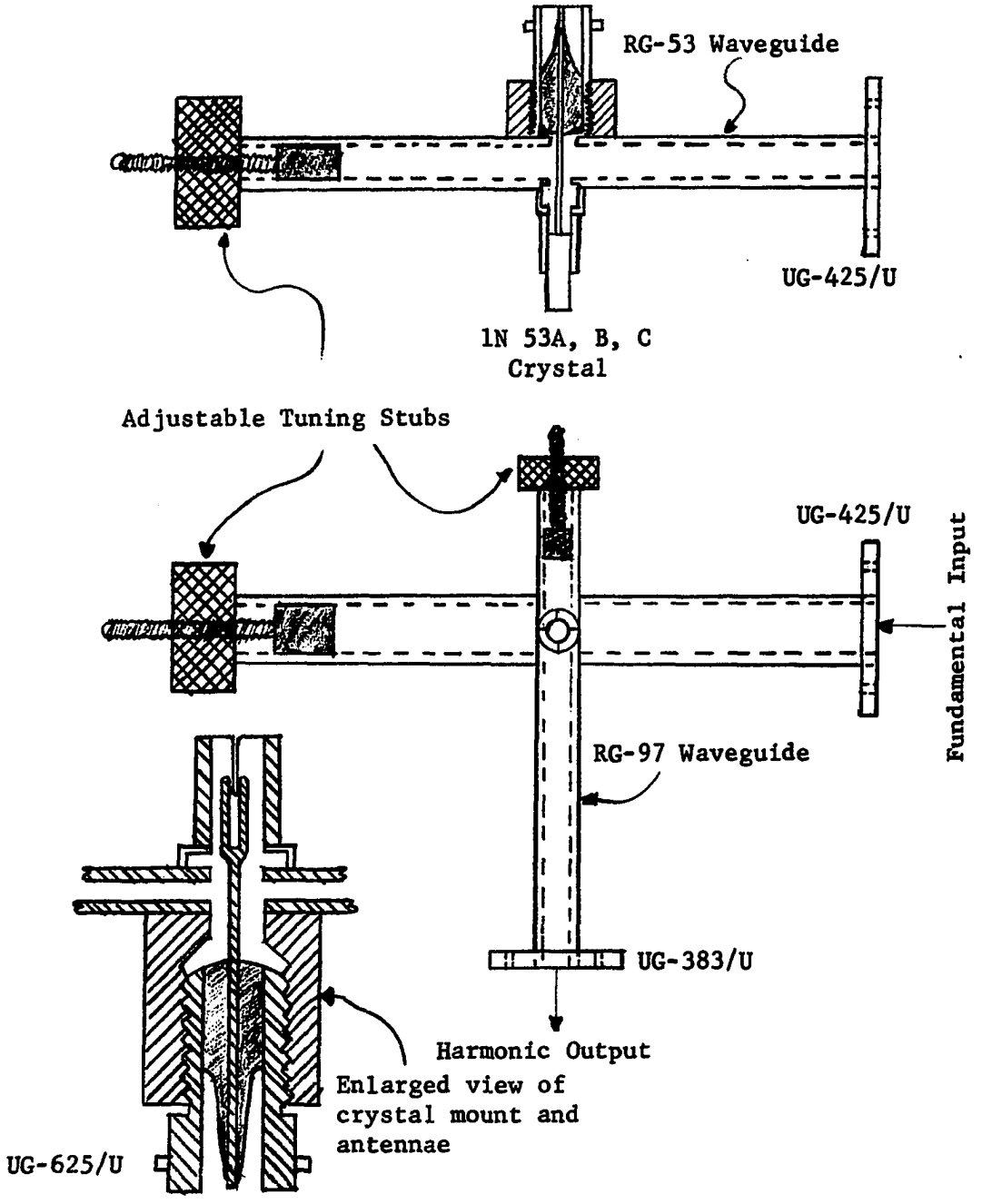

Figure 12. Design of the Frequency Multiplier for Generation of Harmonics From a Fundamental Source

source to be usable in making line width measurements. One must use extreme care in using the frequency multiplier to be assured that the harmonic being observed is the desired one. An effective method of determining the nature of the frequency spectrum output of the multiplier is the following. By using a detector with calibrated micrometer travel it is possible to determine approximately the wave length of the radiation output. Once the radiation wave length has been determined roughly, a wave meter and interpolation receiver can be used to determine the frequency of the output of the frequency multiplier. The magnitude of the power "dip" at the detector will give an indication of the amount of power occuring at the frequency monitored by the wave meter. Making checks with the micrometer travel and the wave meter it is possible to tune the frequency multiplier to enhance the desired harmonic. Once the desired harmonics are established at the output the process of measuring line widths can be begun. The following discussion indicates the importance of knowing the proper harmonic output of the frequency multiplier.

For rotational spectra of symmetric top molecules it is possible to produce and observe spectral lines which occur approximately at a frequency of 2B (J + 1) cps, whereJ ranges over integers 0, 1, 2 ... It can readily be seen that lines can appear at ν_0 , $2\nu_0$, $3\nu_0$ ..., where ν_0 is given by 2B. When a harmonic generator is used to generate harmonics from a fundamental source of frequency f a spectrum of f, 2f, 3f, ... appears at the output of the frequency multiplier. The frequency components in the spectrum may cause lines of higher J than the desired one to appear in the spectral display. However, the molecule

experiences centrifugal distortion dependent upon the quantum numbers, J and K, and these lines may not all overlap but may be shifted away from the frequencies predicted by the relation 2B (J + 1). Since centrifugal distortion increases with increasing J, this aids in making proper assignments for the origin of the spectral lines.

A spectral map of the absorption lines can be used to sort the spectral lines and make proper transition assignments for each line. It is very important to have available either a constructed graph of the spectral lines with proper frequency notation or a recorded spectral display with lines properly identified. From these displays it is possible to use relative intensity factors to help identify each line. Care must be used if the spectral display originates from transitions induced by harmonics at the output of the frequency multiplier, since lines produced by high order harmonics may occur and mix into the spectral display appearing to be high intensity components at the desired frequency being observed.

Intensity of the spectral lines depends upon the intensity of the stimulating radiation and it seems at first glance that the intensity of observed lines serves as a means of determining the origin of the transition. It must be recalled that spectral line intensities vary approximately as ν^3 and doubling of the frequency produces eight times the absorption for a given length cell. The tuning of the detector becomes more sensitive as frequency is increased such that a seemingly strong line may in reality arise from low intensity source radiation at a high harmonic of the fundamental. Due to proper tuning and the ν^3 effect this gives the appearance that the line originated

from a high power low harmonic of the radiation source. A detailed study of each spectral line will enable proper transition assignment for its origin.

Figure 13 shows a spectral display with rotational lines originating from the OCS molecule.

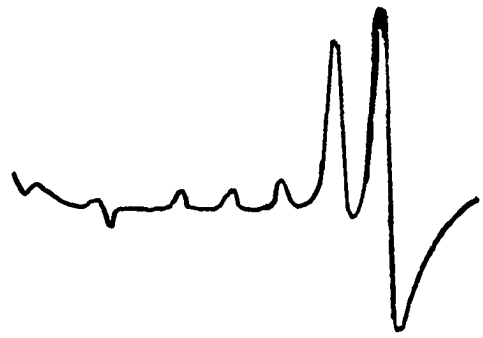

Figure 13. The 8th, 10th, 12th, 16th, 18th and 20th (from right to left) rotational lines of OCS obtained using the 4th to 10th harmonics of a 1.23 cm klystron. [7]

Relative intensity of these spectral lines should not be considered an indication of how to make proper transition assignments for the origin of the spectral lines. Here the importance of knowing what frequency components appear at the output of the frequency multiplier can be seen. The 8th and 10th spectral lines appear to be strong enough that they could both arise from branching of the same parent transition. It is not as difficult, in general, to identify transitions for linear molecules as it is for more complex molecules. The OCS molecular spectra have no fine structure that can cause confusion in the assignments

made to the lines shown in Figure 13.

Since an interpolation receiver is used to measure frequency spacing of the half-power points of the spectral lines it is possible, by making careful measurements of the frequency spacings between the lines, to "map" the spectral display by changing the klystron frequency and carefully measuring the frequency of each spectral line as it appears on the display. Once frequency spacing and relative intensity measurements have been determined the spectral map can be used with confidence.

A spectral display of the rotational spectral lines arising from the transitions $\Delta J = 1 \rightarrow 2$ in the CH_3Cl molecule is shown in Figure 14. The lines in this display have been properly identified both by calculation and by experimental observation. The modulation amplitude used in obtaining these lines produced indication that only 11 lines appear in the display. Line 7 in the display is a double line arising from $\Delta J = 1 \rightarrow 2$, $K = 0$, $\Delta F = 5/2 \rightarrow 7/2$ and $\Delta J = 1 \rightarrow 2$, $K = 0$, $\Delta F = 3/2 \rightarrow 5/2$. Another double line which is too weak to be seen in this display occurs between lines 6 and 7. These two lines arise from the transitions $\Delta J = 1 \rightarrow 2$, $K = 1$, $\Delta F = 5/2 \rightarrow 3/2$, and $\Delta J = 1 \rightarrow 2$, $K = 1$, $\Delta F = 3/2 \rightarrow 1/2$. The remaining allowed transition for this set is $\Delta J = 1 \rightarrow 2$, $K = 1$, $\Delta F = 3/2 \rightarrow 1/2$. This line is not shown as it appears outside the sweep range of this display and is hardly visible for the modulation amplitude used. The intensity of this line increases as the modulation amplitude is increased.

There is another weak line between lines 5 and 6 which is not seen until the modulation amplitude is increased sufficiently high to

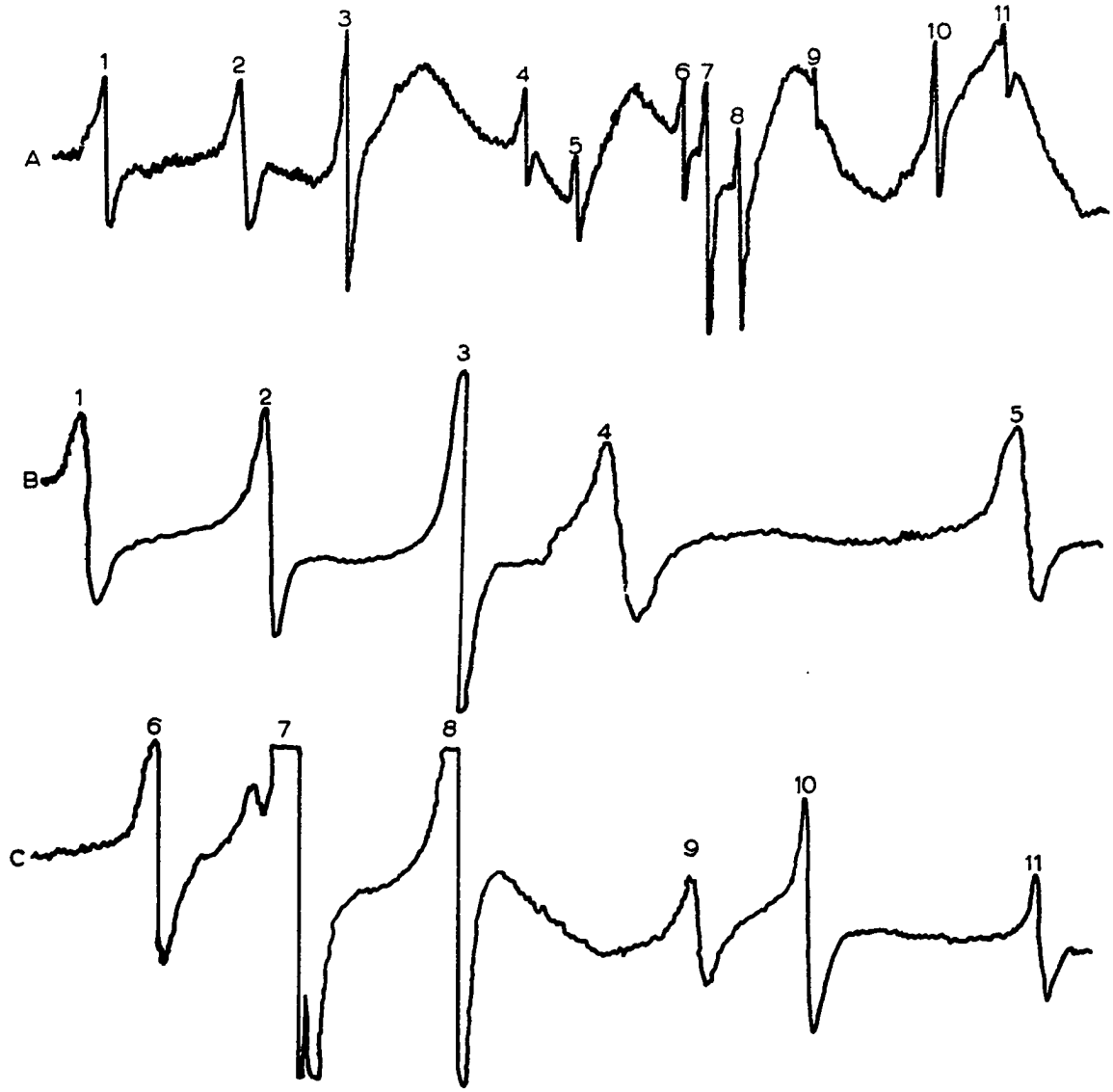

Figure 14. Two frequency traces of the $\Delta J = 1 \rightarrow 2$ transition of the CH_3Cl^{35} molecule. (B and C make an expanded frequency scan of A)

distort the background display. Increasing the modulation to this level distorted much of the spectrum shown. The effect of varying the modulation amplitude is shown in Figure 15. The components of Figures 14 and 15 are identified in Table II.

The observed frequencies do not agree with the first order calculated frequencies. This was expected since the spectrograph used is not primarily designed for absolute frequency measurements, but is designed to make relative frequency measurements. Since these lines were observed using the third harmonic from a 20V10 OKI klystron, there appears to be large error in the absolute frequency measurements. This error is within the frequency measuring ability of the spectrograph. There is very good agreement, however, between the calculated frequency spacing of the spectral lines and the observed frequency spacing for the set of lines given.

A compromise of adjustment between modulation amplitude and power supplied to the absorption cell may be made to shift the standing wave pattern along the frequency region being investigated. Various procedures can be used to eliminate the standing waves or to shift the standing waves along the frequency axis. Over some frequency ranges isolators have been found effective in reducing standing waves. There seems to be no general means or method of eliminating standing waves at all frequencies. A method that works very well at 30-40 kmc/sec can prove to be totally ineffective at 50-60 kmc/sec. The most effective procedure is to try all of the possible remedies and choose the most effective one for the frequency range being investigated.

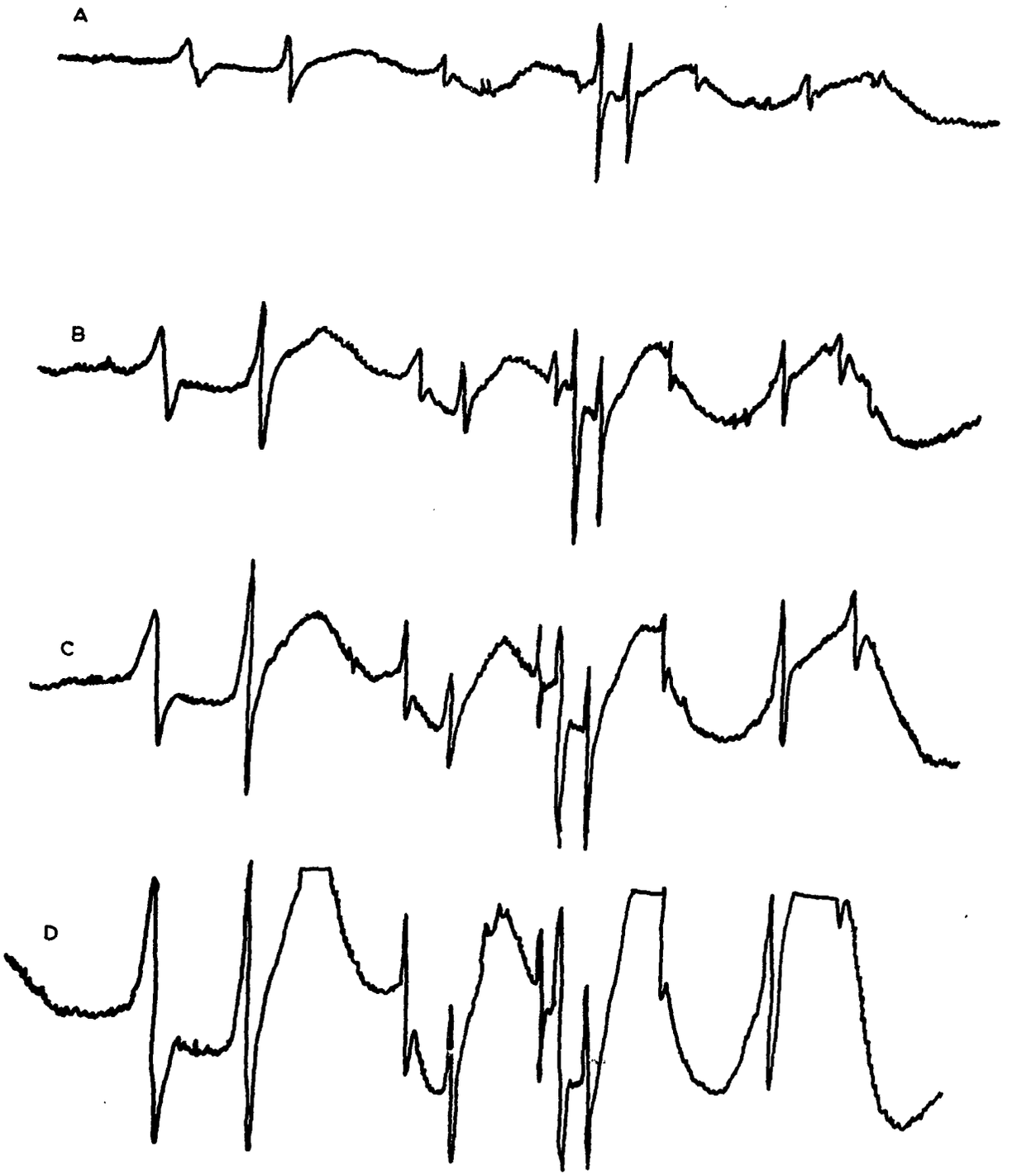

Figure 15. Effect of varying modulation amplitude. (A. ω' = 10 kc/sec B. ω' = 20 kc/sec C. ω' = 80 kc/sec D. ω' = 120 kc/sec) P = 8 microns; $\Delta\nu \sim 185$ kc/sec

TABLE 2.--Identification of components of the spectral display in Figure 14. All spectral lines arise from $\Delta J = 1 \rightarrow 2$ and the transitions tabulated.

Number of Line	ΔF	K	Calculated Frequency (Mc/sec)	Observed Frequency (Mc/sec)
1	1/2→3/2	0	53,152.12	53,152.61
2	5/2→5/2	0	53,153.74	53,153.20
3	3/2→5/2	1	53,155.85	53,156.82
4	3/2→3/2	1	53,162.58	53,163.18
5	5/2→5/2	1	53,165.27	53,166.84
6	1/2→1/2	0	53,170.96	53,171.73
7	5/2→7/2	0	53,172.57	53,173.31
	3/2→5/2	0	53,172.57	53,173.31
8	5/2→7/2	1	53,174.68	53,175.54
9	1/2→3/2	1	53,179.53	53,180.43
10	3/2→3/2	0	53,186.02	53,186.71
11	1/2→1/2	1	53,188.94	53,188.44

CHAPTER V

DETERMINATION OF LINE WIDTHS OF SPECTRAL LINES WHICH ARE NEAR OTHER SPECTRAL LINES

Many spectral lines are found to overlap with nearby spectral lines. A problem arises in determining the line width parameter for these lines since their shape is distorted by the nearby lines. A method has been worked out which enables spectral lines of this type to be measured and the true line width determined for them. Lines for which intensity and frequency spacing values are known can be treated mathematically and the line width determined. This can be done in the following way.

The assumptions are made that all of the overlapping spectral lines are of Lorentzian shape, have the same half-width, $\Delta\nu$, before distortion and that the envelope being measured is the resultant of the addition of these spectral lines. An equation for the lines may be written as f(x), where f(x) is composed of the number of line shape functions which make up the set being observed. If the respective line intensities are I_j and the frequency spacings are a_j then the equation for the composite spectra can be written as

$$\alpha = \sum_{j=1}^{n} I_j \left[(\nu - \nu_o + a_j)^2 + (\Delta\nu)^2 \right]^{-1} \equiv f(x) \qquad \text{(V-1)}$$

Points of steepest slope for the function are given by f'(x), where a prime dentoes the derivative of f(x) with respect to the frequency. The frequency spacing between these points is measured. The measured spacing for composite lines is not a true representation of the points of steepest slope for a single line. In order to determine this spacing, it is necessary to determine the critical points of f'(x) and determine where the single line to be measured has critical points. The roots of the equation $f''(x) \equiv 0$ gives the set of critical points.

For convenience in handling the equation $f''(x) \equiv 0$, the substitution $x \equiv \nu - \nu_0$, which is the difference between klystron frequency and a rather arbitrarily chosen "center" frequency for the system of lines, is made. The equation of f(x) is then

$$f(x) = \sum_{j=1}^{n} I_j \left[(x + a_j)^2 + (\Delta\nu)^2 \right]^{-1} \qquad \text{(V-2)}$$

and f''(x) is given by

$$f''(x) = \sum_{j=1}^{n} I_j \left(\frac{(\Delta\nu)^2 - 3(x - a_j)^2}{\left[(\Delta\nu)^2 + (x - a_j)^2 \right]^3} \right) \equiv 0 \qquad \text{(V-3)}$$

A group of spectral lines which have special interest, and for which Equation (V-1) has ready application, is the group of lines in the NH_3 inversion spectrum for which K = 1. Because of the interaction of the hydrogen nuclear spins with the magnetic field arising due to the rotation of the molecule, the K degeneracy of the energy levels is lifted and a splitting of the energy levels ensues. The hyperfine

structure of the inversion lines of NH_3 with K = 1 has been discussed by Gunther-Mohr et al. [8] Some of the lines for which K = 1 have been treated here to give a solution for the problem since it cannot be solved readily by reducing the pressure until the spectral lines can be resolved.

For various values of $\Delta\nu$, this equation was solved for x, by the computer, for parameters I_j and a_j corresponding to each of the (4,1), (3,1), (2,1) and (1,1) spectral lines. The results were tabulated and used to construct the correction curves for these spectral lines.

From this set of curves and the knowledge of relative position and intensities of the line for which the width is desired, it is possible to locate the theoretical position of the points of steepest slope for a single line. Once these theoretical points have been obtained, they can be related to the observed spacing by means of correction curves produced from the mathematical analysis of the problem. Correction curves determined in this way for the (4,1), (3,1), (2,1) and (1,1) inversion lines of the ammonia molecule are given in Figure 16. These curves can be used to determine the true line width data from observed line width data. From these curves correction terms for the (4,1) and (3,1) inversion lines of ammonia have been obtained. The corrected and raw data curves are plotted in Figure 17 and Figure 18.

From the plot of the (4,1) line data it can be seen that the points below 10 microns of pressure do not fall in line with those points which lie above 10 microns of pressure. After careful analysis of the data for this spectral line, it was determined that the reason

for this is the following. The magnitude of the magnetic interaction between J and I produces a splitting of the main line into two components which are spaced about 120 kc/s apart. This spacing was not considered in keeping the magnitude of the modulation signal at a proper level. The requirement for modulation amplitude is that ω'; the modulation, be kept such that $\omega' \leq \frac{1}{2}\Delta\nu$. [9] This condition was not properly satisfied until the line width observed was 263 kc/sec at a pressure of 13.20 microns. Here the modulation was only 69 kc/sec, which was sufficiently small to allow proper application of the correction formula given in reference 9. In a separate investigation the effect of varying modulation amplitude for this line width region for the (4,1) ammonia line was made. Observed line widths were kept below 300 kc/s and the modulation amplitude varied for each pressure setting. Line widths determined in this way varied for each pressure setting as shown in Figures 17 and 18. Line widths determined in this way varied from 198 kc/s to 175 kc/s as the modulation was varied from 112 kc/s to 30 kc/s. It was concluded that the correction curves may be applied to the line width data providing ω' is kept such that $\omega' \leq \frac{1}{2}\Delta\nu$ of a single component of the complex spectra and when the components of the spectra are not distinguishable as single lines, i.e. the wings of the lines must be sufficiently overlapped to produce shift in the points of steepest slope for the line being measured. From the correction curve for the (4,1) ammonia spectral line it can be seen that the correction curve is quite steep at 200 kc/s. The corrections become doubtful for line widths less than this value. It is obvious that observations are being made on points of steepest slope

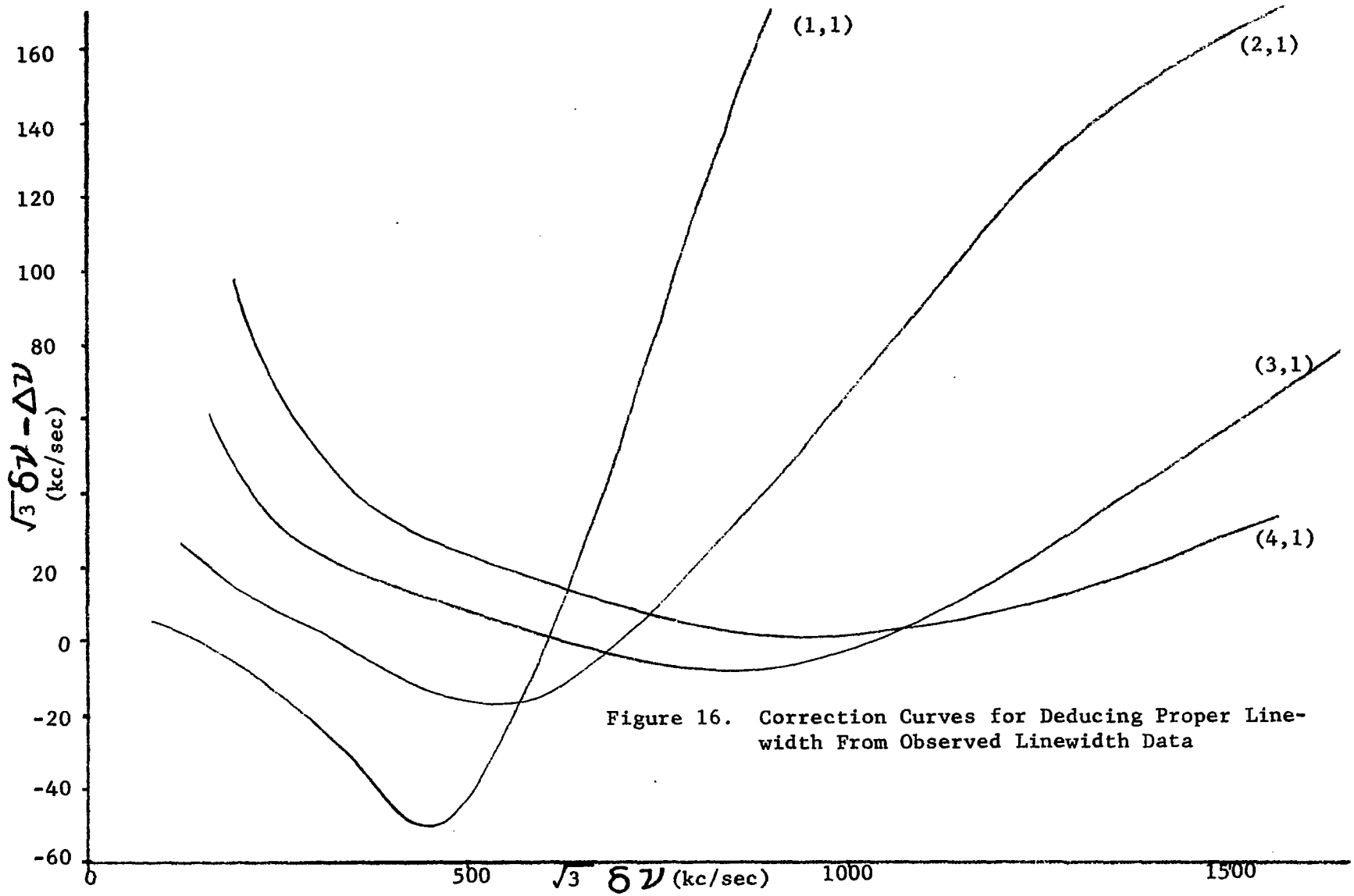

Figure 16. Correction Curves for Deducing Proper Linewidth From Observed Linewidth Data

Figure 17. Linewidth Parameter for the (3,1) Inversion Line of NH_3

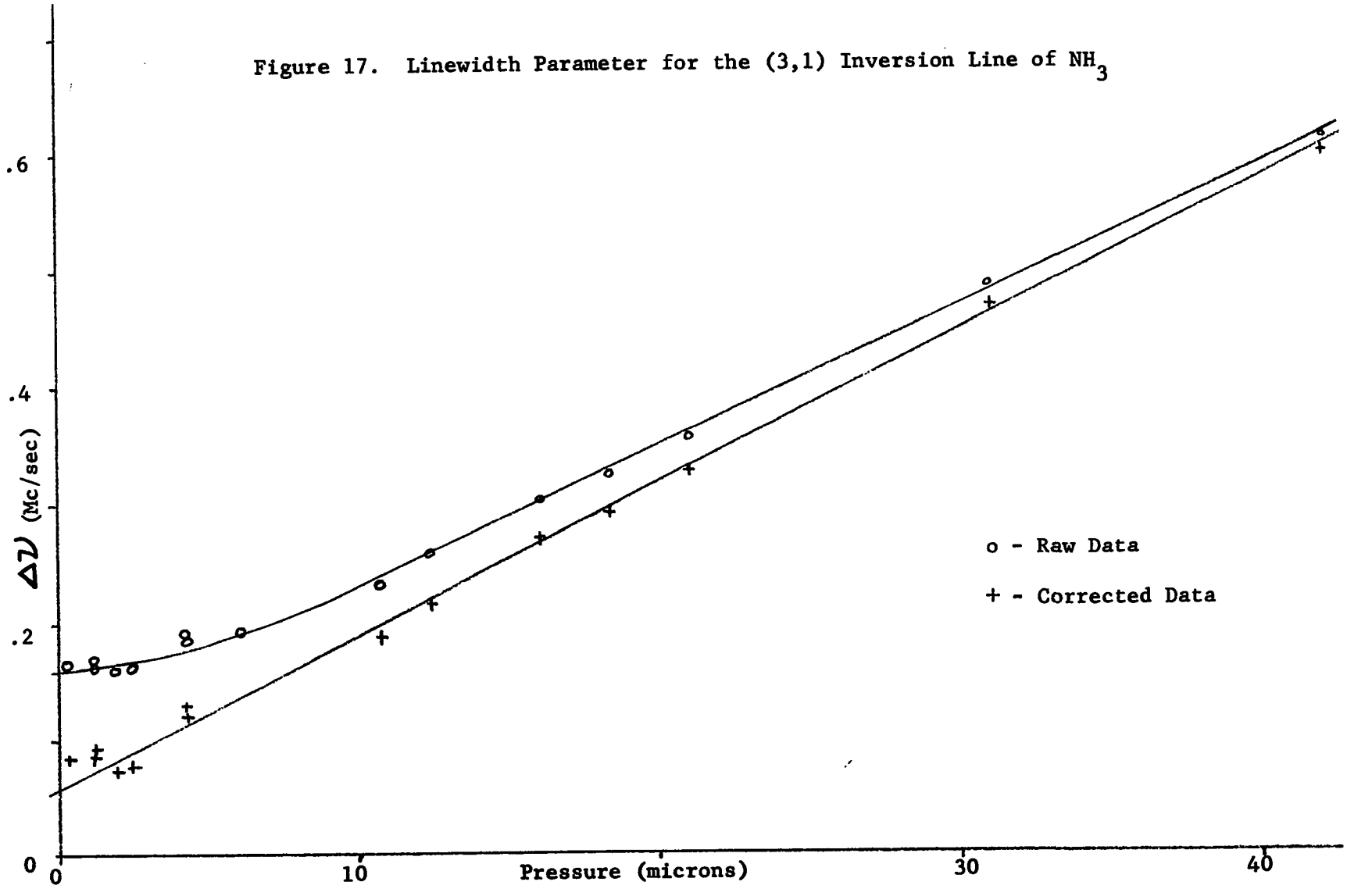

Figure 18. Linewidth Parameter for (4,1) Inversion Line of NH_3

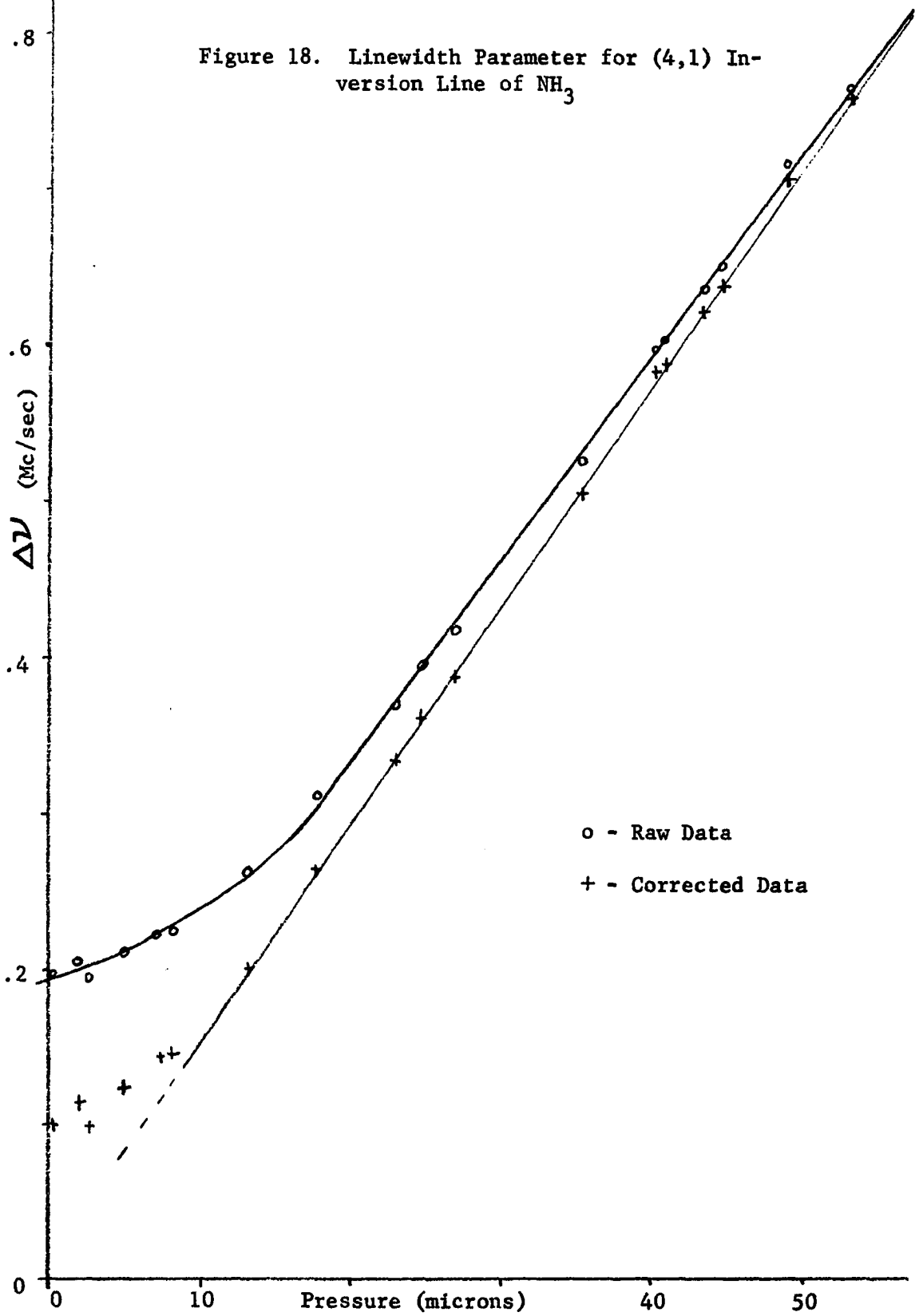

for the outside frequencies of two lines which are not interacting. There will be a fixed spacing between these two lines for any lower pressure after the line width has dropped appreciably below 200 kc/s. This curve will approach a fixed value of 120 kc/s in an asymptotic manner. This merely says that as the line widths of the two lines approach zero the correction procedure for observed line width is to subtract the frequency spacing between the two lines from the frequency observed.

Figure 19 shows a drawing of the progression of the correction term as the pressure of the gas is decreased within the absorption cell.

Sketch (e) of Figure 19 represents the condition when the two lines have become well defined and the correction value for the raw data has become constant.

In the cases listed above, two overlapping lines have been considered in each case except the (1,1) line. It is possible in many cases to have several spectral lines which overlap and influence each other. The (1,1) inversion line of ammonia is an extreme case of overlapping spectral lines and is very complex since there exists four quadrupole satellites which lie near the main line and each of these lines have splitting due to a magnetic interaction of the hydrogen spins with the angular momentum vector. The spectra therefore possess 10 lines which must be considered. In this case Equation (V-1) will have ten terms to be taken into consideration. The corrected slope parameter and raw data for the (1,1) inversion line of ammonia is shown in Figure 20.

As each spectral line is broadened to a very large width the

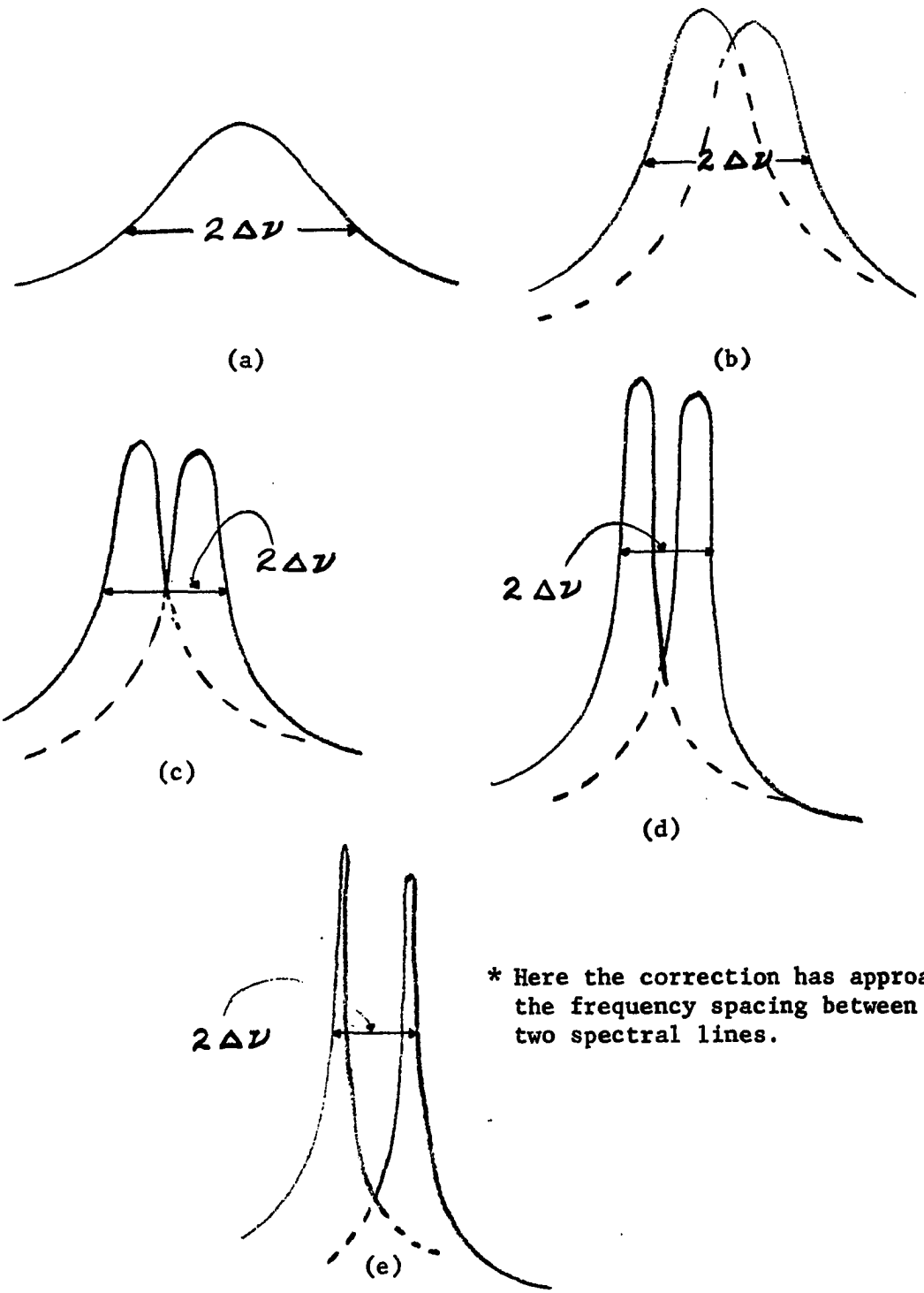

* Here the correction has approached the frequency spacing between the two spectral lines.

Figure 19. Sketches Showing the Progression of Correction Terms for Overlapping Spectral Lines

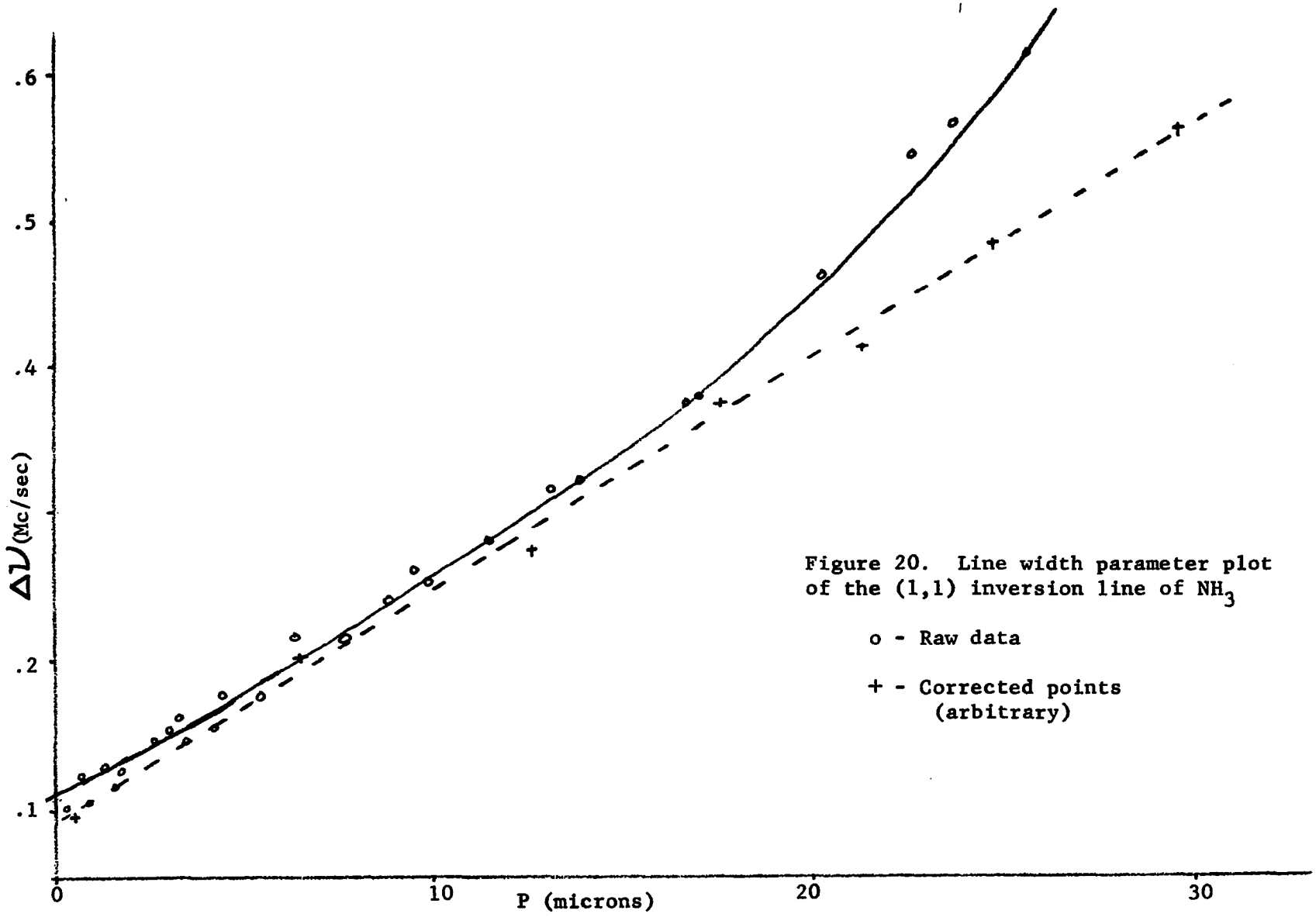

Figure 20. Line width parameter plot of the (1,1) inversion line of NH_3

o - Raw data

+ - Corrected points (arbitrary)

overlapping lines appear as a single line as shown in sketch (a) of Figure 19. When the line has sufficient width the double line may be treated as a single line. The correction curve for the (2,1) spectral line of Figure 16 shows the trend of the correction for widths sufficiently high that the lines lose their identity. The correction term becomes a constant at very high line width values. The line width may then be treated as though measurements are being made on a single, non-distorted spectral line.

Another problem encountered in connection with overlapping spectral lines in an extension of the one above. For many spectral lines there is no overlap at low pressures but as the pressure is increased, broadening the lines, the condition of overlapping spectral lines prevails. This condition has been encountered in the inversion spectra of ammonia because of quadrupole satellites and is a problem for all lines for which $J<7$.

Correction curves have been worked out by means of a computer to correct for the distortion of line shape, hence line width, in the ammonia inversion spectra when lines due to quadrupole interaction are present. The problem is solved by the same procedure as described previously. Here the frequency spacings and line intensities vary more than for the previous cases. The frequency spacings and relative intensities of the quadrupole satellites compared to the main line are well known for the inversion spectra of ammonia and it is possible to make a mathematical analysis of the line width problem for a given line. These results have been worked out and correction curves plotted for the (2,2), (3,3), (4,4) and (7,7) inversion lines of ammonia. Correction

curves for these spectral lines are shown in Figure 21.

Correction terms have been applied to the (2,2) inversion line of ammonia from the correction curve and the results plotted in Figure 23. The validity of the correction terms rested upon the assumption that a true behavior for line width versus pressure for this molecular spectra should describe a straight line. The uncorrected data, as can be seen in Figure 22, did not describe a straight line. The (2,2) spectral line was chosen for analysis because the correction terms became large for reasonably narrow line widths. Because of the modulation scheme used, it was necessary to restrict line widths to less than two megacycles per second. The restriction arose because for larger line widths the standing wave problem was encountered.

When standing waves are present they must be treated with care and line width determinations obtained when they are present should not be taken as conclusive. [10] Standing waves produce the same effect on observed spectral lines as do other spectral lines which are near the observed line. The standing wave problem cannot be solved mathematically since the shape of the standing wave is not well defined; hence, it cannot be given a functional shape. The only solution is to eliminate the standing waves entirely or reduce their amplitude to an insignificant value relative to the spectral line being observed.

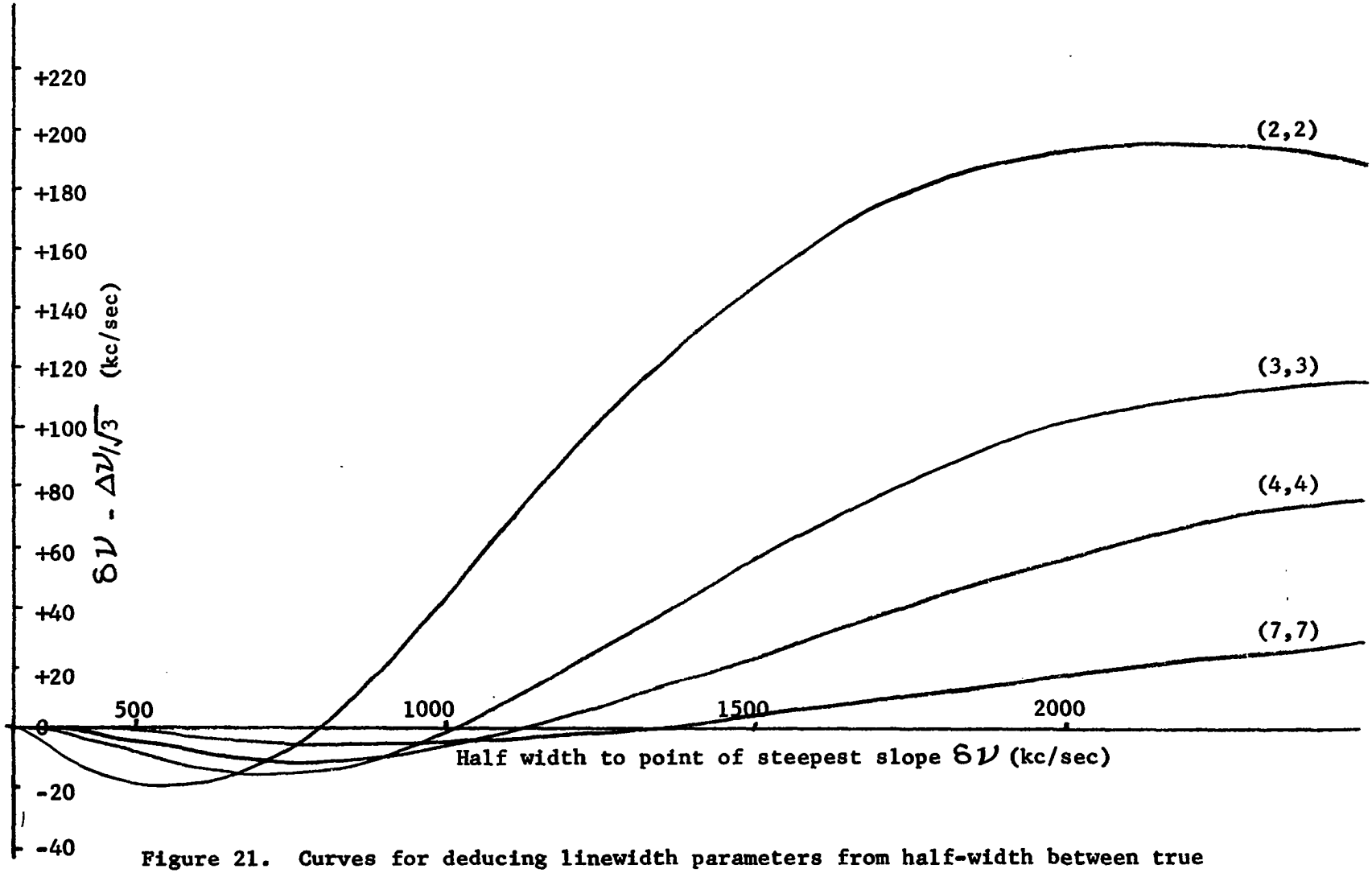

Figure 21. Curves for deducing linewidth parameters from half-width between true points of steepest slope

Figure 22. Linewidth Parameter of the (2,2) Inversion Line of NH_3 (No Correction)

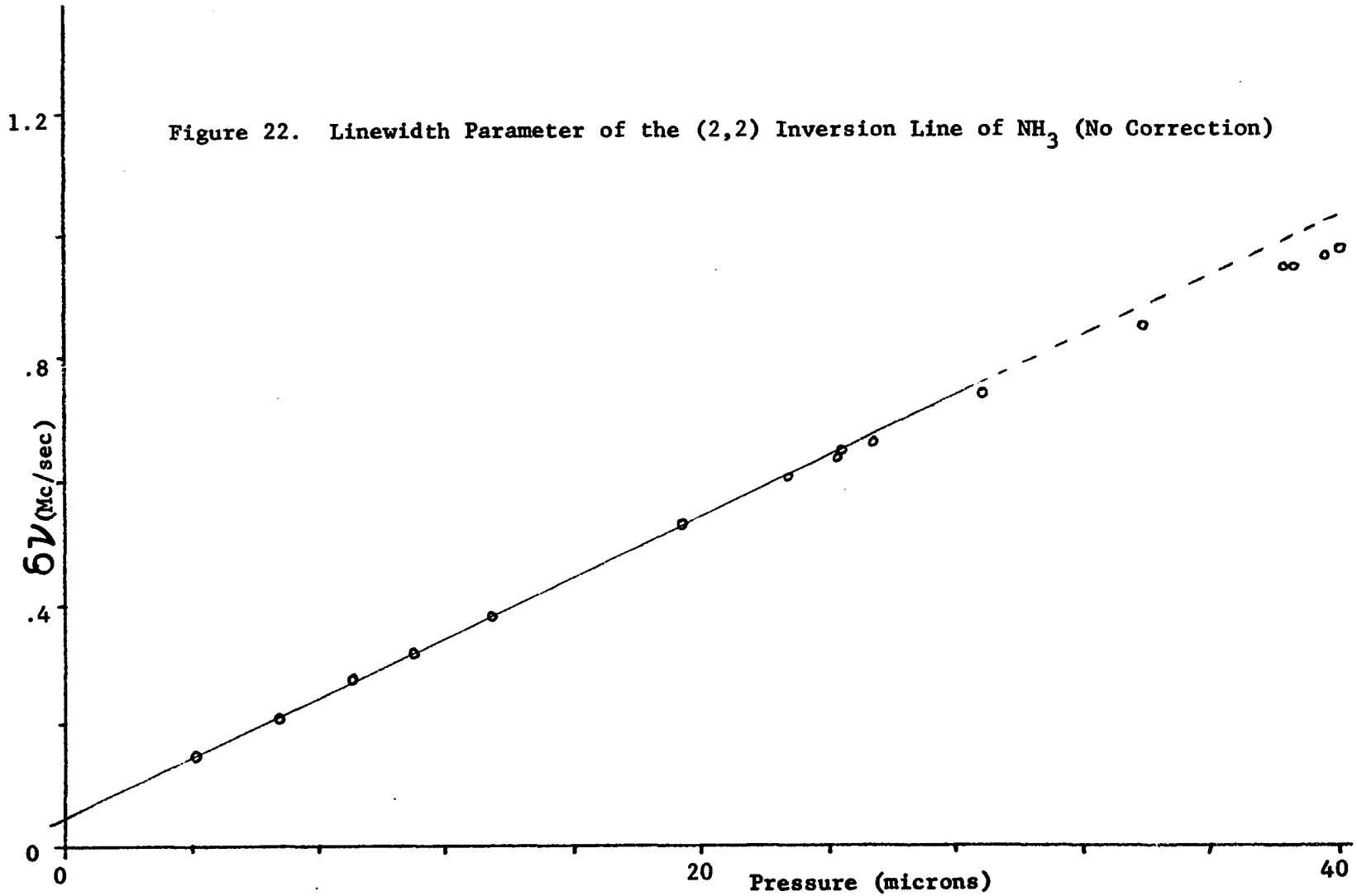

Figure 23. Linewidth Parameter of the (2,2) Inversion Line With Quadrupole Correction Terms Applied

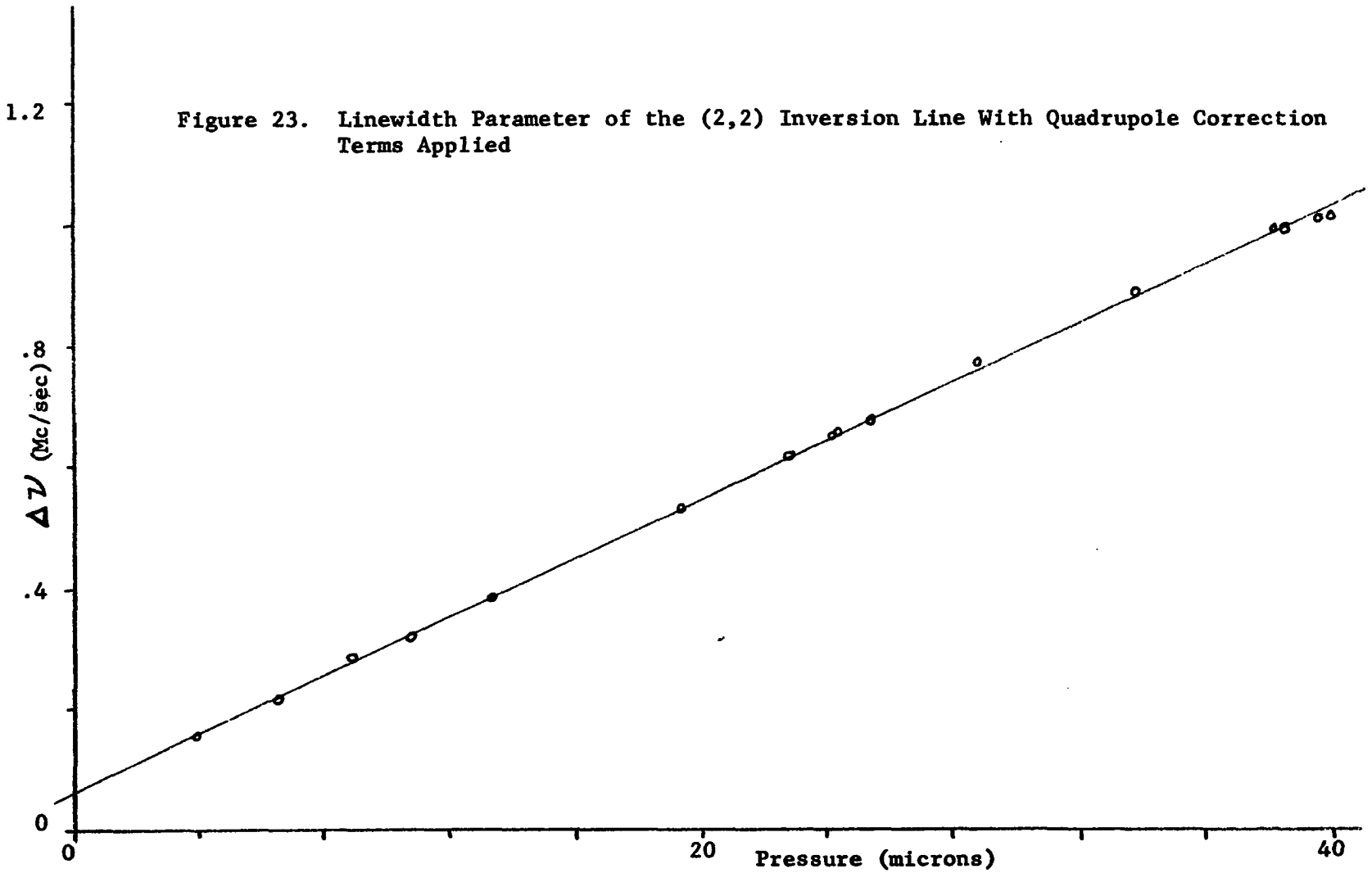

CHAPTER VI

DOPPLER BROADENING OF MICROWAVE SPECTRAL LINES

The doppler effect occurs when a molecule is moving parallel to the direction of propagation of the radiation being absorbed. There is an apparent shift in the radiation frequency, as seen by the moving molecule, given by

$$\delta\nu = \pm \nu (v/v_p) \qquad \text{(VI-1)}$$

Doppler broadening does not become dominant until the pressure of the gas in the absorption cell is reduced to a small value. Then the molecules are able to travel more freely; hence, they describe longer paths (before they experience collisions with one another) as compared to the paths that they travel at high pressures. At high pressures the doppler broadening contribution to the line width approaches a constant value which is usually small when compared to other types of broadening.

For very low pressures broadening of the spectral line due to the doppler effect becomes the dominant width factor. This contribution to line width must be considered if accurate line width determinations are to be made for a given spectral line.

The relationship between line width and mean time between collisions, τ, for a molecular aggregate is given by the following equa-

tion

$$\tau = \left[2\pi\sqrt{3}\,\delta\nu\right]^{-1} \qquad \text{(VI-2)}$$

Over a large range of pressures there exists a linear relationship between $\Delta\nu$ and the pressure, P. From accurate measurements of $\Delta\nu$ and P it is possible to deduce a relationship between the mean time between collisions and the number density of molecules in the absorption cell. With this relationship and the equation for collision cross sections, $\sigma = 2\pi\delta\nu / Nv$, it is possible to deduce an effective cross section for the collision processes taking place in the molecular aggregate.

In general, it is possible to write the overall line width contribution in the following way

$$\Delta\nu = \Delta\nu_1 + \Delta\nu_2 + \Delta\nu_3 + \ldots = \sum_i \Delta\nu_i \qquad \text{(VI-3)}$$

where each $\Delta\nu_i$ is an effective line width associated with each process to be considered in the line broadening scheme. This equation may also be written as

$$\sigma = \sigma_1 + \sigma_2 + \sigma_3 + \ldots = \sum_i \sigma_i \qquad \text{(VI-4)}$$

Here each σ_i is related to a partial line width contribution arising from the respective interaction processes. Some of these factors produce constant contributions to the line width and need not be considered in determining the line width parameter for a given line, since they serve merely to translate the $\Delta\nu$ versus P graph without altering its slope. When all of the broadening effects are considered

it is found that doppler and pressure broadening do not remain constant but interact with each other and produce line distortion of varying degrees over a reasonable pressure range; producing greatest line distortion at low pressures.

A correction method has been worked out to compensate for the line width error due to doppler broadening. This was done in the following way.

The symbol, x, denotes the direction of propagation of radiation of frequency ν_o. If molecules are within the absorption cell some will have velocities of $\pm V_x$. These molecules moving with a velocity V_x will "see" a radiation source of frequency

$$\nu' = \nu(1 \pm V_x/c) \qquad \text{(VI-5)}$$

Assuming a Maxwellian distribution for the molecules in the system, the following equation can be written for the number of molecules per unit volume having a velocity V_x.

$$\delta N_{V_x} = N[m/(2\pi kT)]^{\frac{1}{2}} [\exp(-\tfrac{1}{2}mV_x^2/kT)] \delta V_x \qquad \text{(VI-6)}$$

The contribution that they make to the power absorption coefficient α is given from the Van Vleck-Weisskopf equation as [11]

$$\delta \alpha = 8\pi^2 f |\mu_{ij}|^2 \nu'^2/(3ckT) \left\{ [(\nu' - \nu_o)^2 + (\Delta\nu)^2]^{-1} + [(\nu' + \nu_o)^2 + (\Delta\nu)^2]^{-1} \right\} \delta N_{V_x} \Delta\nu \qquad \text{(VI-7)}$$

with the line shape profile obtained by integrating Equation (VI-7) to obtain the total contribution of all these elements to the line shape.

where: $\Delta\nu = 1/(2\pi\tau_1)$ is the line width parameter.

ν_o = frequency of molecular transition induced.

μ_{ij} = matrix element for this transition.

f = fraction of molecules in the lower of the two transitions.

For microwave transitions observed at low pressure, the approximation holds that $\nu_o \ll \Delta\nu$. Thus, it is possible to neglect the second terms in the brackets in Equation (VI-7). Then combining Equations (VI-5), (VI-6), and (VI-7) produce an equation for the approximate line shape as

$$\alpha(\nu) = A(T)N(\Delta\nu)\int_0^\infty \frac{\exp\left[-\beta(\nu-\nu')^2\right]}{(\nu'-\nu_o)^2 + (\Delta\nu)^2}\, d\nu' \qquad \text{(VI-8)}$$

where the constants A(T), characteristic of the gas for given temperatures, and $\beta = mc^2(2kT\nu_o^2)^{-1}$ have been introduced for convenience.

Values of $\alpha(\nu)$ have been calculated from Equation (VI-8) and plotted, see Figure 24, as a function of ν for a proper molecular transition of ν_o = 25 Gc/sec. This line-shape profile was calculated for ammonia at a temperature of 26°C. To make a comparison between the true line shape and the distorted line shape, the corresponding line of Lorentzian shape is plotted, after proper normalization, so that the peaks of the two lines coincide. Examination of the two curves indicates that all line width determinations made at low pressures will yield larger line width values than should be observed.

Line widths are not measured directly in the scheme employed in this work but each line width is determined by determining the fre-

Figure 24. Line Profile for Doppler and Non-Doppler Broadened Spectral Line of Lorentzian Shape

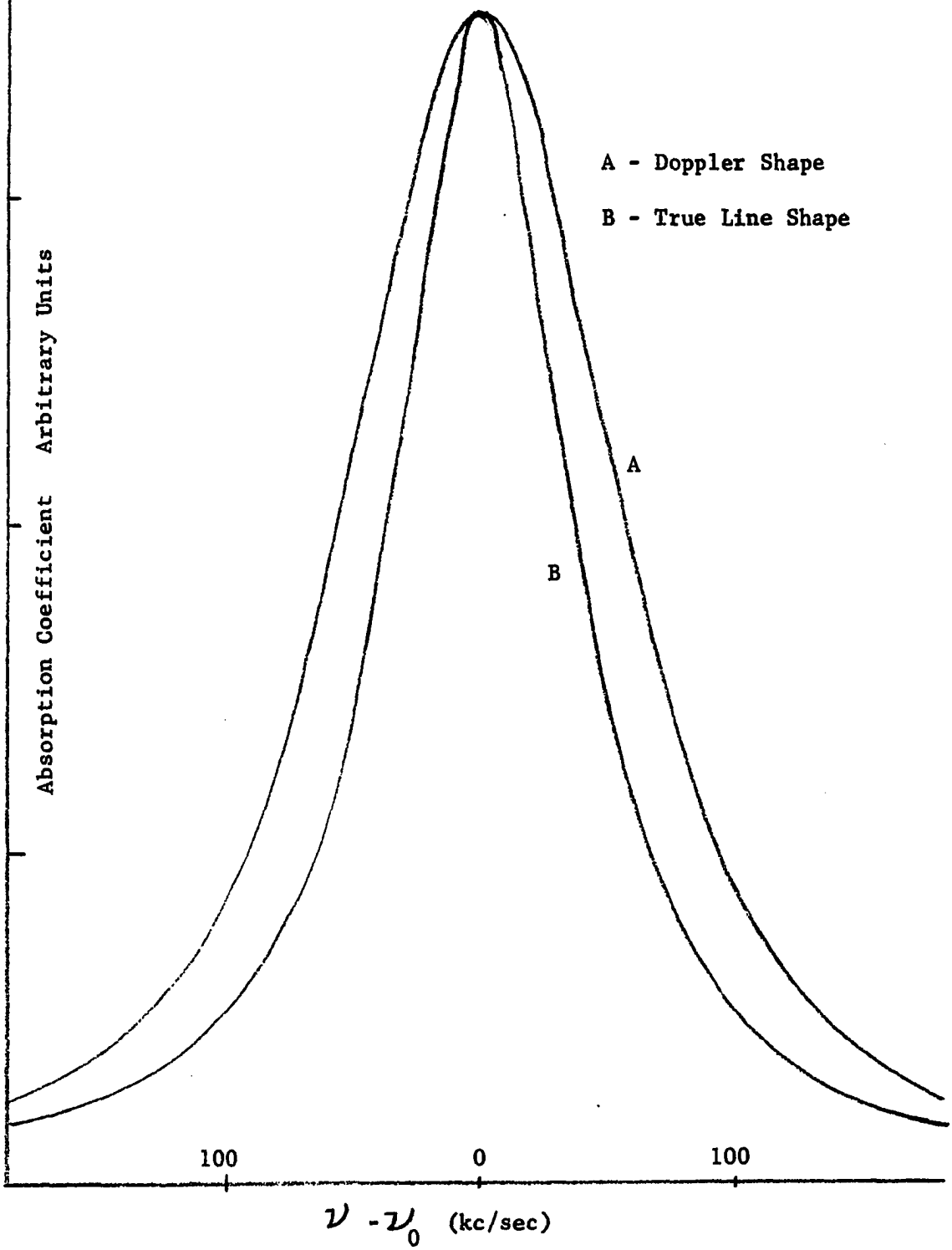

quency spacing between points of steepest slope for the line. This frequency spacing is related to the half-power points approximately by the following equation

$$\Delta\nu = \delta\nu\sqrt{3}\left[\ 1 + 1/3\ (\omega'/\Delta\nu)^2\right]^{-1} \qquad \text{(VI-9)}$$

In order to obtain points of steepest slope the line shape is differentiated by means of a square-wave modulation signal applied to the repeller electrode of the reflex klystron. Then the points of zero slope for the differentiated line shape are measured using frequency markers. When the pressure is very low, Equation (VI-8) describes the line shape. The points of steepest slope for this line are given from the derivative of this function by solving the following equation.

$$\alpha'(\nu) = \int \frac{(1 - \beta x^2)\exp(-\beta x^2)}{(\nu - \nu_o - x)^2 + (\Delta\nu)^2}\,dx = 0 \qquad \text{(VI-10)}$$

In order to correct for the doppler error in line width determination, a set of correction curves has been worked out using a computer program to solve Equation (VI-10). These correction curves for 15, 20, 25 and 30 Gc/sec are plotted in Figure 25. The corrections for other frequencies can be obtained by interpolation of these curves.

If doppler correction were ignored in considering a series of measurements as the self-broadening of the (J,K) = (6,6) inversion line of NH_3, there would be an error of approximately 1% introduced. Measurements made of gas mixtures in the foreign-gas broadening scheme, however, could lead to an error of nearly 8% for the foreign gases which had small slope parameters.

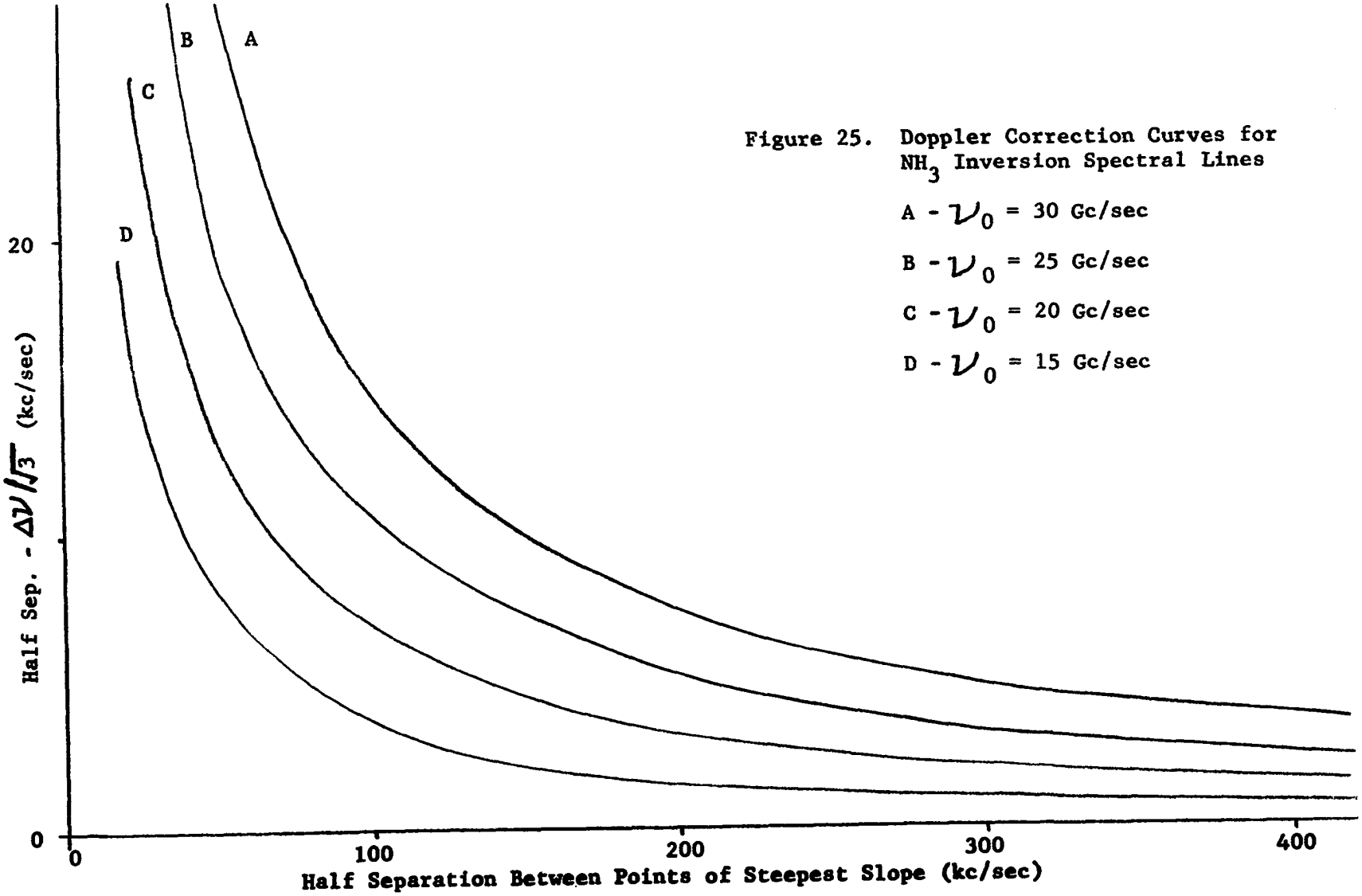

Figure 25. Doppler Correction Curves for NH_3 Inversion Spectral Lines

A - ν_0 = 30 Gc/sec

B - ν_0 = 25 Gc/sec

C - ν_0 = 20 Gc/sec

D - ν_0 = 15 Gc/sec

The most critical range for the doppler contribution to line width for the inversion spectrum of ammonia was for line widths of 100 to 250 kc/sec. This width range corresponded to a pressure range of 1 to 10 microns of pressure of ammonia. For foreign gas measurements the pressure went as high as 200 microns.

Figure 26 shows a linewidth parameter plot of the (3,3) inversion line of NH_3 broadened by argon. The points at low pressures require greater correction for doppler effect than do those points which occur at very high pressures. The pressure of NH_3 within the absorption cell had to be kept very low compared to the pressure of the perturbing gas. For this reason the foreign gas line width parameters which were small produced greater differences in observed slope and doppler corrected slopes. The largest difference was found to be for H_2 which offered a difference of 8% between the observed slope and doppler corrected slope parameters.

It was found that for small linewidth parameters the initial pressure of NH_3 could be increased to have a spectral line of greater width than 200 kc/sec before introducing the foreign gas into the cell. This reduced the difference between observed line widths and corrected line widths, but it increased the error encountered in neglecting the effect of the $NH_3 \longleftrightarrow NH_3$ collisions upon the line width as the foreign gas pressure is increased.

In order to obtain data accurate to better than 2%, it is necessary to take into consideration the distortion to line width due to doppler broadening.

Figure 26. Linewidth parameter for (3,3) Inversion line of NH_3 broadened by argon

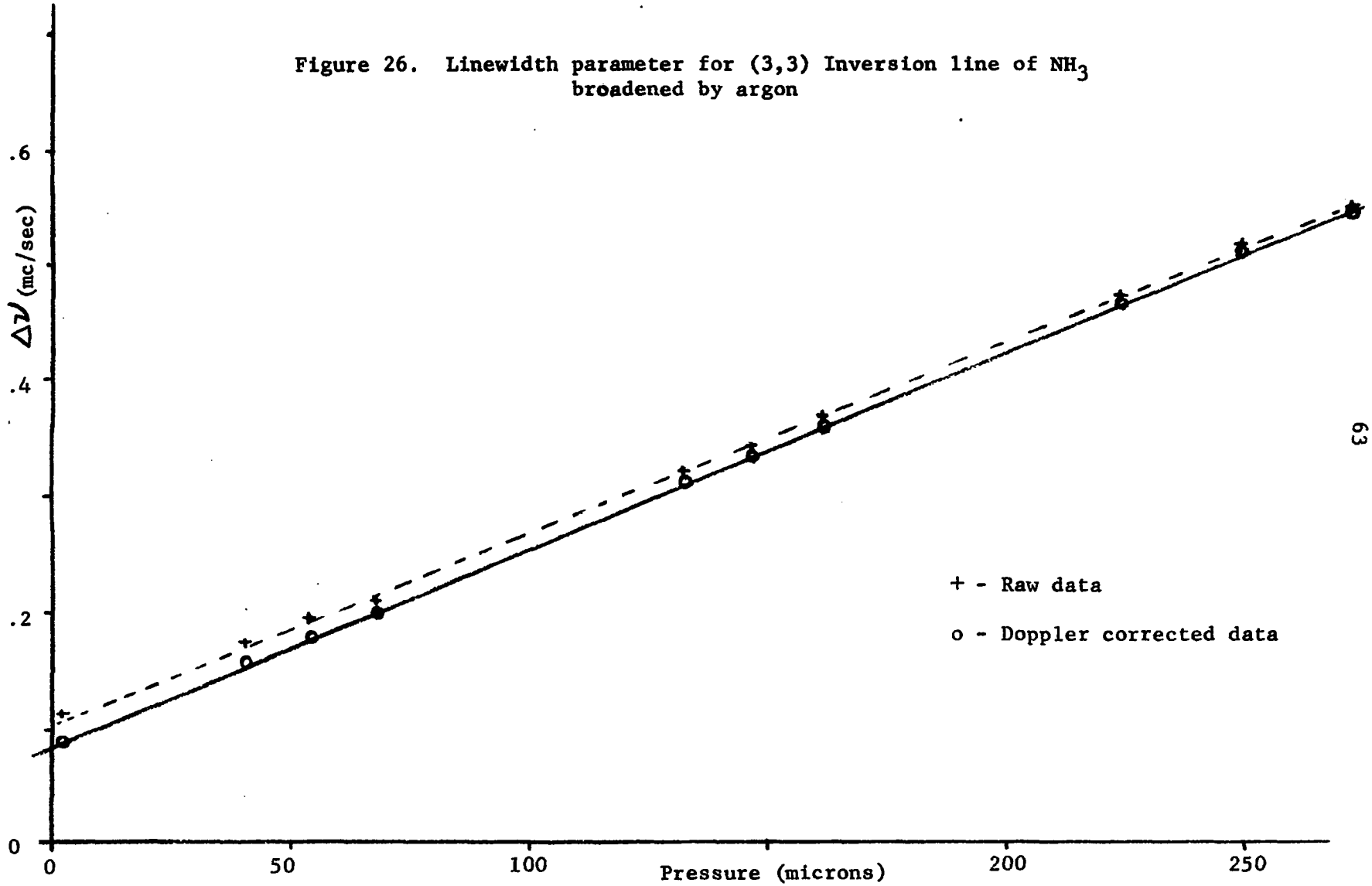

CHAPTER VII

EXPERIMENTAL PROCEDURE FOR MEASURING MICROWAVE LINE WIDTHS

In order to obtain accurate line width data, a systematic and well controlled procedure for measuring line widths of spectral lines must be followed closely. The repeatability of line width data has been found to depend somewhat upon the procedure used in determining the line width measurements. The systematic procedure used and found to be very effective for obtaining consistent line width data is the following.

The entire electronic complement of the spectrograph shown in Figure 5 is given a warm-up time of two hours before any data is taken. During this period of time the gas sample to be measured is allowed to stabilize within the absorption cell. All electronic equipment is checked to be sure each component is functioning properly.

When a known spectral line is to be measured and it is not necessary to search over a large frequency range, the reflex klystron is adjusted for the proper line frequency during the warm-up time of the apparatus. It is often necessary to "touch up" this frequency at the end of the warm-up time.

Once the equipment is completely stabilized and functioning

properly, fine adjustments must be made for all variables of the system. Some of the fine adjustments may produce large errors in the line width determinations if they are not carefully made.

It is imperative that all flange connectors be aligned in such a way that minimum standing waves appear at the detector. There is not a standard procedure proposed for this other than acquire minimum vswr by any method that works. Various methods have been tried which extend from orthodox to "black magic" and have worked to varying degrees.

The most critical adjustments are those connected with the detector mount. It is imperative that the tuning stubs and detector depth adjustment be made in such a way that minimum vswr and maximum crystal current occur at the detector. Variations in line width have been found to be sensitive to crystal current variations when the current is not properly adjusted.

Proper crystal loading is determined from curves similar to those given in Figure 11. The detector load is adjusted with the proper load resistance so that it produces square-law response output.

If a wide range of frequencies is to be observed with the spectrograph it is necessary to readjust the marker mixer for strong harmonic output. This adjustment can be difficult if much adjustment is needed. A procedure has been developed which makes it very easy to obtain strong, well-defined markers. Initially the mixer is tuned for maximum power input from the klystron. In order to determine when maximum power is being coupled into the presently used mixer, the 1000 Mc/sec input connector is shorted allowing the crystal current to be monitored via the 100 Mc/sec connector. The mixer is then tuned

for maximum crystal current at the frequency setting of the klystron. Once the current has been maximized the marker generators are then properly coupled to the mixer. Each transmission line is tuned for maximum crystal current at the mixer. If 1000 Mc/sec markers are desired, the power level is adjusted on these for maximum marker signal out of the mixer via the interpolation receiver. Once the 1000 Mc/sec markers are properly adjusted, the signal from the 100 Mc/sec source is fed into the mixer and proper adjustment made upon the amplitude to produce the desired 100 Mc/sec markers. This procedure is continued until the required marker increment is obtained. This increment is dictated by the range of the radio receiver. A Collins 51J-4 receiver, which covers a range of 0-30 Mc/sec, was used in this work and markers of 10 Mc/sec increment were utilized. The markers were obtained from General Radio Company frequency standards type 1112-A and type 1112-B.

After fine adjustments have been made and the line derivative with frequency markers obtained on the oscilloscope display, the measurements can be begun. The display oscilloscope used was a Tektronix Model 535A. This oscilloscope has dual beam trace scan which is utilized by applying the frequency markers on one trace and the line derivative on the other trace. A single trace oscilloscope may be used and the line signal mixed with the markers. This procedure was found to produce some undesirable distortion of the line signal display. By using two traces very little interference between the markers and the line derivative occurs.

The objective of the measurements is to determine precisely the location of points of steepest slope for the spectral line. Figure 2(b)

of Chapter I shows a sketch of the derivative of the line shape with P_1 and P_2, points of steepest slope for the spectral line, identified. The frequency spacing between P_1 and P_2 is determined by making several measurements with the interpolation receiver for each pressure setting of the gas.

The derivative curve may appear to be symmetric about P_1 and P_2 in the region being observed. Because of this some difficulty arises in locating the points of steepest slope for the spectral line. The operator of the spectrograph is inclined to center the marker on the peaks of the derivative curve. This does not produce much error for very narrow lines, but as the spectral lines are broadened by high pressures the error will be increased if the operator persists in centering the frequency markers on the peak of the curve. The "tails" of the peaks have smaller gradients than do the inside sections of the curve between P_1 and P_2. For this reason the frequency markers should always appear slightly away from the center of the peaks to locate properly the points of steepest slope for the lines.

Locating the proper points along the derivative curve in order to obtain the points of steepest slope for spectral lines produces the greatest problem in this method of line width spectroscopy. The greatest error in all the measurements made is believed to lie here. Very strong lines offer well-defined points, P_1 and P_2, which correspond to the points of steepest slope. As the spectral line intensity decreases, so does the resolution of P_1 and P_2 with an ensuing error increase in location of P_1 and P_2.

When a square wave modulation signal is applied each single

marker will be "split" according to the amplitude of the modulation signal. This frequency spacing is measured as this corresponds to ω', the modulation amplitude of Equation (I-1).

When the initial data taking is begun, the klystron power at the absorption cell is set at the minimum workable value and kept at this level over the entire range of the experiment. An ideal situation would be to completely decouple the klystron and marker generator section from the absorption cell. This is, of course, not possible but it is approximated by use of isolators and low power input to the absorption cell.

The oscilloscope appears with a line shape derivative on one trace and two markers, whose splitting corresponds to the modulation amplitude, on the other trace. Frequency spacing between these two markers and frequency spacing between P_1 and P_2 are measured by the interpolation receiver and recorded. When half of the measurements for a given pressure setting have been made, the pressure is measured for the sample of gas in the absorption cell. Measurements are continued while the mercury in the McLeod gauge is rising. The pressure reading is recorded along with the appropriate values of ω' and $2\delta\nu$. When the number of desired readings for this pressure setting has been obtained, another sample of gas is admitted, along with the first, into the cell and allowed to stabilize until sufficient time has elapsed for the gas to come to equilibrium within the cell. This time depends upon the gas sample and is usually taken as about 30 minutes. While the gas is stabilizing, the line width, $\Delta\nu$, is calculated by use of Equation (I-1). Each point is calculated and checked for consistency with pre-

vious data points to obtain an "on the spot" check of any deviations which may arise in the measuring of a given line. This allows recheck of data points to determine what errors arise during the measuring procedure and enables corrections to be made in case any parameters have shifted to cause erroneous measurements. It is necessary on some occasions to pump the gas from the absorption cell and "touch up" all the adjustments of the spectrograph and begin anew.

During the measuring time of several line widths the modulation amplitude may need to be adjusted to retain a well-defined line. Extreme care must be utilized in adjusting the modulation level as different modulation amplitudes will produce various standing wave patterns about the line being observed. The effect of varying the modulation amplitude can be seen from Figure 15. A general "rule of thumb" for setting the modulation level is to keep the level as low as can be tolerated and still retain a well-defined spectral line.

Investigations of the line widths for several pressure settings are generally made within a period of five hours or less after the equipment has become stabilized. A longer period than this enables much drift in the power supplies due to fluctuations of line voltages. The tendency is to correct for this by making one adjustment rather than go through a complete overall adjustment of the spectrograph. There is interaction between repeller voltages and focus electrode voltage settings which can produce power variations to the absorption cell and consequently fine adjustment of the focus voltage to recover a given frequency may vary the power output of the klystron. If the power level at the detector is readjusted by adjustment of an attenuator in

the waveguide, the same standing wave pattern is not present and erroneous data may be obtained. The most effective method of keeping the power constant to the cell, with minimum interaction between the attenuator dielectric and the standing wave pattern, has been to couple through a 20 d.b. coupler and attenuate at the input to the coupler. Some attenuators have produced such gross standing wave patterns at specific frequencies that they were found to be unusable.

When the line width data and pressure measurements have been obtained for a given spectral line, the process of analyzing the data and making any corrections which might be required in connection with the discussions found in Chapters I through VI is carried out.

The first correction to be made is a correction due to the finite modulation amplitude. This is achieved via Equation (I-1) where the term $(\nu/\Delta\nu)^2$ is neglected, since $\nu \ll \Delta\nu$ generally since $\nu \sim 5$ kc/sec and $\Delta\nu$ is several hundred kilo-cycles per second. Once the condition of zero modulation for the line width has been established, the line width can be corrected for doppler contribution and distortion due to the presence of other spectral lines, if the case need be. Graphs of the uncorrected and corrected line width parameters are given in Chapters V and VI. Figure 22 of Chapter V shows the raw data for the (2,2) inversion line of NH_3 with only doppler correction applied to the line widths. Figure 23 shows the result of application of all needed corrections for the (2,2) line of NH_3.

The result of application of correction terms to the (3,3) inversion line of NH_3 broadened by A is given in Figure 26. The error in line width due to doppler broadening is not evident from observation

of the raw data, but it can be readily seen that the slope parameter is altered when doppler contribution to the line width is considered.

When all corrections have been made to the observed line widths, all data points should describe a straight line over a very wide pressure range, when $\Delta\nu$ is plotted versus P. This has been found to be true for the data obtained in this work. Those line width parameters which are not constant over a large pressure interval are checked to determine the cause. Usually for weak lines at high pressures the standing wave patterns become more important than the spectral signals themselves.

Standing waves are not very sensitive to the pressure change intervals needed to obtain reliable line width data. The amplitude of these standing waves remain constant whereas the spectral lines may become so weak as to not appear in the spectrum. For this reason extreme care must be exercised to get reliable data for spectral lines of intensity less than $10^{-6}cm^{-1}$.

It is believed that the spectrograph developed is among the best available and the data obtained with it is believed to be very reliable when properly analyzed.

Graphs are supplied in Appendix III to give results for spectral lines having intensities of $10^{-4}cm^{-1}$, $10^{-5}cm^{-1}$ and $10^{-6}cm^{-1}$.

Appendix IV contains tabulated data obtained from spectral lines having an intensity of $10^{-4}cm^{-1}$ to $10^{-7}cm^{-1}$ intensity. An idea of the high resolution capabilities of the spectrograph can be obtained from these data.

CHAPTER VIII

INVESTIGATIONS OF THE ANDERSON COLLISION THEORY AS APPLIED TO SYMMETRIC TOP MOLECULES

The first attempt to make microwave line width measurements was done by Bleaney and Penrose in 1947. [12] Several lines of NH_3 were measured by using a cavity technique. The method was new and crude by today's standards, but it gave reasonably good results. This investigation prompted further experimental work and stimulated some activity from a theoretical point of view. P. W. Anderson in 1949 advanced, as part of his doctoral dissertation, a theory of collision broadening of spectral lines. [13] He assumed a scheme of time dependent perturbation for the molecular system to account for interaction between the molecules moving within the abosrption cell. As a test of this theory, Anderson used the data obtained by Bleaney and Penrose.

Because of the difficulty encountered in instrumentation and a lack of understanding of the effect of different measuring techniques, several investigators set about to check the results of Bleaney and Penrose and improve instrumentation techniques, as well as attempt to refine Anderson's theory. The very intense spectral lines were the first observed because of difficulty in sensitivity of apparatus. The early work of Bleaney and Penrose was not reliable, since the investi-

gations were made using crude measuring techniques. However, the results which they obtained were used as a test of the theory later proposed by Anderson to account for collision processes of molecules.

Even though the application of Anderson's theory to the results of Bleaney and Penrose did give satisfying results, a general application of this theory was not very rewarding. More work was done to test the validity of the newly proposed Anderson theory with the following results.

TABLE 3.--Comparison between Anderson's theory and experimental results

Transition	Gas	Anderson's Theory
$\Delta J = 0 \rightarrow 1$	OCS	Inconclusive since q is not known accurately and calculations are sensitive to the value of q.
$^{9}_{1,9} \longrightarrow {}^{8}_{2,6}$	SO_2	Too difficult to calculate; the authors did not calculate the result.
$^{2}_{2,0} \longrightarrow {}^{3}_{1,3}$	H_2O	Good agreement with Anderson's theory.

In addition to the above investigations others were made on foreign gas broadening to determine molecular quadrupole moments. The results were not conclusive and did not agree from one experiment to the other and from one molecular transition to the other.

It was obvious from these investigations that a systematic and well controlled investigation must be made to ascertain the accuracy of the Anderson collision theory.

After solving the instrumentation problem, a detailed study of

the quantum number dependence of the line width for different rotational transitions for the same molecule was made. The experimental results were compared with the calculations based upon Anderson's theory. These results for ammonia are listed for comparison in Table 4.

The quantum number dependence of the collision cross section was studied since a study of the ratio of line widths for sets of quantum numbers could be taken and these results compared to the relative behavior of line widths predicted from Anderson's theory. A difference of 20 - 25% could be encountered between the Anderson theory calculations and experimental results by shifting the value of S(b) to obtain different values of b_0. If a relative behavior of $\Delta\nu_p(J,K)$ is considered the error is greatly reduced, since the internal consistency of Anderson's theory is not extremely sensitive to the choice of S(b). Comparing an absolute result based on an arbitrary choice of S(b) with an experimental value may indicate a gross error between experiment and theory.

A graph of the results of $\Delta\nu_p(J,K)$ for NH_3, based on the Anderson theory and experimental results, is plotted, for comparison, in Figure 27. As can be seen from this plot the results predicted from Anderson's theory indicate a sharp rise in $\Delta\nu_p$, hence, a sharp rise in $\sigma(J,K)$, as the quantum numbers increase from 1 to 4. The most sensitive result is for the (1,1) line and greatest difference is expected for this line. In Chapter V, part of the reason for this large difference is explained.

For J = K the Anderson theory and experimental results give reasonably good agreement for $J \leqslant 10$. From Table 4 it can be seen that

TABLE 4.--Linewidth parameters (Mc/Torr) of self-broadening of NH_3. $(\Delta\nu_p)_{calc}$ was obtained by using Anderson's collision theory and normalizing to the (4,4) transition.

Lines	$(\Delta\nu_p)_{Obs}$	$(\Delta\nu_p)_{Calc}$	Lines	$(\Delta\nu_p)_{Obs}$	$(\Delta\nu_p)_{Calc}$
(1,1)	16.3	19.6	(4,3)	22.10	20.1
(2,2)	22.9	22.6	(4,2)	16.1	14.5
(3,3)	24.0	23.9	(4,1)	13.4	10.3
(4,4)	24.4	(24.4)	(6,5)	22.0	22.0
(5,5)	24.6	24.7	(6,4)	19.6	18.4
(6,6)	24.0	24.9	(6,3)	16.6	14.9
(7,7)	24.6	25.0	(6,2)	13.8	11.5
(8,8)	24.7	25.1	(8,7)	21.9	22.5
(9,9)	24.6	25.2	(8,6)	19.8	19.5
(10,10)	23.8	25.3	(3,2)	17.6	17.6
(11,11)	22.1	25.4	(3,1)	12.8	11.0
(12,12)	24.8	25.5			

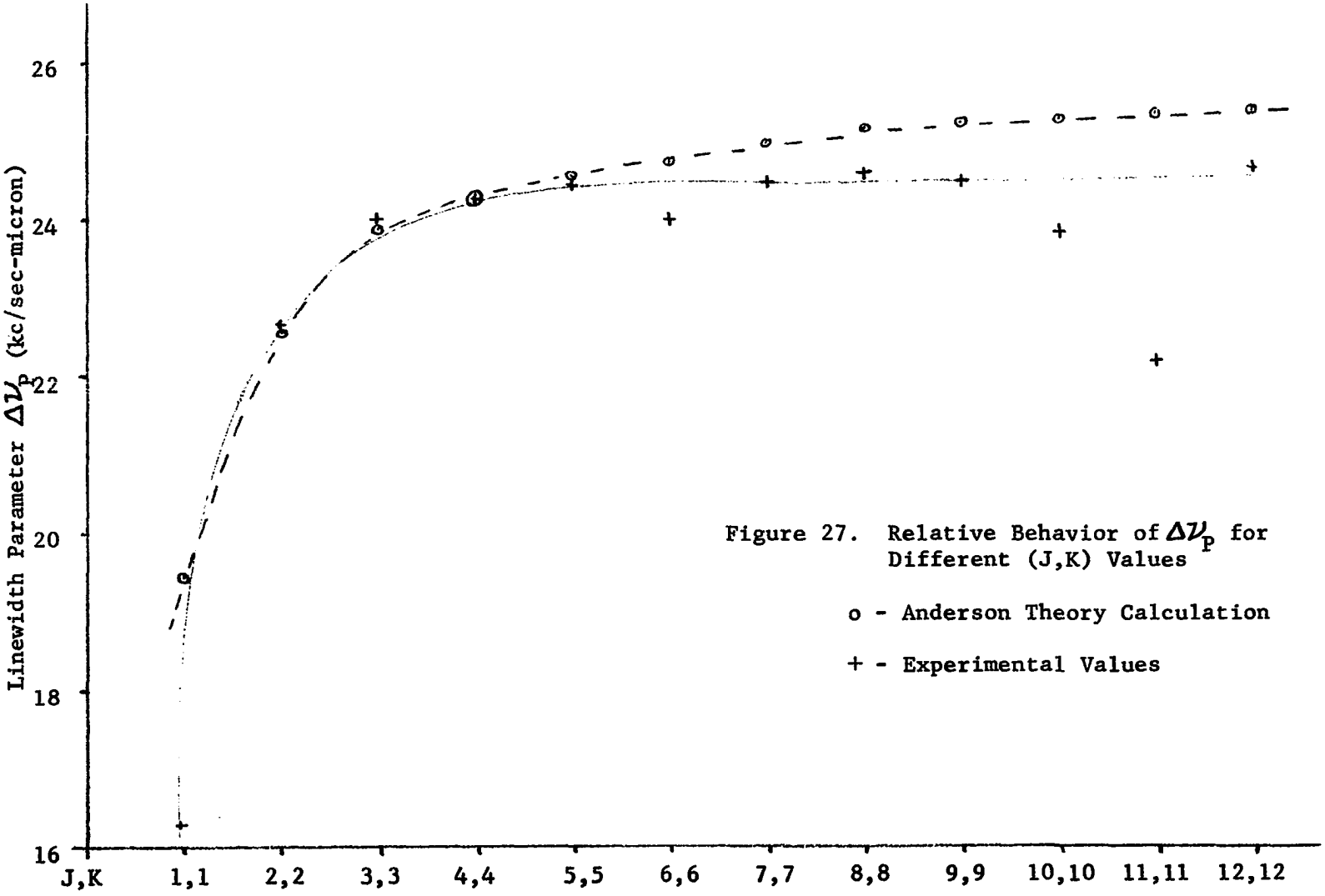

Figure 27. Relative Behavior of $\Delta\nu_p$ for Different (J,K) Values

o - Anderson Theory Calculation

\+ - Experimental Values

as J - K increases the results of experimental measurements deviate more and more from the Anderson theory prediction. For $J>4$ there is only a slight increase in $\Delta\nu_p(J,K)$ predicted from the Anderson theory. This same result does not follow in the experimental case and from J = 4 to J = 9 the values of $\Delta\nu_p(J,K)$ are approximately constant. Relative behavior between theory and experiment is quite good for J = 2 to J = 5. For values larger than J = 5 the theoretical results and experimental results begin to diverge from each other. Of particular interest is the gross deviation of the (11,11) line from the prediction of Anderson's theory and the other experimental results. It is not understood at this time why there is such a large difference between experimental and theoretical values of $\Delta\nu_p$ for this line. The experimental results were repeatable for several investigations made on this transition. There was not sufficient variation in the data to allow for an error large enough to bring the line width parameter into better coincidence with the other experimental results. Further investigation of this transition at this time appears to be fruitless, but as experimental techniques are better refined it is believed that this problem can be clarified.

The experimental results for the self-broadening of the ammonia inversion spectrum gives good overall agreement with the theoretical predictions of Anderson's collision theory. The discrepancies between theory and experimental results do not indicate a serious defect in the Anderson theory and it is believed that refinement of the simplifying assumptions in Anderson's theory along with a close examination of the experimental results will produce better agreement between Anderson's

theory and the observed results.

Because of the importance of foreign gas broadening in determination of molecular quadrupole moments, a detailed study of the foreign-gas broadening of the (3,3), (4,4) and (6,6) inversion lines of the ammonia spectrum has been made and the results compared with the predictions of $\Delta\nu_p$ based on Anderson's collision theory. These results are listed in Table 5.

According to the Anderson theory the variation for $\Delta\nu_p$ is given as

$$\Delta\nu_p \propto \left[\frac{K^2}{J(J+1)}\right]^n \qquad \text{(VIII-1)}$$

the value of n dependent upon the dominant type interactions which are taking place between the molecules. For dipole-dipole interaction, n = 1/2, whereas for dipole-quadrupole interaction n = 1/3. For both cases $\Delta\nu_p$ is expected to increase for increasing J and K. This trend was not generally borne out by the data of Table 5.

It is not surprising that the results show no definite trend. If the results followed the same trend as Anderson's theoretical result for self-broadening of NH_3, there is only a 4% difference between the calculated value of the slope parameter for the (3,3) line and the (6,6) line. If, on the other hand, the results followed the same trend as observed experimentally for the self-broadening of NH_3, there would be only 2.4% difference between the minimum value and the maximum value of the slope parameter. The microwave spectrograph used in obtaining these results can reproduce data with an accuracy of 2% or better,

TABLE 5.--Linewidth parameters (Mc/Torr) of foreign-gas broadening of NH_3.

Gases*	Linewidth parameters (3,3)	(4,4)	(6,6)
A	1.71	1.75	1.59
He	1.04	0.94	0.91
H_2	3.05	3.07	3.03
N_2	3.69	3.85	3.40
O_2	2.16	2.10	1.96
N_2O	5.96	6.17	6.20
CO	4.34	3.91	4.20
CO_2	6.35	6.37	6.44
CH_3Cl	16.7	16.3	17.0
CH_2CF_2	15.0	15.1	15.2
CH_4	3.11	3.10	2.97
SO_2	10.7	10.6	10.8
H_2O	7.81	7.60	8.16
CH_3Br	15.3	15.1	15.0
CHF_3	29.6	30.2	31.8
$CHCl_3$	20.4	20.6	-

* All gases were admitted into the absorption cell where NH_3 constituted less than 2 microns of partial pressure within the cell.

dependent upon the line intensity. Most of the foreign gases reduced the intensity of the spectral lines somewhat when the gases were added to the absorption cell. It is probable that the accuracy of the data needs to be relaxed to an error of 5% to take into consideration the low intensity of the spectral lines as the foreign gas is admitted into the cell.

If the error in line width determination is considered to be as much as 5%, all of the error in the line width parameters except those for A, He, N_2, O_2, and CO may be considered to be due to scatter since the difference between the (3,3), (4,4), and (6,6) results for all the other foreign gases is less than 5%. Therefore, the results for the foreign gas broadening are not conclusive in establishing a trend of $\Delta\nu_p$ as a function of J and K. There is no well established trend for the gases A, He, N_2, O_2, and CO for all lines observed. All of these gases, except CO, have the common property that they have no dipole moment. Even CO has only a very small dipole moment, being 0.10 Debye. The hydrogen molecule should fall into this same class, but the data of Table 4 do not indicate the same behavior as for the above listed gases. This discrepancy in the line width parameters for these molecules indicates a decrease from (4,4) to (6,6) for the line width parameter for all the gases A, He, N_2 and O_2. However, CO is an exception to this trend. This is the same trend observed in the self-broadening scheme of NH_3. This trend should be expected if the dominant interaction forces between NH_3 and A, He, H_2, N_2, O_2 and CO are all of the dipole-induced dipole type. For He and CO the trend of increasing $\Delta\nu_p$ from the (3,3) to (4,4) lines of NH_3 does not hold within 5%

error of determination of $\Delta\nu_p$. Therefore, it is concluded that the foreign gas data follow the same trend as the self-broadening data within an experimental error of 5% in all cases except for He and CO.

A more detailed study of the interaction between NH_3 and CH_3Cl was made to attempt to understand more fully the interaction between ammonia and a foreign gas molecule of symmetric top type which had a strong dipole moment. A detailed study of nine transitions of the inversion spectrum of NH_3 was made using CH_3Cl as the perturbing molecule. The results of this study are listed in Table 6. A similar trend holds in the quantum number dependence of $NH_3 \leftrightarrow CH_3Cl$ interaction as holds in the $NH_3 \leftrightarrow NH_3$ interaction scheme as (J-K) increases. This is an expected trend since the dominant interaction between NH_3 and CH_3Cl is of the dipole-dipole type.

Since CO_2 does not possess a dipole moment but does possess a molecular quadrupole moment, a study of $NH_3 \leftrightarrow CO_2$ interaction was made to try to understand the nature of interaction between dipole and quadrupole moments. The results obtained did not indicate a well defined behavior for the line width parameters as J and K are varied. The only definite trend is that as (J-K) increases the line width parameter decreases as was true for self-broadening of the NH_3 lines. The results of this investigation are listed in Table 7 with observed line width parameters and line width parameters calculated using Anderson's collision theory with n = 1/3 in Equation (VIII-1).

Table 8, listing collision diameters obtained from experimental results and collision diameters based on kinetic theory calculations, is given for making comparisons of these two methods of obtaining the

TABLE 6.--Line width parameters (Mc/Torr) of NH_3 due to broadening by CH_3Cl

Lines	$(\Delta\nu_p)_{Obs.}$	$(\Delta\nu_p)_{Calc.}$
(3,3)	16.7	15.8
(4,4)	16.3	(16.3)
(6,6)	17.0	16.9
(4,3)	14.1	12.3
(5,3)	12.2	10.1
(6,3)	10.5	8.5
(7,6)	15.0	14.7
(8,6)	14.6	12.9
(9,6)	13.7	11.6

TABLE 7.--Line width parameters (Mc/Torr) of NH_3 due to broadening by CO_2

Lines	$(\Delta\nu_p)_{Obs.}$	$(\Delta\nu_p)_{Calc.}$
(2,2)	6.58	5.98
(3,3)	6.35	6.23
(4,4)	6.37	(6.37)
(6,6)	6.44	6.52
(6,4)	5.93	4.98
(6,2)	4.18	3.12

TABLE 8.--Collision radii determined from foreign gas broadening of the (3,3) inversion line of NH_3 compared with collision radii determined from kinetic theory calculations.

Gas	b_0 in Å units (from line width data)	Kinetic Theory
He	2.16	3.3
A	3.82	4.04
H_2	2.71	3.58
O_2	3.93	4.02
N_2	5.45	4.09
CO	5.92	3.96
CO_2	7.43	4.46
CHF_3	16.49	---
N_2O	7.15	4.35
H_2O	7.69	---
CH_3Br	12.01	---
CH_3Cl	12.16	5.14
CH_2CF_2	11.69	---
CH_4	4.71	---
$CHCl_3$	13.98	---
SO_2	9.87	---
NH_3	13.18	4.43

collision diameter for interaction between two types of molecules. In each case where the interaction processes are of long range type, dipole-dipole, the collision diameters are found to be larger experimentally, than those calculated on the basis of a kinetic theory approach. This indicates that the process of radiation interruption for molecular collisions is more effective than the momentum transfer scheme employed in the kinetic theory approach to collision interaction.

Those cases of interaction which are believed to depend upon short range forces do not indicate the same trend between kinetic theory calculations and experimentally observed results. In all cases, except N_2 and CO_2, in which the perturbing molecule does not possess a permanent dipole moment, the observed values of b_o are less than those calculated from kinetic theory approach.

The reason for this deviation is not fully understood at this time. It is possible that the emitter molecule is able more readily to induce a dipole moment in these two molecules than in the other molecules which have no permanent dipole. If this occurs the dipole-induced dipole interactions will begin to play a greater role in line broadening and produce a larger collision cross section than is expected for dipole-quadrupole interaction alone.

Because of a definite conclusion could not be drawn concerning the Anderson collision theory, additional investigations were made. The gases of interest as observed from earlier discussion and as seen in Table 5 seemed to be A, He, H_2, N_2, and CO_2. A study of the interaction processes between these gases and molecules which have strong

dipole moments seemed to offer the most fruitful pursuit. Another molecule besides NH_3 was chosen as the emitter. The symmetric top molecule CH_3Cl was chosen, with the transition $\Delta J = 0 \longrightarrow 1$, $\Delta F = 0$, to be studied.

The investigation of CH_3Cl was done as follows. Measurements were made at 26°C on binary gas mixtures with the microwave spectrograph described earlier, and the line widths were corrected for the doppler contribution as described by Parsons and Roberts. [14] If τ_1 and τ_2 are the mean intervals between self and foreign-gas broadening collisions respectively, then

$$\Delta\nu = (2\pi\tau_1)^{-1} + (2\pi\tau_2)^{-1} \qquad \text{(VIII-3)}$$

$$= (\alpha - \beta)P_1 + \beta P \qquad \text{(VIII-4)}$$

where P is the total pressure in mm of Hg, P_1 the partial pressure, in mm of Hg, of methyl chloride, and the coefficients α and β are given in terms of the mass of the absorbing molecule and the broadening molecule and the hard-sphere collision diameters b_1 and b_2 for self and foreign-gas broadening collisions by Jeans. [15]

$$\alpha = 2b_1^2\left[N_o/(\pi M_1 kT)\right]^{\frac{1}{2}} \qquad \text{(VIII-5)}$$

and

$$\beta = b_2^2\left[2N_o/(\pi MkT)\right]^{\frac{1}{2}} \qquad \text{(VIII-6)}$$

where N_o is the number of molecules per cubic cm, $1/M = 1/M_1 + 1/M_2$, and M_1 and M_2 are taken as masses of the individual absorbing and broadening molecules respectively. For given value of P_1, the width

of the line of frequency 26.57077 Gc/sec, which corresponds to the transition $\Delta J = 0 \rightarrow 1$, $\Delta F = 0$, was measured as a function of the total pressure P. Values of β were found by a least squares analysis of the data. These values are tabulated, along with the values of b_2 deduced from them, in Table 9. It should be pointed out that there may also be systematic errors arising, for example, from calibration errors in the apparatus, but it is believed that the total error in should be less than twice that listed in Table 9.

The line width measurements were corrected for doppler distortion since the observed widths were all within the region where the doppler effect gives a significent contribution to the observed line widths. This was true for these gases because they all have a very small line width parameter.

TABLE 9.--Line broadening parameter β and collision diameters b_2

Foreign Gas	H_2	He	N_2	A	CO_2
β in mc/sec-torr	6.46	3.47	5.73	5.54	11.98
b_2Å	4.7	4.1	7.7	8.0	12.0
b_2Å (K.T.)	3.50	3.33	3.88	3.75	4.04

Table 10 gives the uncorrected data used to obtain the results of this study. The errors in reading of the modulation, ω', and the line widths, $\Delta\nu$, are assumed to be less than 2% for gases except CO_2. In making measurements of the line width parameter for CO_2 it was found that the intensity of the CH_3Cl line diminished considerably as

TABLE 10.--Uncorrected line width data used to obtain $\Delta\nu_p$ for the CH_3Cl transition $\Delta J = 0 \rightarrow 1$ upon being broadened by several foreign gases.

Foreign Gas	P(m-Torr)	ω'(kc/sec)	$\Delta\nu$(kc/sec)
N_2	2.73	43	122
	6.30	43	144
	8.68	43	156
	10.95	43	172
	14.98	80	201
	22.76	80	
	28.10	80	284
	33.88	135	334
He	7.93	53	242
	10.72	53	255
	21.43	63	297
	31.12	63	335
	40.17	123	373
	49.35	123	416
H_2	3.41	58	169
	10.09	101	216
	16.24	99	265
	22.40	98	302
	28.55	147	365
	34.76	180	410

TABLE 10--Continued

Foreign Gas	P(m-Torr)	ω'(kc/sec)	$\Delta\nu$(kc/sec)
CO_2	14.60	27	408
	22.31	35	487
	28.83	64	563
	35.72	104	677
	42.35	90	740
	49.06	61	860
	57.81	56	1000
A	9.25	72	279
	15.38	72	323
	21.04	77	354
	26.73	109	402
	32.07	102	429
	37.78	103	462
	43.06	136	500

the gas CO_2 was introduced into the cell. This diminution of intensity decreased the resolution of the apparatus and produced a larger probable error in the line width determination. The errors in $\Delta\nu$ and ω' for CO_2 are assumed to be less than 4%. Measurements were also made of the self-broadening of the spectral line and from these the parameter $\Delta\nu_p$ was found to be 20.3 $\pm$ 0.4 mc/sec/mm Hg, which yields a collision diameter of 15.9A; this is in good agreement with the result of Bird. [16] In addition, some measurements were made on the line frequency 26.58949 Gc/sec, which corresponds to the transition $\Delta J = 0 \rightarrow 1$, $\Delta F = \frac{3}{2} \rightarrow \frac{5}{2}$, but the results for $\Delta\nu_p$ were the same, to within the experimental error, as those given above.

From Anderson's collision theory, collision diameters for the foreign gas broadening of the inversion spectrum of the symmetric top molecule NH_3 may be calculated. [17] Anderson assumed that the dominant interactions were those between the dipole and quadrupole moments of the emitting or absorbing molecule with the dipole moments induced in the foreign gas molecule. If these interactions were also dominant in the present case, it would be expected that the collision diameter b_2 would vary as $(a\sqrt{M})^{1/6}$, where a is the polarizability of the foreign gas. This, however, does not appear to be the case as may be seen from Figure 28 in which log b_2 is plotted against log $(a\sqrt{M})$: the best straight line gives a very poor fit to the experimental points, and its slope is 0.28, which is almost double the expected value. A somewhat similar discrepancy was reported by Birnbaum and Maryott in their analysis of the data on non-resonant absorption. [18] Part of the discrepancy may arise from interactions between the dipole moment of methyl chloride

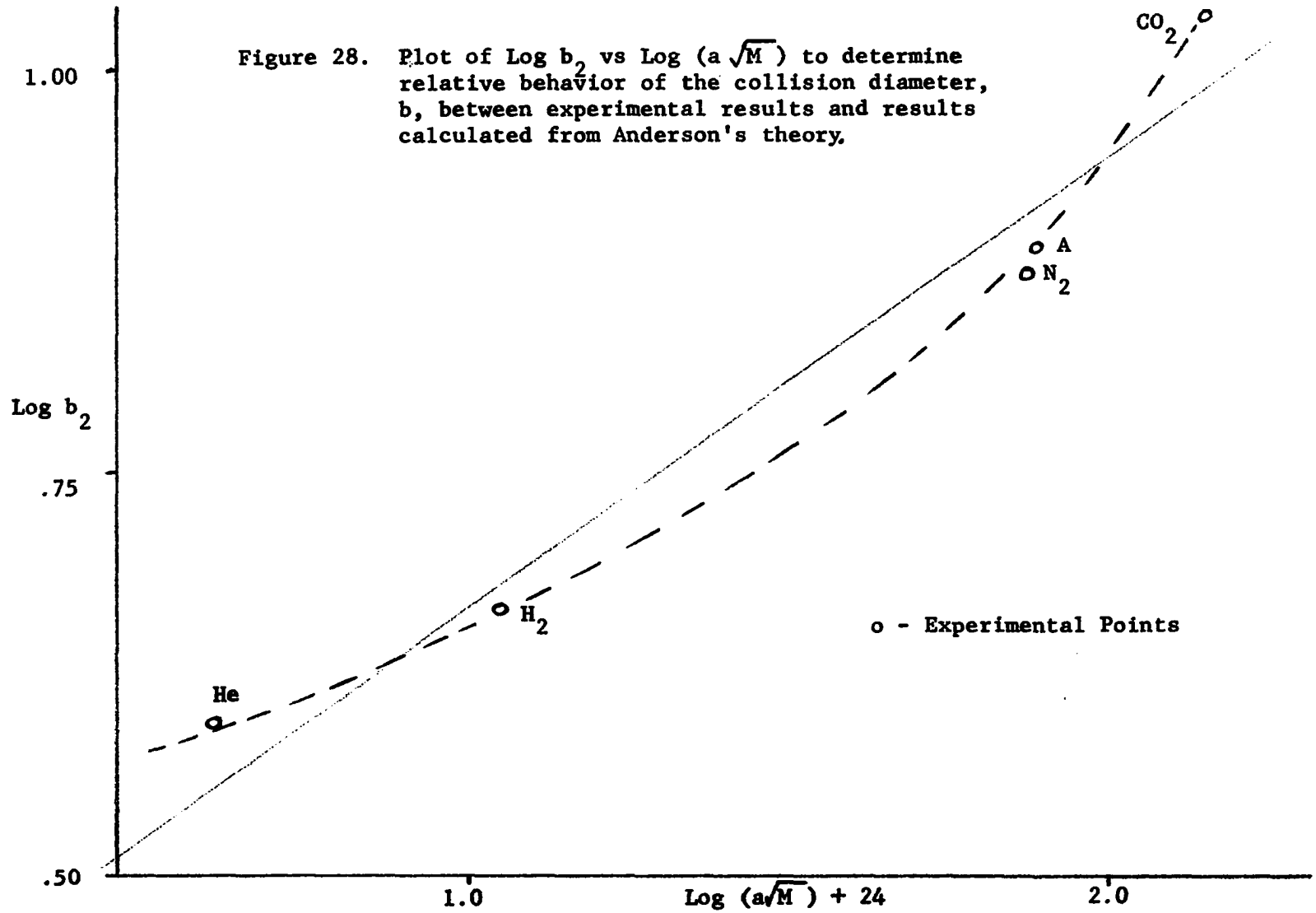

Figure 28. Plot of Log b_2 vs Log ($a\sqrt{M}$) to determine relative behavior of the collision diameter, b, between experimental results and results calculated from Anderson's theory.

and the permanent quadrupole moments of the foreign gases in the manner discussed by Smith. [19] This cannot be so in the case of broadening by argon since in this case the foreign gas has no quadrupole moment.

In order to enlarge the scope of the experimental results and attempt to clarify the direction to take in analyzing Anderson's theory from a broader point of view, a group of symmetric top molecules was studied. It was hoped that from this study a definite quantum number behavioral trend of the collision cross section could produce a well-established trend to point out a direction of refinement within the framework of Anderson's theory.

The molecules chosen to be analyzed were all of the methyl group, since they were the most easily obtained and possessed spectra that were reasonably well resolved. The discussion of overlapping spectral lines in Chapter V points out the need for observing non-overlapping spectral lines. All of the molecules which possessed spectral lines having fine structure showed lower slope parameters for $\Delta J = 1 \rightarrow 2$ than for $\Delta J = 0 \rightarrow 1$. The one molecular specie, C_3H_4, which did not have fine structure, showed a different trend of $\Delta\nu_P$ between $\Delta J = 0 \rightarrow 1$ and $\Delta J = 1 \rightarrow 2$ than did the other molecular sample. Within experimental error all molecules indicated the same trend of K dependence for the line width parameter within a given J transition.

A separate study of the collision cross section dependence upon quadrupole transitions for three different sets of J and K indicated that the collision cross sections are independent of the quadrupole transitions for a given J and K value. The results of this study are contained in Table 11. These results indicate that any F dependence of

TABLE 11.--Line width data for several symmetric top molecules.

Molecule	ΔJ	K	ΔF	$\Delta\nu_p$ (mc/s-Torr)
CH_3Br^{79}	0 → 1	0	3/2 → 5/2	15.71
	1 → 2	0	3/2 → 5/2	8.58
		1	5/2 → 7/2	12.25
	2 → 3	0	7/2 → 7/2	12.83
		0	5/2 → 5/2	12.15
		0	7/2 → 9/2	12.69
		0	5/2 → 7/2	
		1	7/2 → 9/2	11.79
		2	1/2 → 3/2	11.93
	3 → 4	0	5/2 → 7/2	12.83
		0	3/2 → 5/2	
		1	7/2 → 9/2	13.80
		2	9/2 → 11/2	12.60
		3	7/2 → 9/2	12.00
CH_3Cl^{35}	0 → 1	0	3/2 → 5/2	19.46
		0	3/2 → 3/2	19.43
	1 → 2	0	5/2 → 7/2	17.56
		1	5/2 → 7/2	15.63
CH_3Cl^{37}	0 → 1	0	3/2 → 5/2	20.17
	1 → 2	0	5/2 → 7/2	17.87
		1	5/2 → 7/2	17.00

TABLE 11--Continued

Molecule	Δ J	K	Δ F	$\Delta\nu_p$ (mc/s-Torr)
CH_3Cl^{37}	2 → 3	0	7/2 → 7/2	11.25
		2	3/2 → 5/2	12.80
CH_3Br^{81}	0 → 1	0	3/2 → 5/2	15.20
	1 → 2	0	5/2 → 7/2	10.30
		0	3/2 → 3/2	8.26
		1	5/2 → 7/2	12.88
	2 → 3	0	3/2 → 3/2	14.73
		1	7/2 → 9/2	12.60
		2	1/2 → 3/2	14.63
	3 → 4	0	9/2 → 9/2	14.85
		1	7/2 → 9/2	13.23
		2	9/2 → 11/2	12.90
		3	3/2 → 5/2	12.66
CH_3CN	0 → 1	0	1 → 2	94.17
	3 → 4	3	3 → 4	77.70
C_3H_4	0 → 1	0		8.75
	1 → 2	0		12.25
		1		13.75
	2 → 3	0		7.25
		1		8.45
		2		8.39

TABLE 11--Continued

Molecule	ΔJ	K	ΔF	$\Delta\nu_p$ (mc/s-Torr)
C_3H^4	3 → 4	0		8.48
		1		8.60
		2		7.88
		3		7.91
CH_3I	0 → 1	0	5/2 → 7/2	13.28
	1 → 2	0	7/2 → 9/2	10.77
		1	7/2 → 9/2	9.58
	2 → 3	0	9/2 → 11/2	9.45
		1	9/2 → 11/2	11.08
		2	9/2 → 9/2	9.53
	3 → 4	0	3/2 → 5/2	9.54
		0	5/2 → 7/2	9.92
		0	7/2 → 9/2	9.65
		0	9/2 → 9/2	
		0	11/2 → 11/2	9.58
		0	11/2 → 13/2	9.88
		0	9/2 → 11/2	10.31
		1	11/2 → 11/2	9.46
		2	11/2 → 13/2	9.58
		3	11/2 → 13/2	8.79
	4 → 5	0	11/2 → 13/2	9.83
		1	13/2 → 15/2	9.65

TABLE 11--Continued

Molecule	ΔJ	K	ΔF	$\Delta\nu_p \frac{mc}{(s\text{-}Torr)}$
CH_3I		2	13/2 → 15/2	9.90
		3	13/2 → 15/2	9.71

the collision cross section for a given transition must contribute less than 4% to the line width parameter, since the spectrograph was believed to have an overall resolution capability of better than 4% for all transitions observed. In this case, overall resolution refers to the repeatability of the data and does not imply that the data are all good to better than 4%. Many of the spectral lines were observed at frequencies above 30 Gc/sec. Although the apparatus responds well even at frequencies near 80 Gc/sec, all of the parameters related to line width measuring have not been thoroughly analyzed at these higher frequencies. In many cases standing waves within the absorption cell became a problem to contend with. In general all of the data are accurate to better than 4% with only a few transitions subject to doubtful validity in determination of $\Delta\nu_p$. Those lines which have doubtful values of $\Delta\nu_p$ have been checked and the values which seemed most accurate, based on low scatter, have been taken to be the correct values.

The results of the self-broadening study for the set of symmetric tops investigated are listed in Table 11.

The greatest deviation between determined line width parameters and calculated line width parameters, assuming dipole-dipole interaction,

occurred for CH_3CCH. This can readily be seen from Table 15 of Appendix IV. Some of the calculated values of the slope parameters for CH_3CCH were less than half of the observed values. The greatest difference was found to be 63% for the error in calculated value compared to the experimentally observed value. The smallest difference between calculated and observed line width parameters occurred for the transition $\Delta J = 2 \rightarrow 3$, $K = 0$. This difference was 22%. All the other transitions yielded differences greater than 32% for this molecule. The maximum difference between observed and calculated line width parameters for the other molecules of the group was 31%. Most of the results for these molecules agreed to better than 15% with only ten of the forty-two transitions studied yielding errors greater than 15%.

The theoretical calculations for the line width parameters in Table 15 were made assuming dipole-dipole interactions only, with no normalization scheme employed. The calculated values were obtained using Anderson's approximation number 2 in his interpolation scheme. [21] The results are not normalized to the experimental line width parameter of a given transition as was done in the case of NH_3. The normalization procedure is justifiable when exact resonance is involved. [22] Because the inversion energies for NH_3 are small compared to the rotational energy levels, the inversion energies were assumed to be zero for purpose of calculation. Since these energy differences are small, the relative behavior of $\Delta\nu_p$ for NH_3 is independent of the interpolation scheme employed. The normalization scheme cannot be employed for the other symmetric top molecules studied as the rotational energy differences dominate the calculations of $\Delta\nu_p$ and these results are sen-

sitive to the interpolation scheme used. Therefore, absolute calculations were made for the general group of symmetric tops studied.

The molecule CH_3CCH has a dipole moment of only .75 debye units which is comparatively small. This may in part account for the large discrepancy between calculated results and experimental data. Therefore, it is concluded that higher order interactions need to be considered to clarify the differences between experimental and calculated results for the CH_3CCH molecule.

As can be observed from Appendix III, the expected error in line width determination of all the spectral lines observed should be less than 6%, as all observed spectral lines had an intensity of $10^{-6} cm^{-1}$ or larger. All of the transitions studied, except six, yielded differences between experimental results and theoretical results in excess of 6% with an average difference for all molecules, except CH_3CCH, of 17.5%. It is believed to be more than coincidence that calculated values of $\Delta\nu_p$ for CH_3Cl, CH_3Br and CH_3I are larger than observed values of $\Delta\nu_p$. The difference between these results is not sufficiently small that the error can be attributed to instrumentation effects or possibly a small error in determination of some of the constant parameters of the molecules.

The largest group of transitions studied was for the molecule, CH_3I. Very good agreement was found for the low J transitions with the difference between experimental and calculated results increasing as J and K increased.

The two molecules, CH_3CN and CH_3CCH, need further analysis to better clarify the differences in theoretical and observed values. Al-

though there is limited data for CH_3CN, the results are very good. It was not possible to resolve the spectral lines of CH_3CN to make measurements for several transitions. A method is proposed to resolve this spectra into components by applying a d.c. stark field to the molecule.

It is believed that the data recorded in Table 11 is the best available to date. Some refinement of measurements must be made for the weaker spectral lines and a more careful analysis of the response of the spectrograph at frequencies above 40 kmc/sec must be made to completely solve the line width problem for the symmetric top molecules studied. Aside from the CH_3CCH molecule and a few isolated transitions of some other molecules, the overall agreement between experimental results and Anderson's theory is better than 20%. The agreement for NH_3 was better than this, but normalization was made to the (4,4) transition. Whereas, for these molecules, absolute values were computed. The overall agreement between theory and experiment is believed to be very good considering that only dipole-dipole interactions were assumed in calculating the line width parameters recorded in Table 15. Further analysis of fine points of the theory, no doubt, will lead to better understanding of the reason for the difference between the calculated and observed values of $\Delta\nu_p$.

APPENDIX I

CIRCUIT DIAGRAMS OF AUXILLIARY CIRCUITS

Some of the circuits used were not a necessary part of the spectrograph, but they served to improve the data output and to produce a more dependable system. It was necessary to construct an amplifier that could amplify the 100 kc/sec output trigger from the electronic counter. This trigger was used to synchronize the marker generator systems to a crystal controlled source. With amplification the signal was dependable and the long time stability of the output of the marker generator was greatly improved. The schematic diagram of this circuit is shown in Figure 29 and is recorded primarily for reference.

Another apparatus utilized is the one schematically shown in Figure 30. This apparatus is commercially available as an harmonic generator for testing radio receivers but it has been found to be stable and adaptable as a standard locking device for stabilizing the carrier signal generator. Because of the prevalence of 100 kc/sec signal already in the system, a crystal was selected which locked the carrier at non-integral multiples of 100 kc/sec. No modulation of the markers or klystron mode has been observed at the carrier frequency due to presense of the carrier signal feeding to the repeller electrode.

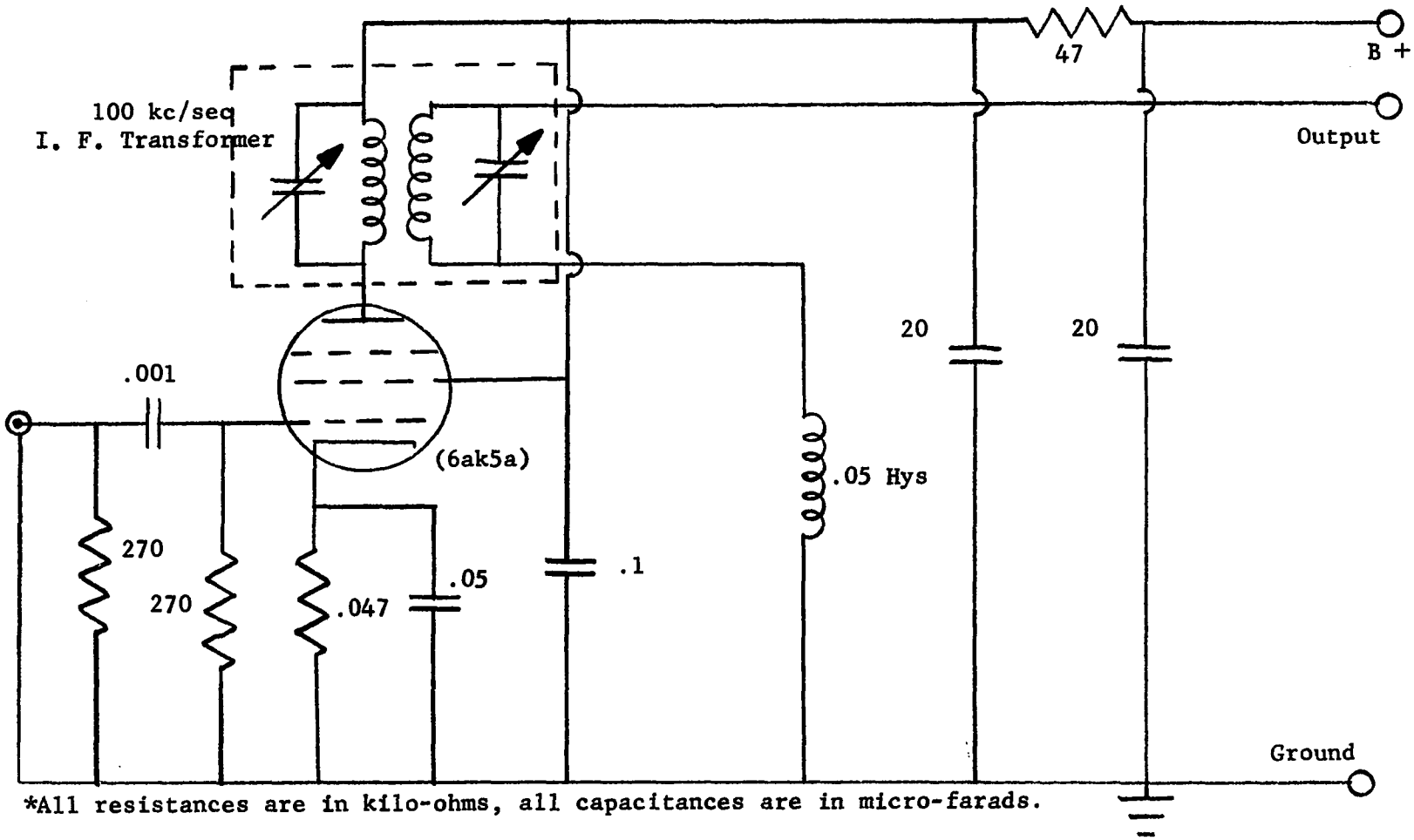

*All resistances are in kilo-ohms, all capacitances are in micro-farads.

Figure 29. 100 kc/sec Trigger Amplifier for Marker Generator

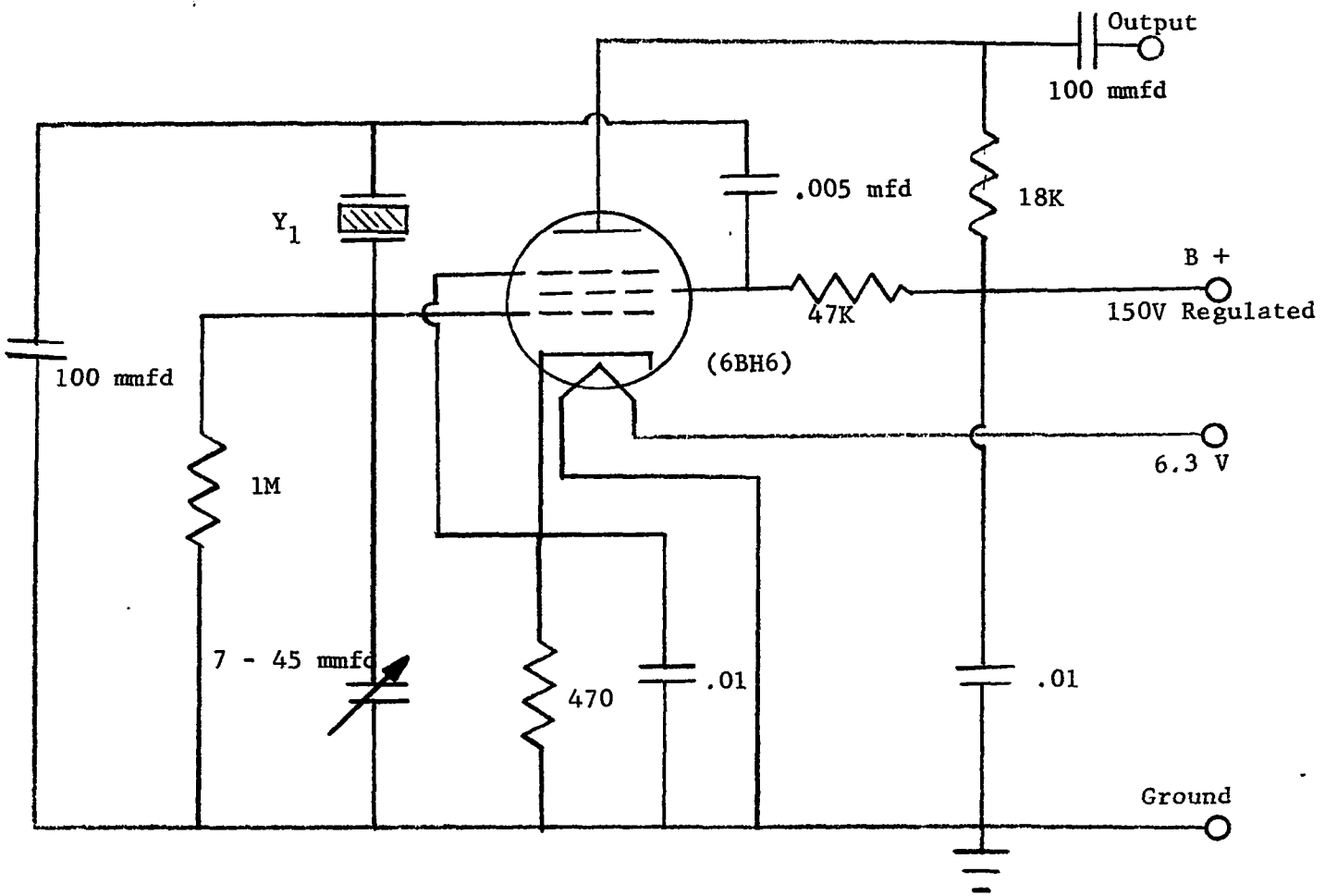

Figure 30. FO - 1L Schematic

APPENDIX II

QUANTITATIVE INVESTIGATION OF THE LINE WIDTH PARAMETER OF THE SO_2 MOLECULE FOR SELF AND FOREIGN GAS BROADENING

A qualitative investigation of the dependence of collision cross sections of asymmetric top molecules on quantum numbers has been made. Both self-broadening and foreign-gas broadening of the slightly asymmetric top molecule, SO_2, have been investigated. The results of the self-broadening are listed in Table 12.

The same general trend of quantum number dependence on collision cross sections has been found to hold for the slightly asymmetric top molecule, SO_2, as was found for inversion spectra of symmetric top molecules. For increasing J there was found to be an increase in the line width parameter until J = 7 at which point the line width parameter seemed to become constant with perhaps a small dependence on K. A similar trend has been found for linear molecules by other investigators. [19, 20]

Because of the interesting trend found in gases H_2, He, N_2, A and CO_2 a study was made of the interaction of these foreign gases with the SO_2 transitions. The same general trend was noted here as was found for the symmetric top molecules studied. This was expected

TABLE 12.--Self broadening parameters for the asymmetric top molecule, SO_2.

Transition	$\Delta\nu_p$ $\frac{mc}{(s\text{-}Torr)}$	ν_o (mc/sec)
$2_{0,2} \rightarrow 2_{1,1}$	10.25	53,529.16
$4_{0,4} \rightarrow 4_{1,3}$	13.48	59,225.00
$3_{1,3} \rightarrow 4_{0,4}$	13.67	29,321.22
$6_{1,5} \rightarrow 5_{2,4}$	15.56	23,414.30
$7_{2,6} \rightarrow 8_{1,7}$	16.46	25,392.80
$9_{1,9} \rightarrow 8_{2,6}$	16.73	24,083.39
$13_{2,12} \rightarrow 12_{3,9}$	18.09	20,335.47
$16_{3,13} \rightarrow 17_{2,16}$	15.21	28,858.11
$22_{4,18} \rightarrow 21_{5,17}$	17.61	24,039.50
$23_{5,19} \rightarrow 24_{4,20}$	16.83	22,482.51
$24_{5,19} \rightarrow 25_{4,21}$	17.92	26,777.20
$34_{7,27} \rightarrow 35_{6,30}$	17.41	25,049.13

as the dominant interaction forces are still dipole-quadrupole and dipole-induced dipole for interaction of SO_2 with the gases listed.

The results of the foreign gas collision investigations of SO_2 are listed in Table 13. The results of the line broadening parameter determinations did not yield a general trend to the line width parameters as a function of J and K. Most of the variations indicated for different J and K can be attributed to scatter in the cases of foreign gas broadening of the SO_2 lines given. The trend for $SO_2 \longleftrightarrow SO_2$ interaction indicates a definite increase in $\Delta\nu_p$, hence an increase in $\sigma(J)$, when J is increased to J = 7. Higher values of J did not produce sufficient variation in $\Delta\nu_p$ to indicate a definite trend. The results indicate approximately a constant value of $\Delta\nu_p$ for $J > 7$. This is the same result, with only one exception, indicated by the inversion spectra of NH_3 for J = 4 to J = 12.

TABLE 13.--Table of self and foreign-gas broadening for several transitions of the SO_2 molecule.

Gas	$2_{0,2} \rightarrow 2_{1,1}$ 53,529.16	$4_{0,4} \leftarrow 3_{1,3}$ 29,321.46	$4_{0,4} \rightarrow 4_{1,3}$ 59,225.00	$5_{2,4} \leftarrow 6_{1,5}$ 23,414.25	$7_{2,6} \rightarrow 8_{1,7}$ 25,392.81	$9_{1,9} \rightarrow 8_{2,6}$ 24,083.39
SO_2	10.25	13.67	13.48	15.56	16.46	16.73
CH_3Br	13.97	13.23	13.50	16.93	16.63	15.93
H_2	6.25	5.46	5.76	6.30	6.00	6.30
He	2.83	2.54	2.60	2.70	2.81	3.04
N_2	4.48	4.58	4.52	4.77	4.75	5.00
Ar	2.58	2.81	2.48	2.77	2.88	2.92
CO_2	8.92	7.78	7.84	7.80	7.91	7.75

APPENDIX III

LINE WIDTH PARAMETER CURVES FOR SEVERAL MOLECULAR TRANSITIONS

Several line width parameter graphs are included in this appendix to indicate the high resolution capability of the line width spectrograph used to obtain data for this work. From an overall analysis of available data it has been concluded that the following rules hold for accuracy of repeatability of the data.

TABLE 14.--Resolution capabilities of the line width spectrograph

Intensity of spectral line	Percent accuracy expected for obtained data
10^{-4} cm^{-1}	2%
10^{-5} cm^{-1}	4%
10^{-6} cm^{-1}	6%

Spectral lines which are directly observable without aid of a phase detector produce better accuracy in line width determinations than do those which require the use of a phase detector. The spectrograph has been used to observe directly spectral lines of an intensity of 10^{-7} cm^{-1} with resulting data of low scatter. The scatter of data

has been found to increase as the spectral line intensity decreases. The increased scatter in the data is not totally responsible for requiring that the data accuracy be relaxed to 6% for 10^{-6} cm^{-1} intensity lines. The chief contributing factor is that standing waves become more important as the spectral line intensity decreases. Presense of these standing waves requires that the modulation amplitude be kept low to compensate for their presense. This reduces the excursion of the frequency of the klystron along the line. The greater the excursion of the klystron frequency, the better average is obtained over the "noisy" section of the line. Therefore a large modulation amplitude averages through the noise and indicates less scatter for a given spectral line.

It has been observed that even 10^{-6} cm^{-1} spectral lines produce data of low scatter when there are no standing waves present and the modulation amplitude can be increased to approximately one-half the spectral line width.

Figure 31. Linewidth parameter of the (9,9) inversion line of NH_3
(Intensity $\sim 10^{-4}$ cm^{-1})

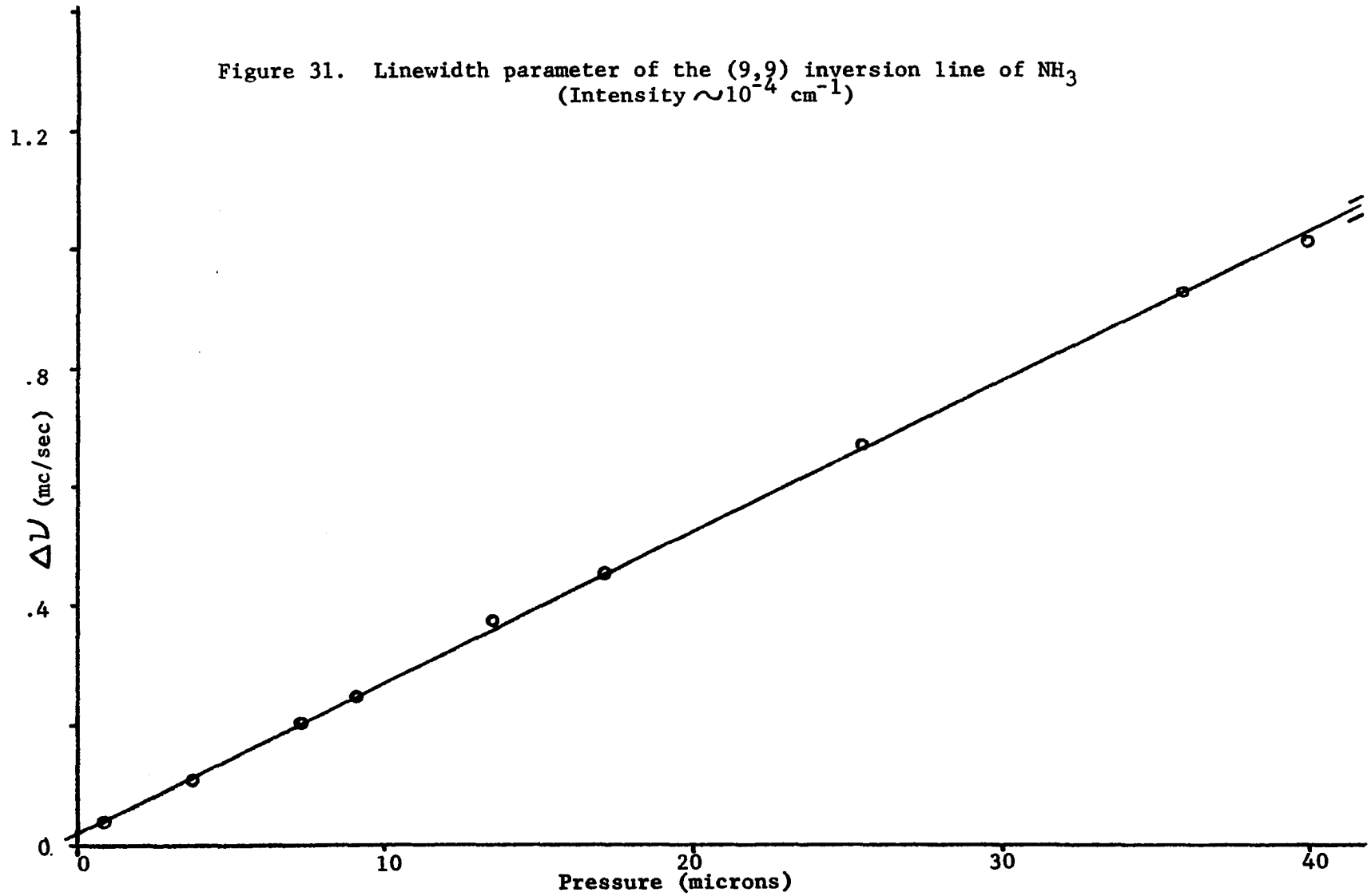

Figure 32. Linewidth parameter of the (12,12) inversion line of NH_3
(Intensity $\sim 10^{-5}$ cm^{-1})

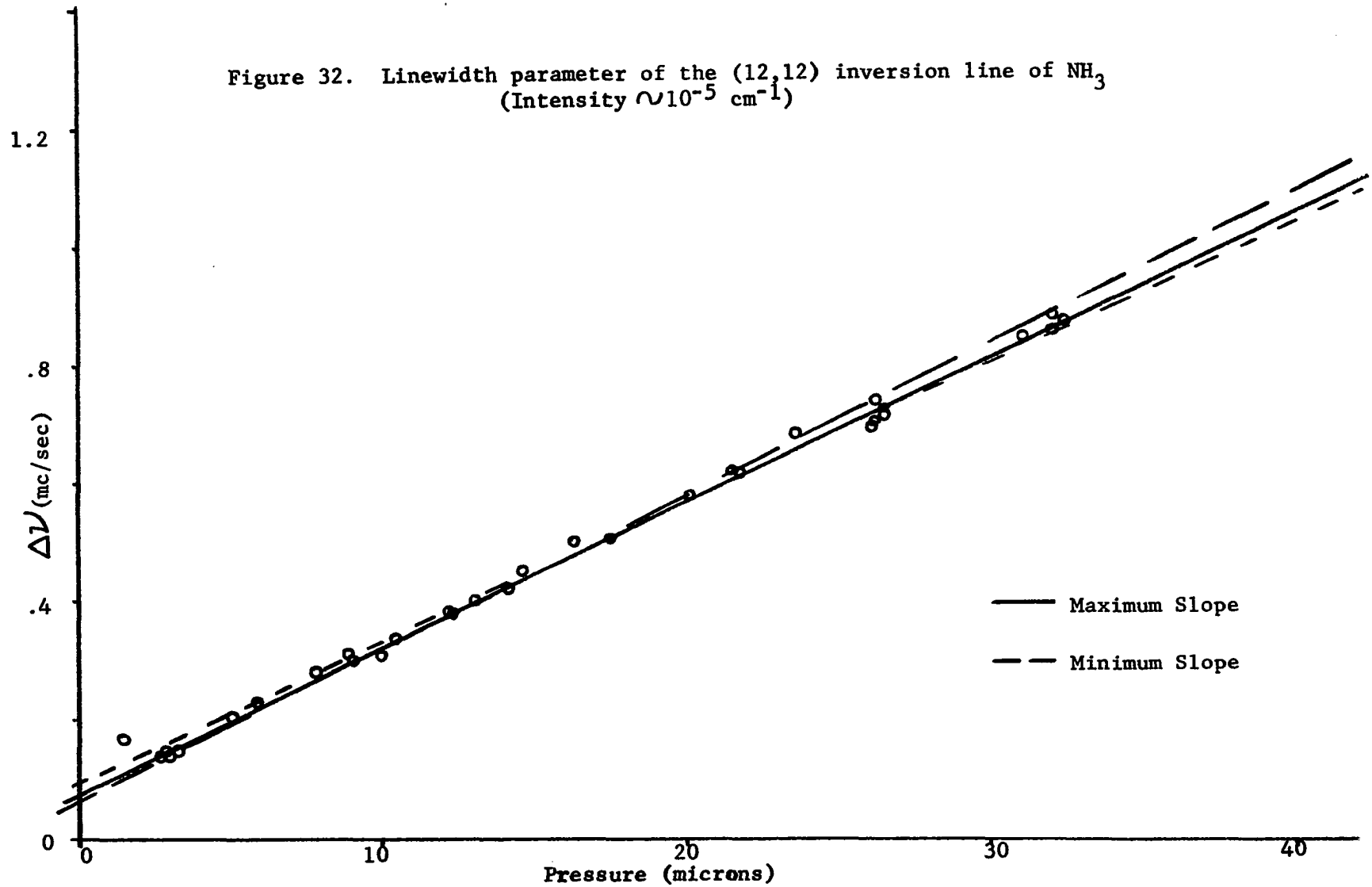

Figure 33. Linewidth parameter of the (0⟶1, 0, 3/2⟶5/2) transition of CH_3Br (Intensity $\sim 10^{-6}$ cm^{-1})

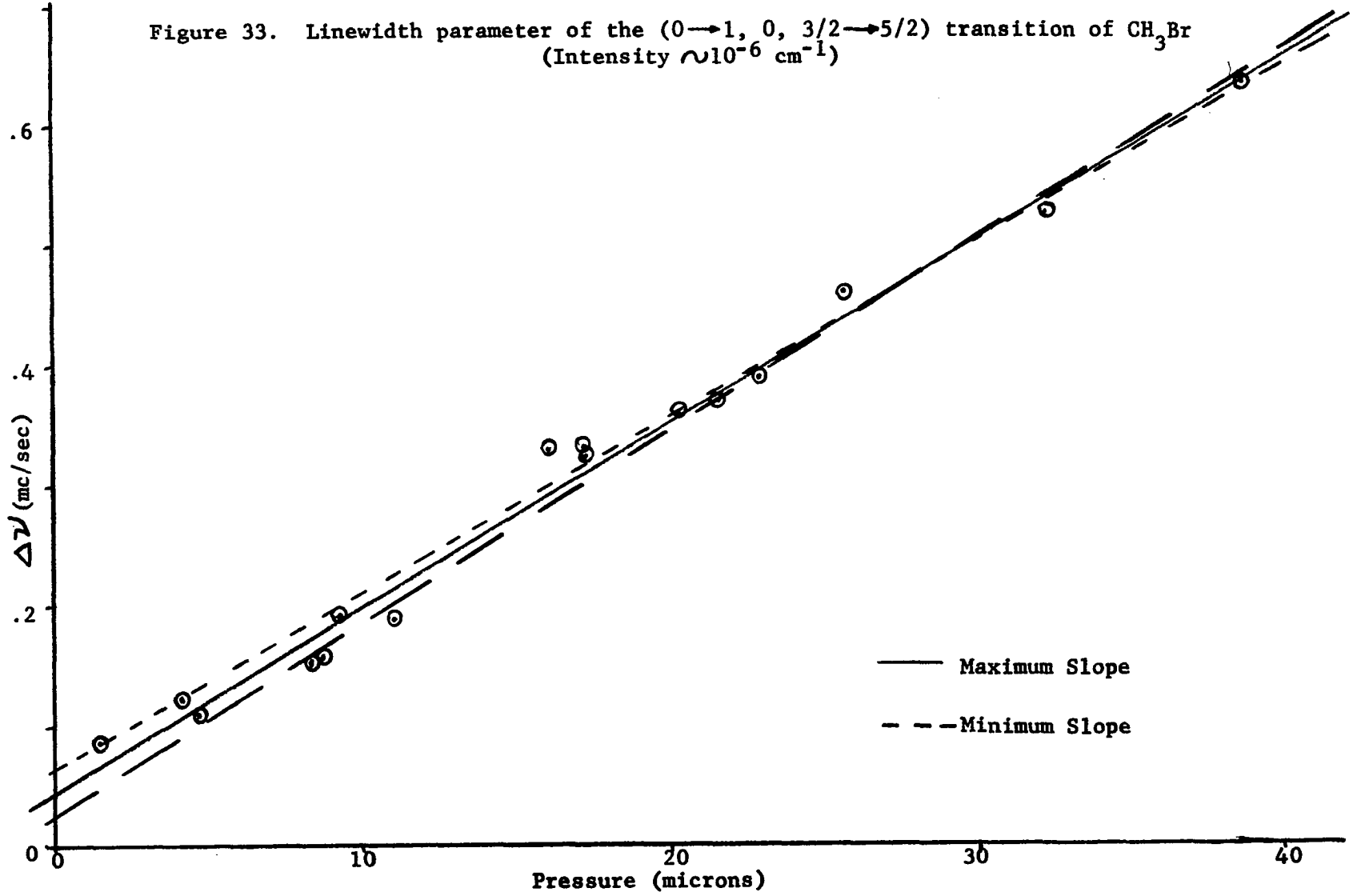

APPENDIX IV

MISCELLANEOUS TABLES

This appendix contains some tables needed to make comparisons between the theoretical calculations and experimental results.

Several tables of data obtained for various intensity spectral lines are given to indicate the nature of scatter for the data obtained using the line width spectrograph discussed in this work. As has been pointed out earlier, the scatter of the data points cannot be totally attributed to the low intensity of the spectral lines. Several interacting parameters can produce large scatter in the data and produce erroneous slope parameters, even for strong spectral lines, if the procedure for measuring line widths as discussed in Chapter VII is not followed.

Table 15 gives comparison data needed to compare detailed calculations made using Anderson's theory with the results obtained experimentally.

Tables 16, 17, and 18 give raw and corrected data obtained for spectral lines of $10^{-4}cm^{-1}$, $10^{-5}cm^{-1}$ and $10^{-6}cm^{-1}$ intensity. These results indicate the degree of precision with which data is repeatable for this work. Some spectral lines of $10^{-7}cm^{-1}$ intensity have been observed but the resulting data is subject to greater doubt than that

listed here. Spectral lines of $10^{-7}cm^{-1}$ intensity can be measured more accurately by using a phase sensitive detector, but this entails a procedure for generating markers of 100 Kc/sec increment. These markers must have good long range stability to be usable as standards.

The most accurate data of this investigation are assumed to be the data obtained for spectral lines of $10^{-4}cm^{-1}$ intensity.

TABLE 15.--Calculated and observed line width parameters for several symmetric top molecules

Gas	ΔJ	K	ΔF	$\Delta\nu_p$(obs.)	$\Delta\nu_p$(calc.)
CH_3Br^{79}	0→1	0	3/2→5/2	15.71	17.70
	1→2	1	3/2→5/2	12.25	13.43
	2→3	0	7/2→7/2	12.83	13.00
		1	7/2→9/2	11.79	12.48
		2	1/2→3/2	11.93	10.63
	3→4	0	5/2→7/2	12.83	11.55
		1	7/2→9/2	13.80	11.35
		2	9/2→11/2	12.60	10.67
		3	7/2→9/2	12.00	9.12
CH_3Br^{81}	0→1	0	3/2→5/2	15.20	17.60
	1→2	0	5/2→7/2	10.30	15.12
		1	5/2→7/2	12.88	13.32
	2→3	0	3/2→3/2	14.73	12.84

TABLE 15.--Continued

Gas	ΔJ	K	ΔF	$\Delta\nu_p$(obs.)	$\Delta\nu_p$(calc.)
CH_3Br^{81}	2→3	1	7/2→9/2	12.60	12.36
		2	1/2→3/2	14.63	10.53
	3→4	0	9/2→9/2	14.85	11.42
		1	7/2→9/2	13.23	11.22
		2	9/2→11/2	12.90	10.56
		3	3/2→5/2	12.66	9.03
CH_3Cl^{35}	0→1	0	3/2→5/2	19.46	22.47
	1→2	0	5/2→7/2	17.56	19.65
		1	5/2→7/2	15.63	17.34
CH_3Cl^{37}	0→1	0	3/2→5/2	20.17	22.23
	1→2	0	5/2→7/2	17.87	19.39
		1	5/2→7/2	17.00	17.12
	2→3	0	7/2→7/2	11.25	16.79

TABLE 15.--Continued

Gas	ΔJ	K	ΔF	$\Delta\nu_p$(obs.)	$\Delta\nu_p$(calc.)
CH_3Cl^{37}	2→3	2	3/2→5/2	12.80	13.76
CH_3CN	0→1	0	1→2	94.17	80.86
C_3H_4	0→1	0		8.75	5.62
	1→2	0		12.25	5.63
	1→2	1		13.75	5.14
	2→3	0		7.25	5.67
	2→3	1		8.45	5.46
	2→3	2		8.39	4.70
	3→4	0		8.48	5.72
	3→4	1		8.60	5.50
	3→4	2		7.88	5.20
	3→4	3		7.91	4.38
CH_3I	0→1	0	5/2→7/2	13.28	13.43

TABLE 15.--Continued

Gas	ΔJ	K	ΔF	$\Delta\nu_p$(obs.)	$\Delta\nu_p$(calc.)
CH_3I	1 → 2	0	7/2 → 9/2	10.77	11.65
	1 → 2	1	7/2 → 9/2	9.58	10.26
	2 → 3	0	9/2 → 11/2	9.45	9.97
	2 → 3	1	9/2 → 11/2	11.08	9.59
	2 → 3	2	9/2 → 9/2	9.53	8.13
	3 → 4	0	3/2 → 5/2	9.54	8.86
	3 → 4	1	11/2 → 11/2	9.46	8.70
	3 → 4	2	11/2 → 13/2	9.58	8.16
	3 → 4	3	11/2 → 13/2	8.79	6.94
	4 → 5	0	11/2 → 13/2	9.83	8.31
	4 → 5	1	13/2 → 15/2	9.65	8.23
	4 → 5	2	13/2 → 15/2	9.90	7.94
	4 → 5	3	13/2 → 15/2	9.71	7.39

TABLE 16.--Line width parameter data for the (6,6) inversion line of NH_3 broadened by CH_2CF_2

P_1	P_2	$\delta\nu$	P_1	P_2	$\delta\nu$	P_1	P_2	$\delta\nu$
13.955	14.062	.107	13.910	14.143	.233	13.886	14.266	.380
13.903	14.012	.109	13.861	14.093	.232	13.761	14.141	.380
.052	.050		.049	.050		.125	.125	
13.954	14.062	.108	13.910	14.143	.233	13.885	14.267	.382
13.903	14.013	.110	13.859	14.092	.233	13.761	14.141	.380
.051	.049		.051	.049		.124	.126	
13.954	14.062	.108	13.910	14.142	.232	13.885	14.266	.381
13.903	14.012	.109	13.860	14.093	.233	13.760	14.141	.381
.051	.050		.050	.049		.125	.125	
13.955	14.063	.108	13.910	14.143	.233	13.886	14.266	.380
13.904	14.013	.109	13.860	14.093	.233	13.761	14.141	.380
.051	.050		.050	.050		.125	.125	
13.954	14.062	.108	13.911	14.143	.233	13.886	14.267	.381
13.903	14.012	.109	13.801	14.093	.232	13.761	14.142	.381
.051	.050		.050	.050		.125	.125	

Pressure = .34 microns: $\omega' = .050$, $\delta\nu = .109$, $\Delta\nu = .088$

Pressure = 8.78 microns: $\omega' = .050$, $\delta\nu = .233$, $\Delta\nu = .199$

Pressure = 17.09 mic.: $\omega' = .125$, $\delta\nu = .381$, $\Delta\nu = .319$

13.880	14.422	.542	13.829	14.508	.679	13.794	14.585	.795
13.645	14.184	.539	13.592	14.273	.681	13.556	14.357	.801
.235	.238		.237	.235		.238	.232	
13.881	14.420	.539	13.830	14.509	.679	13.798	14.588	.790
13.645	14.185	.540	13.594	14.272	.678	13.557	14.356	.799
.236	.235		.236	.237		.241	.232	
13.881	14.421	.540	13.830	14.510	.680	13.796	14.587	.791
13.644	14.186	.542	13.593	14.272	.689	13.555	14.354	.799
.237	.235		.237	.238		.241	.233	
13.882	14.420	.538	13.829	14.508	.679	13.797	14.586	.789
13.645	14.186	.541	13.594	14.271	.687	13.557	14.356	.798
.237	.234		.235	.237		.240	.230	

Pressure = 25.36 microns: $\omega' = .236$, $\delta\nu = .540$, $\Delta\nu = .440$

Pressure = 33.56 microns: $\omega' = .237$, $\delta\nu = .681$, $\Delta\nu = .567$

Pressure = 41.92 mic.: $\omega' = .235$, $\delta\nu = .796$, $\Delta\nu = .670$

TABLE 17.--Line Width Parameter Data for the $\Delta J = 0 \rightarrow 1$, $K = 0$, $\Delta F = 3/2 \rightarrow 5/2$ Line of CH_3Br^{79} ($I = 1.5 \times 10^{-6} cm^{-1}$)

P_1	P_2	$\delta\nu$	P_1	P_2	$\delta\nu$	P_1	P_2	$\delta\nu$
17.608	17.753	.145	17.548	17.822	.174	17.470	17.885	.415
17.578	17.727	.149	17.508	17.798	.190	17.457	17.865	.408
.030	.026		.040	.024		.013	.020	
17.609	17.751	.143	17.538	17.815	.177	17.477	17.888	.411
17.580	17.724	.144	17.517	17.798	.181	17.452	17.859	.407
.029	.027		.021	.017		.025	.029	
17.612	17.756	.144	17.540	17.814	.174	17.456	17.881	.416
17.581	17.724	.143	17.511	17.796	.185	17.441	17.863	.422
.031	.032		.029	.018		.024	.018	
17.609	17.752	.143	17.542	17.821	.179	17.472	17.876	.404
17.580	17.722	.142	17.519	17.794	.175	17.442	17.856	.414
.029	.030		.023	.030		.030	.020	
Pressure = 4.05 microns			Pressure = 11.29 microns			Pressure = 17.13 microns		
ω' = .030			ω' = .030			ω' = .030		
$\delta\nu$ = .144			$\delta\nu$ = .179			$\delta\nu$ = .412		
$\Delta\nu$ = .123			$\Delta\nu$ = .168			$\Delta\nu$ = .356		
17.447	18.023	.576	17.419	18.145	.726			
17.399	17.988	.589	17.345	18.092	.747			
.038	.035		.074	.053				
17.434	18.019	.585	17.414	18.151	.737			
17.384	17.959	.565	17.333	18.075	.742			
.050	.060		.081	.076				
17.456	18.016	.560	17.418	18.126	.708			
17.373	17.964	.591	17.321	18.091	.770			
.083	.052		.097	.035				
17.422	18.036	.614	17.419	18.147	.728			
17.368	17.968	.590	17.331	18.079	.749			
.054	.068		.088	.068				
Pressure = 32.22 microns			Pressure = 38.61 microns					
ω' = .050			ω' = .075					
$\delta\nu$ = .584			$\delta\nu$ = .738					
$\Delta\nu$ = .505			$\Delta\nu$ = .637					

TABLE 18.--Line width parameter data for the (6,2) inversion line of NH_3 (I = 1.3 X 10^{-5} cm^{-1})

P_1	P_2	$\delta\nu$	P_1	P_2	$\delta\nu$	P_1	P_2	$\delta\nu$
25.285	25.556	.271	25.268	25.577	.309	25.180	25.674	.494
25.199	25.472	.273	25.180	25.491	.311	25.098	25.586	.488
.086	.084		.088	.086		.082	.088	
25.285	25.556	.271	25.270	25.578	.308	25.185	25.673	.488
25.199	25.472	.273	25.183	25.491	.308	25.097	25.583	.486
.086	.084		.087	.087		.088	.090	
25.286	25.554	.268	25.267	25.578	.311	25.179	25.672	.493
25.200	25.472	.272	25.183	25.491	.308	25.097	25.585	.488
.086	.082		.084	.087		.082	.087	
Pressure = 12.67 microns			Pressure = 15.80 microns			Pressure = 27.12 mic.		
ω' = .086			ω' = .086			ω' = .086		
$\delta\nu$ = .272			$\delta\nu$ = .309			$\delta\nu$ = .489		
$\Delta\nu$ = .228			$\Delta\nu$ = .261			$\Delta\nu$ = .419		
25.232	25.793	.561	25.151	25.868	.717	25.136	25.893	.757
24.993	25.551	.558	24.910	25.628	.718	24.905	25.663	.758
.239	.242		.241	.240		.231	.230	
25.232	25.794	.562	25.157	25.862	.705	25.137	25.888	.751
24.993	25.554	.561	24.915	25.631	.716	24.092	25.646	.744
.239	.240		.242	.231		.235	.242	
25.230	25.793	.563	25.154	25.868	.714	25.138	25.889	.751
24.994	25.553	.559	24.916	25.628	.712	24.905	25.651	.746
.236	.240		.238	.240		.233	.238	
Pressure = 29.60 microns			Pressure = 40.07 microns			Pressure = 42.27 mic.		
ω' = .240			ω' = .240			ω' = .235		
$\delta\nu$ = .561			$\delta\nu$ = .715			$\delta\nu$ = .751		
$\Delta\nu$ = .458			$\Delta\nu$ = .597			$\Delta\nu$ = .630		

LIST OF REFERENCES

1. Edgar A. Rinehart, R. L. Legan and Chun C. Lin, Rev. Sci. Instr., 36, 511 - 517 (1965)

2. Edgar A. Rinehart, R. H. Kleen and Chun C. Lin, J. Mol. Spectry., 5, 458 - 473 (1960)

3. Edgar A. Rinehart and R. L. Legan, Rev. Sci. Instr., 35, 103 - 104 (1964)

4. P. W. Anderson, Phys. Rev., 76, 647 (1949)

5. International Crystal Manufacturing Company, Inc., Oklahoma City, Oklahoma

6. C. H. Townes and A. L. Schawlow, Microwave Spectroscopy, 458 - 462 (McGraw-Hill Book Company, Inc., New York, New York, 1955)

7. W. C. King and W. Gordy, Phys. Rev., 93, 407 (1954)

8. G. R. Gunther-Mohr, R. L. White, A. L. Schawlow, W. E. Good and D. K. Coles, Phys. Rev., 94, 1184 (1954)

9. Rinehart, Kleen and Lin, loc. cit.

10. Robert L. Legan, "Measurements of Line Widths of the Microwave Spectrum of Ammonia" (unpublished Master's Thesis, Department of Physics, University of Oklahoma, 1964)

11. J. H. Van Vleck and V. F. Weisskopf, Revs. Mod. Phys., 17, 227 (1945)

12. B. Bleaney and R. P. Penrose, Proc. Phys. Soc., 59, 418 (1947)

13. Anderson, loc. cit.

14. R. W. Parsons and J. A. Roberts, J. Mol. Spectry., 18, 412 - 417 (1965)

15. J. H. Jeans, The Dynamical Theory of Gases, pp. 37, 252. (Cambridge University Press, Third Edition, 1921)

16. G. R. Bird, Phys. Rev., 95, 1686 (1954)

17. P. W. Anderson, Phys. Rev., 80, 511 (1950)

18. W. V. Smith, J. Chem. Phys., 25, 510 (1956)

19. Chester O. Britt and James E. Boggs, J. Chem. Phys., 45, 3877 (1966)

20. Roy Anderson, Phys. Rev., 97, 1654 (1955)

21. Anderson, P. W., loc. cit.

22. Robert L. Legan, James A. Roberts, Edgar A. Rinehart and Chun C. Lin, J. Chem. Phys., 43, 4337 - 4345 (1965)